The role of iron bound carbon for organic matter preservation and global climate systems: an experimental approach.

Benjamin J. Fisher

Submitted in accordance with the requirements for the degree of

Master of Science by Research

The University of Leeds

School of Earth and Environment

June 2020

The candidate confirms that the work submitted is their own, except where work which has formed part of jointly authored publications has been included. The contribution of the candidate and the other authors to this work has been explicitly indicated below.

The candidate confirms that appropriate credit has been given within the thesis where reference has been made to the work of others.

The work in Chapter 3 of the thesis has been submitted to Chemical Geology for publication as follows:
Experimental evaluation of the extractability of Fe-bound organic carbon as a function of carboxyl content: Implications for understanding Fe-bound organic carbon in marine sediments. **Fisher. B**, Moore. O, Faust. J, Peacock. C, März. C *(in revision)*

I was responsible for experimental design, conducting the experiments, data analysis and writing the manuscript. The contribution of the other authors was supervision, joint planning of experimental design, assistance in interpretation of the data and feedback on manuscript drafts.

The work in Chapters 3 and 4 of this thesis have appeared in published conference proceedings of the European Geosciences Union under DOI: 10.5194/egusphere-egu2020-855. Further details of conferences can be found in *Appendix 1.*

Abstract:

Burial of organic carbon (OC) in marine sediments is a crucial process for the drawdown of atmospheric CO_2 over geological timescales. Association of OC with reactive iron (Fe_R) phases represents the largest described mechanism by which OC is preserved in marine sediments (accounting for ~22% of preservation). Despite its importance, little is known about which Fe_R phases are involved in OC uptake, or the binding mechanism of OC to these reactive iron minerals. Moreover, the effect of different OC moieties on the stability and preservation of Fe-bound OC is not fully understood. To determine the importance of the OC-Fe_R mechanism, a citrate-dithionite-bicarbonate (CDB) extraction is used to dissolve the 'easily reducible iron oxide' fraction and release associated OC from sediments. However, natural samples contain a range of Fe_R phases extractable by CDB, and phases are defined by their susceptibility to chemical reduction. Therefore, factors affecting mineral stability, including association with OC, may influence estimates of the amount of OC bound to Fe_R phases. Here, OC-Fe composites were synthesised with known Fe_R phases and OC moieties and spiked into OC-free marine sediment followed by treatment with CDB to determine the impact of OC moiety on Fe release. It is shown that CDB treatment results in only partial dissolution of the most susceptible Fe phase and that greater losses of Fe occur for carboxyl rich organominerals due to increased structural disorder. Further findings indicate that the strength of OC bound to Fe, determined by structure, can affect quantification of the OC-Fe pool and effort is made to reconstruct the CDB method in order to improve its accuracy. A developed understanding of this molecular level characterisation will improve understandings of OC-Fe quantifications from sediment analysis, and subsequently in determining the extent to which Fe bound OC preservation is important for global carbon cycling.

Acknowledgements

Firstly, I'd like to thank my primary supervisor, Dr Christian März for taking a chance and giving me the opportunity to pursue my interest in biogeochemistry by supervising this project. I also extend my thanks to the rest of my supervisory team, Dr Johan Faust, Dr Oliver Moore and Prof Caroline Peacock who have each brought immeasurable insight from my first days in the lab through to analysing puzzling data and writing this thesis.

My experimental work would not have been possible without the help and advice of the technical staff both in Cohen Geochemistry and the School of Geography, in particular I wish to thank Dr Andy Hobson, Dr Bob Jamieson, Fiona Keay, Lesley Neave and David Ashley for all their kind support.

Many others have also provided thoughtful inputs on my methodology and results throughout which were crucial to shaping the path of my research. I thank the MINORG team for involving me in your insightful (and biscuit filled) weekly coffee meetings. To the ChAOS team, participating in the 2019 post cruise meeting was a real eye opener for me, who knew there were so many things you could measure in marine sediments! And for those ChAOS members who retrieved the sediment samples I used for this project.

I thank Quaternary Research Association for allowing me to give my first conference presentation of this project in a very friendly environment and the EGU for the chance to present at my first international conference (albeit virtually from my bedroom, thanks to COVID-19). I also extend thanks to the European Association of Geochemistry for offering me a travel grant which will be repurposed for a future conference.

Finally, to acknowledge the everyone in the Earth Surface Science Institute at Leeds who are the nicest group of people I could have hoped to meet, it has been a pleasure to spend the year with such a great group of people who I hope will remain friends for a long time to come!

Table of Contents

Table of Figures

Table of Tables

Abbreviations

1 COOH	Valeric acid ($CH_3(CH_2)_3COOH$
2 COOH	Adipic acid $(CH_2)_4(COOH)_2$
3 COOH	1,2,4-Butanetricarboxylic acid $C_7H_{10}O_6$
AAS	Atomic absorption spectroscopy
C4MIP	Coupled Climate Carbon Cycle Model Intercomparison
CDB	Citrate-dithionite-bicarbonate (chemical extraction)
CO_2	Carbon dioxide
COOH	Carboxyl group
CRAM	Carboxyl rich alicyclic molecule
DI	Deionised water
DOC	Dissolved Organic Carbon
DOM	Dissolved Organic Matter
Fe	Iron (element)
$Fe(NO_3)_3.9H_2O$	Iron(III) nitrate nonahydrate
Fe_R	Reactive Fe phase
Fh	Ferrihydrite (iron phase)
Fh-OC	Organic Carbon bound to ferrihydrite
FTIR	Fourier-transform infrared spectroscopy
g	Gram / Gravitational force (unit)
HCL	Hydrochloric acid
IC	Inorganic Carbon
KOH	Potassium hydroxide
MAR	Mean accumulation rate
MQ	Milli-Q (ultrapure) water
Na	Sodium
NaCl	Sodium chloride
$NaHCO_3$	Sodium bicarbonate
NEXAFS	Near edge X-ray absorption fine structure
OC	Organic Carbon
OC-Fe	Organic Carbon bound to reactive iron phases.

OM	Organic Matter
Pg	Peta-grams
POC	Particulate Organic Carbon
PPE	Perturbed physics ensemble
QC	Quality Control
rDOC	recalcitrant Dissolved Organic Carbon
RSD	Root square deviation
SEM	Standard error of the mean
SEM	Scanning electron microscopy
Sln	Solution
STXM	Scanning X-ray transmission microscopy
TEM	Transmission electron microscopy
TOC	Total Organic Carbon
XAS	X-Ray absorption spectroscopy
XRD	X-ray diffraction

Chapter 1- Introduction

1.1 Thesis outline

This thesis explores an understudied area of overlap between experimental geochemistry and marine biogeochemistry integrated in to two larger work packages, “Changing Arctic Ocean Seafloor “(ChAOS, NERC) and “Carbon cycling in marine sediments: mineral-promoted preservation and burial” (MinORG, ERC). Specifically, this work expands on previous studies by exploring the role of molecular organic structure in determining the strength of the preservative effect conferred upon organic carbon by reactive iron minerals.

Chapter 1 provides a literature review and introduction to the topic of iron bound carbon preservation, placing this in a global context. This chapter critically analyses our knowledge to date, particularly in terms of methodology, and identifies the gaps which this thesis aims to address.

Chapter 2 details the chemical and physical methods which have been used for experimental synthesis (e.g. mineral coprecipitation), preparation of samples and the subsequent elemental and physical analysis methods.

Chapter 3 presents results from experiments aimed at investigating the influence of carboxyl richness on the stability of iron bound carbon. Additionally, data related to physical parameters (particle size, crystallinity) are shown. This chapter primarily focuses on experimental biogeochemistry using synthesised coprecipitates to probe the molecular level iron-carbon interaction.

Chapter 4 builds on conclusions drawn from Chapter 3 relating to the completeness of the reductive dissolution method (used as a proxy for iron-carbon bond stability). This chapter tests physical parameters of the reductive dissolution method and quantifies its efficiency using known synthetic standards before validating this against natural Arctic marine sediment.

Chapter 5 concludes the thesis and provides a short commentary on the overall implications of the work conducted. This chapter links the results from both Chapters 3 and 4 together and considers how these could be applied to methods for environmental sample analysis and included mechanistically in global biogeochemical models. The thesis ends with suggestions of further work which may be beneficial but was beyond the scope of this project.

1.2 Global carbon cycling

The presence of carbon on Earth is essential for life, both as an organic building block, and in creating habitable environmental conditions through control of atmospheric carbon dioxide (CO_2) concentrations, and indirectly temperature (Hansen et al., 1981; Dasgupta and Hirschmann, 2010). The role of carbon is central to biogeochemical cycles, with the importance of these cycles in mediating planetary responses to rapid environmental change being increasingly realised in the context of modern climate change. Broadly, carbon can be considered in two forms within an environmental context, organic and inorganic. Inorganic carbon (IC) exists as dissolved or gaseous species of CO_2 (with bicarbonate dominating most aqueous solutions on Earth's surface) and in solid carbonate minerals (e.g., calcite, aragonite). Atmospheric or dissolved CO_2 is the primary carbon source for photosynthesis, resulting in the production of most organic matter (OM) at Earth's surface using solar energy to build biomass consisting of organic carbon (OC)-based molecules (Wetzel, 2001). Models suggest that marine and terrestrial settings make equal contributions to overall net primary production (NPP) of the biosphere (Field et al., 1998). In marine environments, surface productivity is dominated by phytoplankton species, while plants account for roughly the same amount of productivity in marine and terrestrial environments (le B. Williams, 1998). Subsequently, OM can sink through the oceans or fall onto the ground, then become buried within seafloor sediments or soil. Once turned into "dead" OM, it immediately acts as an energy source, allowing the persistence of heterotrophic life on Earth at depths beyond the penetration of light, where photosynthesis cannot occur (Lang et al., 2019).

OM is often referred to as being dissolved or particulate in nature, where dissolved organic matter (DOM) is defined as those molecules small enough to pass through a 0.5 μm filter while particulate organic matter (POM) are larger than this arbitrary cut off (Lush and Hynes, 1973;

Kaushik and Hynes, 1971). While these terms may be useful for describing size of OM compounds, some caution should be given to their overinterpretation as it is noted that "there is a fair amount of interchange" (Lush and Hynes, 1978) between the two states, and therefore DOM and POM should be regarded as dynamic, not distinct OM pools. Several mechanisms exist for the transformation of DOM to larger POM fractions, including: Brownian motion induced aggregation (perikinetic coagulation), adsorption of DOM on to suspended particles (predominantly in riverine environments), and photo regulated processes including photo-irradiation (e.g. enhanced degradation of DOM producing smaller fractions which subsequently adsorb to other particles) (He et al., 2016 and references therein). The structure of OM may also influence its fate both in terms of transformation, with Ward (2008) suggesting the presence of carboxyl functional groups enhance the DOM to POM transformation, and overall OM reactivity (see *1.4.1)*. Due to size, and therefore density, DOM sinks more slowly than POM and typically resides in the water column for a longer period of time (Volkman and Tanoue, 2002). Residence time for DOM has been estimated to be up to 1320 years for surface fractions and 6240 years for deeper refractory DOM (Williams and Druffel, 1987), with photodegradation to inorganic components and labile organic fractions postulated as the dominant removal process for refractory DOM (Ward, 2008). Any OM not removed in the water column will with time (dependent on sedimentation rate) reach the seafloor.

1.2.1 Surface to sediment: The transport of organic carbon.

OM in marine sediments can be considered in two distinct forms. Insoluble OM exists as kerogen, stored in deep sedimentary rocks where it is refractory in nature and remains stable on geological timescales (Schillawski and Petsch, 2008). This fraction contains approximately 15 $x10^6$ Pg C which by far outweighs the total mass of all other OC pools in soils, non-lithified sediments, and living ocean biomass (*Figure 1.1*)

(Berner, 1987; Hedges, 1992). Additionally, a comparatively smaller pool of 'labile' sedimentary organic matter overlays kerogen and marine carbonates. While this pool is less significant in terms of mass, it is much more dynamic in nature with the ability to be decayed and released into the ocean or sequestered on geologically relevant timescales via preservation processes. Therefore, the C stored here is much more vulnerable to environmental change and is of greater relevance in the context of molecular level mechanisms implicated in the marine C cycle.

Typically, the TOC concentration profile of marine sediment is expected swiftly decrease beyond the OM rich 'fresh' surface, Recently, we have begun to understand the extent to which preservative processes facilitate OC persistence in these deeper oligotrophic sediments. Estes et al. (2019) have shown low but significant levels of OC preservation to sediment depths of 25 m (~24 million years) in the North Atlantic and South Pacific oceans . This study provides an estimation of between 6.4 $x10^{21}$ and 1.6 $x10^{22}$ g of OC stored within such deeply buried oxic sediments, representing 50-120% of current estimates for total OC stored in the seafloor. Additionally, in my recent work (Faust et al., *in prep*) we have demonstrated the persistence of OC at 25-30m sediment depth, facilitated by the presence of reactive iron phases, indicating long term efficiency of mechanisms associated with the sedimentary carbon sink.

In surface sediments, marine DOM is the main OC source mostly produced autochthonously by photosynthetic plankton and subsequently acts as a substrate for heterotrophic microbial populations and as an N&P source for autotrophs (Hansell et al., 2009). Additional OC sources are spatially and seasonally variable and can either act as a sink/source themselves (often leaching into sedimentary OM over time) or can be a direct flux, the main accumulation pathways are shown in *Figure 1.1.* An example of an OC flux would be riverine transport (0.45 Pg C yr^{-1}) (Meybeck, 1982; Li et al., 2017) while inputs from other OC sinks includes

OC in groundwater liberated from summer permafrost thaw (14-71 kg km (shoreline) day $^{-2}$) (Connolly et al., 2020) and terrestrial inputs (e.g. slope transport of soil and vegetation in fjord sediment) (Smith et al., 2015). The subsequent flux of oceanic DOC to the sediment is estimated to be 0.2 Pg C yr $^{-1}$ (IPCC, 2013) as shown in *Figure 1.1.*

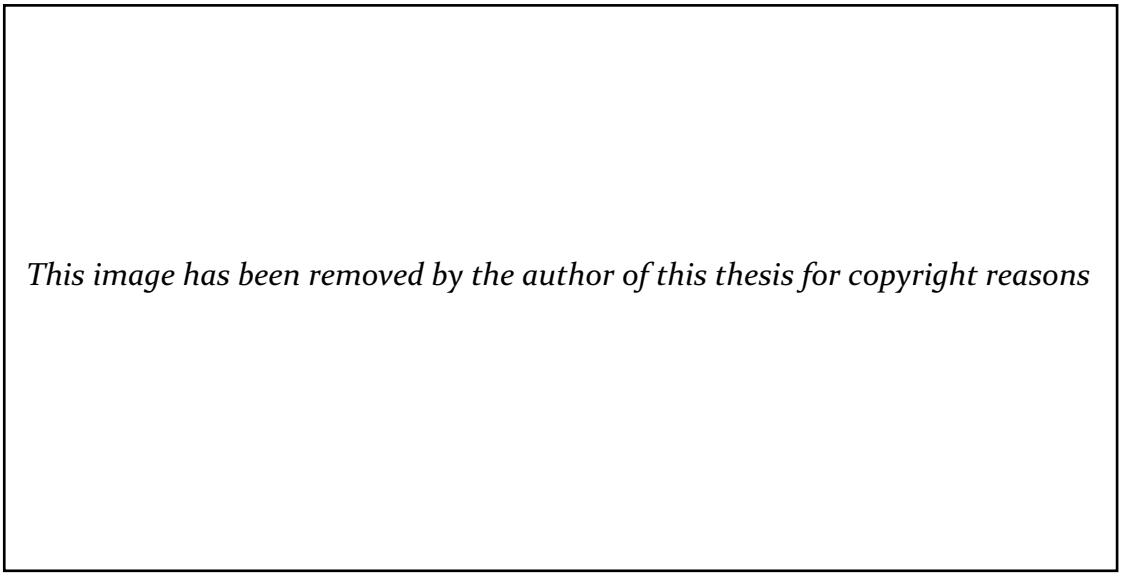

Figure 1.1 Schematic of carbon cycle fluxes. Adapted from (Lang et al., 2019). Light orange boxes indicate OC pools, dark orange show OC fluxes in the direction dictated by the arrows. Red ellipses highlight the most mobile natural OC pools, 0.2 Pg C yr^{-1} ocean to sediment flux added from (IPCC, 2013).

The OC content of labile soil and sediment pools is spatially and temporally variable, dependent upon the balance between preservation of OC, resulting in its incorporation into the lithosphere, and OC degradation, resulting in respiratory release as CO_2 back to the atmosphere. The term "labile", when applied in the context of OM, indicates the susceptibility of OM towards microbial degradation (Bongiorno et al., 2019). Mayer (1995), however, notes that degradability cannot be used to describe OM in itself as it is not an inherent property of OM and is dependent upon interactions between OM and the environment.

This interaction highlights the importance of environmental processes in mediating both production, transportation and storage of OM on Earth's surface, defined by Arndt et al. (2013) as a "reaction-transport problem", with chemical, physical and biological processes being jointly involved in degradation. Chemical factors could include OM composition (e.g. non hydrolysable substrates which resist decomposition) (Canfield, 1994; Hedges, J.I. and Keil, R., 1995), electron acceptor availability (see *1.5*), microbial inhibition by metabolites (Aller, R. and Aller, J., 1998), and the (an)oxic conditions of the water column (Arndt et al., 2013 and references therein). Physical factors which influence OM degradation include sedimentation rate, particularly where the bulk OM is refractory enough to avoid degradation in the upper mixed sediment layer (Arndt et al., 2013 and references therein). Additionally, physiochemical protection of OM by adsorption to minerals protects OM particles against microbial degradation (see *1.4.3*). Macrobenthic activity represents a physiobiological level of control on OM degradation through movement within the sediment (bioturbation) and drawing down of overlaying water in to burrows within the sediment (bioirrigation) creating short term redox oscillations which may promote OM degradation (Arndt et al., 2013).

Water depth, light availability, and benthic faunal community composition are significant environmental factors controlling OC deposition at the seafloor (Middelburg, 2019a). Regional effects, particularly in high latitude settings are generally more susceptible to changes in external forcing of Earth's climate (driven by orbital parameters and resulting insolation changes) (Koç and Jansen, 1994), and therefore respond quicker and more sensitively, with potential feedbacks on the global climate system (e.g., changes in global sea level, ocean circulation, ocean gateways) (Ding et al., 2017; Winton et al., 2013). Examples of further climate sensitive localised controls on OC deposition include; those which are physical such as ice sheet extent with implications for

primary productivity (Boetius et al., 2013; Anderson and Macdonald, 2015), chemical e.g. liberation of OC moieties from thawing glaciers (Lawson et al., 2014; Hood et al., 2015) and biological with shifts in the water column ecosystem influencing rates of remineralisation (Lopes et al., 2015).

1.2.2 Palaeo carbon burial

Understanding of how carbon burial has been, and will continue to be, influenced by changing trends in atmospheric CO_2 and temperature can been inferred from palaeoclimate records, particularly over the late Quaternary (Munroe and Brencher, 2019). Here, changes in ice sheet extent and thickness, and subsequent changes in sea levels and ocean circulation, are more profound and free from internal climate variability bias (e.g. from zonal wind anomalies), compared to decadal scale observations (Holland et al., 2019). The late Quaternary can be considered in three stages, the Last Glacial Maximum (LGM, 19-26.5 ka) (Clark et al., 2009), followed by a deglacial period, until commencement of the current epoch, the Holocene (11.65 ka) (Walker et al., 2009). Reconstruction by Cartapanis et al. (2016) *(Figure 1.2)* shows a global marine OC burial maximum of 28.17 Pg C yr^{-1} (± 5.49) at 21 ka (LGM, glacial conditions), in comparison to a modern day (0 ka, interglacial conditions) burial of 16.62 Pg C yr^{-1} (± 0.63).

This trend is replicated across the penultimate glacial-interglacial boundary (marine isotopic stages (MIS) 6/5e, 195-123 and 123-119 ka respectively). The trend between OC accumulation and glaciation is generally presumed to be resultant from enhanced OC delivery and improved preservation (e.g. Poli et al., 2012). However, palaeo studies rarely consider the mechanistic processes which influence OC preservation; indeed, these are only beginning to be fully understood in the context of the modern marine C cycle. A developed understanding of the OC preservation mechanisms in modern marine sediments may be

advantageous in palaeo applications for unravelling gaps in knowledge regarding the palaeo record; for example why OC accumulation is high in the LGM and MIS6 but not under the glacial conditions of MIS4 *(Figure 1.2),* a problem described by Cartapanis et al. (2016) as "an intriguing observation that deserves further attention".

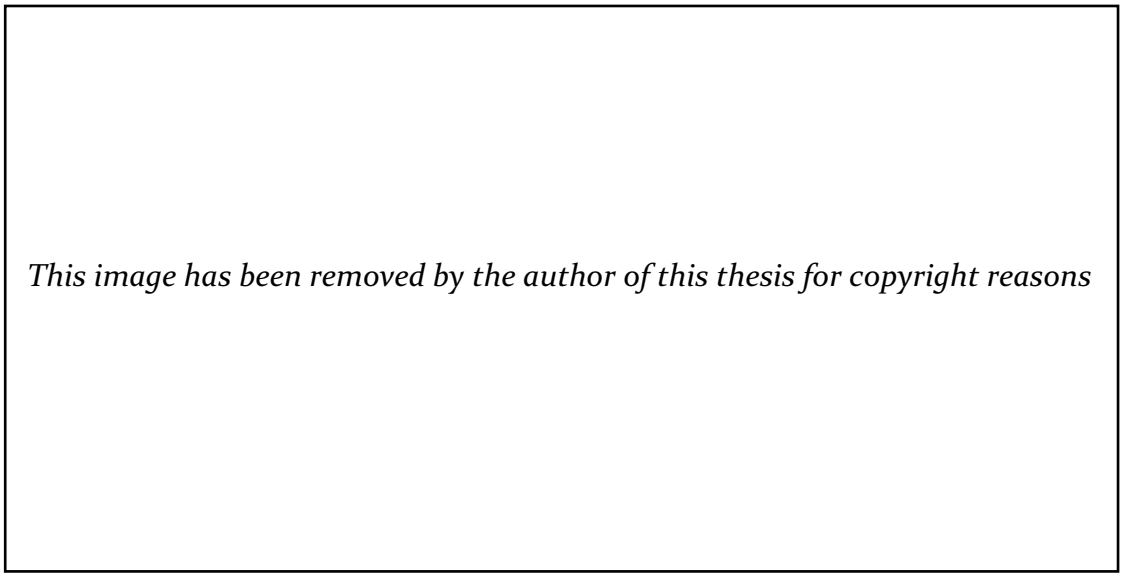

Figure 1.2 Reconstruction of Palaeo TOC Mean Accumulation Rate (MAR) and sea level change throughout the Quaternary. (Cartapanis et al., 2016).

The direct influence of sea ice extent, through limiting light availability for surface primary production, on OC burial is minimal, and under periods of warming primary and export productivity have been shown to be decoupled from carbon burial (Lopes et al., 2015) *(Figure 1.3).* Indirect physical influences are likely to be more significant in increasing OC burial during glacial periods, with a significant decrease in sea levels reducing the distance OC particles have to travel to reach the seafloor. Enhanced nutrient fluxes to the ocean (Shaffer and Lambert, 2018), more efficient transfer of OC through the water column and reduced oxygen exposure (Hoogakker et al., 2014) have all been postulated as contributory factors towards increased OC burial in glacial periods (Cartapanis et al., 2016).

These overriding physiochemical parameters also mask ecological shifts influencing burial efficiency. Water column ecosystems are an important indicator of palaeo and future OC burial through dictating OC molecular structure, which has implications for remineralisation rates. Interglacial periods were dominated by heavy diatom based ecosystems which export OC more efficiently than the costal upwelling type ecosystems found in glacial periods whereby OC is readily remineralised through the water column (Lopes et al., 2015). Size fragmentation is a key factor in determining the remineralisation length scale (RLS, the vertical distance over which the organic particle flux declines by 63%) of OC, of particular importance in oxygen minimum zones (OMZ) (Cavan et al., 2017). RLS has a significant feedback on atmospheric CO_2, whereby a 100 m RLS increase correlates to an atmospheric CO_2 level increase of ~50 ppm (Kwon et al., 2009).

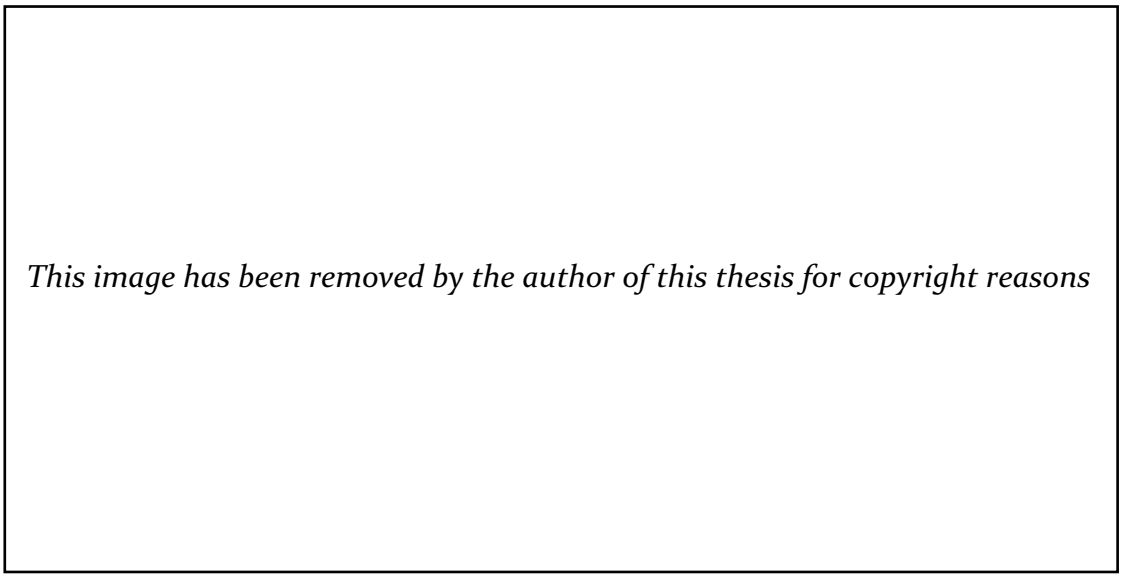

Figure 1.3 Decoupling of primary productivity from carbon burial in the Quaternary shown by reconstructions from diatom flora composition. (Lopes et al., 2015)

Ecosystem function may be of particular importance on longer palaeo timescales whereby reconstructions of physical parameters fail to replicate increased glacial OC burial on longer timescales (e.g. MIS4, 71 kya) (Cartapanis et al., 2016). This multifaceted approach to understanding the

biological, physical and geological parameters required to reconstruct paelo OC burial demonstrates the importance of variability at the organism to molecular scale, such as OC fractionation and ecosystem community composition, in mediating past, present and future OC sequestration.

1.3 Processing and composition of organic carbon in marine sediments.

OM which is not remineralised in the water column reaches the ocean-sediment interface. Most of it is then oxidised at the sediment surface (e.g. Bender and Heggie, 1984; Canfield, 1993; Canfield, 1994 and references therein), and only ~10-20% is preserved relative to the rain rate (Burdige, 2007). OC preserved in marine sediment is predominantly derived from marine phytoplankton with variable inputs from terrestrial detritus, in the form of lipids, lignin, carbohydrates (sugars) and amino acids (derived from proteins) (Burdige, 2007). Due to degradative processes the majority of OC cannot be biochemically classified; however, in modern marine sediments, amino acids account for the largest identifiable source of OC (10-15%) (Cowie, G L. and Hedges, J I., 1992), with carbohydrates contributing another 5-10%, lignin 3-5% (Cowie et al., 1992) and lipids <5% (Tissot and Welte, 1984). The prevalence of carboxyl containing amino acids in oceanic OC inputs pool, once degraded, leaves DOM at the seafloor dominated by carboxyl rich alicyclic molecules (CRAM) (Hertkorn et al., 2006) *(Figure 1.4)*.

This image has been removed by the author of this thesis for copyright reasons

Figure 1.4 Isomers of model carboxyl rich alicyclic molecules (CRAM) as determined by Hertkorn et al. (2006)

While the molecular composition of the TOC pool in marine sediments has only partly been deciphered, there is an even greater gap in knowledge about the composition of the DOM pool. The marine DOM pool is very heterogenous as a result of multiple variables including: i) varying degradation rates sources; ii) OM sources; iii) redox conditions and iv) microbial community composition (Arndt et al., 2013; Moran et al., 2016). The microbial communities of aerobic bottom waters are known to be enhanced for genes involved in aromatic metabolism (e.g. metabolism of organic functional groups) (Wang et al., 2017). This genetic difference likely produces OC depleted of structurally complex carbon (i.e. more labile) in oxic relative to anoxic waters, which may contribute to observations of increased burial of OC under anoxia (Emerson and Hedges, 1988; Hedges, 1999; Canfield, 1994). However, structural comparison of OC deposited under oxic and anoxic waters are of limited use as any structure dependent burial effect is likely to be overshadowed by the high degradation efficiency during oxic burial due to the availability of O_2 as a high energy yielding electron acceptor.

Variation in buried OC structure is further increased by photosynthetic activity at the seafloor of shallow shelves, producing high quality OM which has not been subject to degradation pre-deposition (Middelburg, 2019a). Approximately one third of costal sediments have sufficient light availability for benthic primary production, representing a small, but not insignificant source of OC (0.32 Pg C yr^{-1}) (Gattuso et al., 2006).

The role of variation in OC structure, resultant from differing composition and source on preservation remains largely undefined and it remains largely unknown as to why oxidative and microbial processes are unable to transform the complete OC pool. A developed understanding of preservative processes, and the importance of OC structure towards these, will be necessary in order to characterise refractory sedimentary OC, the controls on which are crucial for creating and maintaining a habitable planet.

1.4 Preservation of organic carbon

As previously discussed, a small but crucial portion of OC is unable to be transformed to IC either by chemical or microbial environmental processes. Many mechanisms describing this phenomenon have been postulated and can largely be grouped in to three categories:

- That preservation is a function of an increasingly recalcitrant OC pool predominantly determined by inherent biochemical properties of the OM (e.g. aromaticity) (Quigley et al., 2019). Refractory OC is therefore typically more structurally complex and resistant to degradation (Hedges and Oades, 1997; Sollins et al., 1996), requiring more complex enzyme processes at higher activation energies in order to be broken down (Romero-Olivares et al., 2017).

- That OC is physically protected from microbial degradation by inorganic complexes, typically through occlusion within or sorption to a mineral matrix (e.g. Hedges, J.I. and Keil, R.G., 1995; Burdige, 2007; Torn et al., 1997; Hemingway et al., 2019). Mineral preserved OC has been observed to be co-localised with iron both in soils (Wagai and Mayer, 2007; Kleber et al., 2015; Zhao et al., 2016; Mu et al., 2016) and in marine sediments (Barber et al., 2017; Lalonde et al., 2012; Salvadó et al., 2015; Peter and Sobek, 2018; Ma et al., 2018; Wang et al., 2019; Dicen et al., 2018), with the interaction easily replicated experimentally (Tipping, 1981; Eusterhues et al., 2008; Eusterhues et al., 2011; Gu et al., 1995; Gu et al., 1994; Henneberry et al., 2012; Chen et al., 2014; Yang et al., 2017; ThomasArrigo et al., 2018).

- That the physical, biological and geochemical environment surrounding OM plays a significant role in determining reducibility (Burdige, 2007; Arndt et al., 2013; LaRowe et al.,

2020; Middelburg, 2019a and references therein). This perspective is better established in terrestrial applications (Wu et al., 2017; Schmidt et al., 2011; Lehmann and Kleber, 2015) but is recently becoming increasingly applied to marine sediments, not least in review by LaRowe et al. (2020).

1.4.1 Intrinsic recalcitrance

The term 'recalcitrance' is poorly defined and applied in a range of differing contexts. Interpretations of recalcitrance have been summarised by Kleber (2010). Environmentally, recalcitrance can be assumed to refer to either an inherent structural property of OC (Baldock and Skjemstad, 2000; Alexander, 1981; Bosatta and Ågren, 1999; Sollins et al., 1996; Hedges and Oades, 1997), those molecules with a long residence time (Davidson and Janssens, 2006; Marschner et al., 2008) with further definitions given based on responses to chemical treatment in an experimental context (See table 1 in Kleber, 2010). LaRowe et al. (2020) suggest moving away from the categorical terms 'labile' and 'recalcitrant' and replacing them with 'reactivity'. While reactivity may more accurately describe a sliding scale of structural stability it could be argued that reactivity in itself is still open to (mis)interpretation; for example, chemical reactivity may differ from biological reactivity and is dependent on the chemical reagents a compound is exposed to (i.e. operationally defined).

Traditionally it has been difficult to examine the structure of preserved OC due to degradation processes and interference of organic solvents in OC extraction from sediments and soils (Mylotte et al., 2016; Hayes, 2006). This has resulted in the components of the OC pool being largely uncharacterised with little evidence for the presence of organic structures which would prevent microbial degradation (Hansell, 2013; Arrieta et al., 2015). More recently, new applications such as comprehensive multiphase nuclear magnetic resonance spectroscopy (NMR) have been applied, with the benefit of not requiring OC extraction. This has shown the dominance

of methylene moieties in preserved OC (representing protein fractions), with the contribution of lignin to total OC also increasing with depth (Mylotte et al., 2016).

Generally, an OC pool is considered to become decreasingly reactive (or increasingly recalcitrant) with time, as the more reactive compounds are progressively degraded. Thus, the refractory DOC (rDOC) pool is characterised by complex structures (Quigley et al., 2019). This simplistic approach, however, ignores the dynamic nature of organic compounds and instead presents a one-way view where large compounds are degraded to leave behind only the small refractory components. Conversely, preservation of carbon has been related to the existence of large organic macromolecular structures (Lalonde et al., 2012). These have been referred to as products of geopolymerisation formed through oxidative polymerisation and sulphidisation reactions (Arndt et al., 2013 and references therein), resulting in the production of large 'bleb' like structures which are difficult to degrade (Lalonde et al., 2012).

Modelling by Mentges et al. (2019) has concluded that while OC molecules can be structurally recalcitrant, their presence is not required to explain the persistence of the aged ocean DOC pool. Instead, that apparent recalcitrance of OC is hypothesised to occur because the growth of the microbial community becomes equal to mortality and the production of DOC balances its degradation. Under these conditions, microbial growth becomes limited by low concentrations of OC existing in a steady state equilibrium, i.e. degradation is limited by the favourability of energy intensive processes and not by physical inability to degrade complex OC structures.

1.4.2 Dilution hypothesis and microbial processes

While the recalcitrant OC theory has been deployed to explain persistence of OC at greater burial depth, we have seen that recalcitrance is not a required parameter for models explaining OC preservation

(Mentges et al., 2019). Similar to the microbial equilibrium theory suggested by Mentges et al. (2019), the dilution hypothesis suggests that the OC compounds present in deeper sediment are structurally labile but

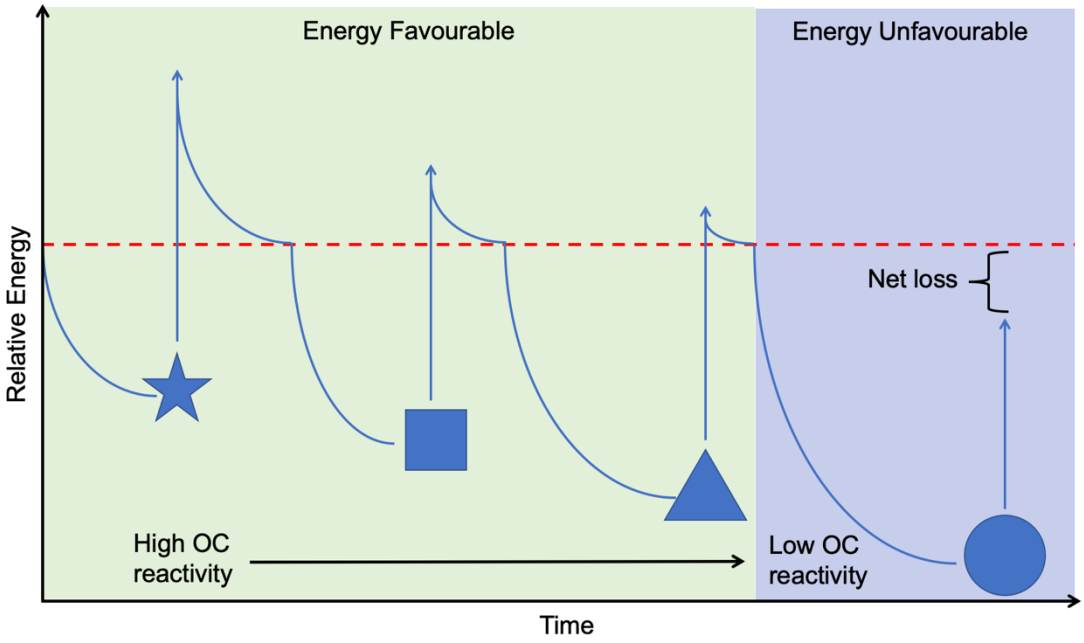

low concentrations prevent degradation. Microbes are central to this theory as they have to make a biological 'choice' about the amount of energy they are willing to investment vs the energy reward from consumption; they will therefore only degrade OC if this will result in a net energy gain (Jannasch, 1994; Jiao et al., 2014) *(Figure 1.5)*. Where a compound is not degraded, it can be considered to be preserved.

Figure 1.5 Schematic demonstrating the energy favourability of the dilution hypothesis. As compounds become less reactive (and less complex), they require more energy to be degraded and release less energy to the degrading organism. The red line indicates a zero-energy state.

The dilution hypothesis has been widely debated after it was originally thought to have been disproved by Barber (1968) in microbial incubation experiments where the concentration of deep water DOC was found to remain constant across a time series. This method was revisited by Arrieta et al. (2015) using comparatively new technology, Fourier-transform ion cyclotron resonance mass spectroscopy (FT-ICR-MS), to characterise

utilisation of OC compounds in microbial incubations on the molecular level. This later study found that consumption of OC in both unamended (i.e. environmental conditions) and concentrated (5x environmental) DOC pools does occur, indicating significant microbial consumption of labile compounds.

In addition to providing a mechanism for carbon preservation (through lack of degradation), the dilution hypothesis also provides an insight in to the microbial carbon pump (Jiao et al., 2010), and therefore the "end state" OC structure. Microbial degradation of labile compounds to their lowest utilisable concentration produces an end state DOC pool characterised by thousands of structurally differing OC compounds of varying ages (Arrieta et al., 2015). This vast and diverse 'community' of carbon structures is at stark contrast to the suggestion of a restricted pool of structurally recalcitrant compounds. The inherent diversity of sediment DOC (e.g. inclusion of functional groups) also facilitates interactions with other inorganic components of sediments (such as minerals) (Zhao et al., 2016), thus facilitating an additional level of OC preservation.

1.4.3 Mineral protection hypothesis

OC can be physically located inside (occluded) or on the surface (adsorbed) of clay based minerals and reactive metal (hydr)oxides (Singh et al., 2018; Feng et al., 2005; Hedges, J.I. and Keil, R.G., 1995; Mayer, 1994; Keil et al., 1994), reducing accessibility for microbes to degrade OC. Compared to phyllosilicates (incl. clay minerals), reactive Fe and Al minerals have been found to have a greater absorption capacity for DOC (Tombácz et al., 2004). Fe (oxyhydr)oxides, herein referred to as Fe_R (reactive Fe) phases, in particular have a significant role in OC stabilisation and preservation (Kaiser and Guggenberger, 2000; Wagai and Mayer, 2007; Lalonde et al., 2012; Mu et al., 2016; Jones and Edwards, 1998). The co-occurrence and subsequent sorption or occlusion of OC to or within Fe_R has been estimated to account for 21.5 % ± 8.6 of OC preserved in marine sediments globally (Lalonde et al., 2012), representing

the largest quantified mechanism of OC stabilisation. The physical protection offered to OC by adsorption to or coprecipitation within Fe_R phases allows bound OC to persist in sediment for millennia relative to unbound OC, as shown by radiocarbon dating (Hemingway et al., 2019).

Adsorption and coprecipitation of Fe and OM represent the most common OC-Fe interactions under environmental conditions (Han et al., 2019). Coprecipitation occurs naturally in marine sediments where reduced, Fe containing water meets oxidised water, resulting in the transition of soluble Fe (II) to insoluble Fe (III). Subsequently, Fe (III) sorbs on to ions, metals and OM to form a mineral coprecipitate with adsorption and occlusion of organic molecules in the interstices between the crystals of newly formed minerals, often ferrihydrite (Fh) (Eusterhues et al., 2014b; Cooper et al., 2017) This process creates chemical differences within Fe_R phases, dependent upon the availability of environmental "contaminants" competing for sorption/coprecipitation spots during precipitation of the phase.

Bonding between OC and Fe has been shown to be facilitated by carboxyl and hydroxyl groups within the OC structure (Karlsson and Persson, 2010, 2012; Mikutta, 2011). Additionally, Fourier-transform infrared spectroscopy (FTIR) has been used to identify the molecular components involved in bonding between ferrihydrite (Fh) experimentally precipitated with DOM and shows a prevalent at 1,400 cm^{-1}, indicating the presence of bonding carboxyl groups (Yang et al., 2012). Carboxyl groups (COOH) are readily available in DOM due to degradation (hydrolysis) and conjugation of carboxyl containing amino acids. Subsequently, DOM can coprecipitate within or adsorb to an iron mineral surface by ligand exchange *(Figure 1.6)* (Fuller et al., 1993; Gu et al., 1994; Henneberry et al., 2012; Eusterhues et al., 2014a).

While no single hypothesis discussed can be considered to fully describe the processes influencing OC persistence in isolation, they each contain their own merits and flaws in biological, chemical and physical terms. It

will be necessary to consider the interactions between these different mechanisms, for example microbial degradation of mineral protected OC, in order to advance our understanding of how organic compounds become selectively preserved under environmental conditions.

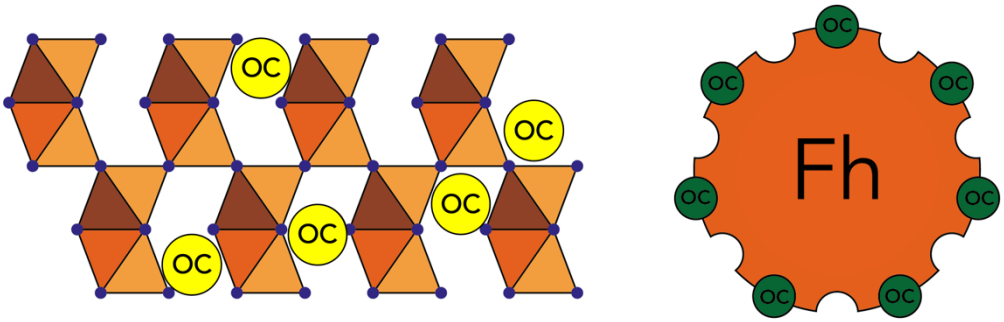

Figure 1.6 Schematic of mechanisms for OC-Fe interactions. Coprecipitation of an OC containing compound within an Fe mineral matrix is shown (left) and adsorption of OC to a ferrihydrite (Fh) is shown (right).

1.4.4 Extraction of iron bound organic carbon

While various techniques have been applied to determine the amount of OC bound to Fe_R, a common wet chemical approach is the application of a chemical extraction technique known as citrate-dithionite-bicarbonate (CDB). The name is given from the reagents involved in the extraction: Dithionite for reductive dissolution of easily reducible Fe_R (see Poulton and Canfield, 2005). Trisodium citrate is added as a surfactant to prevent aggregation of the charged ferrihydrite nanoparticles forming after the dissolution of primary Fe_R phases by reducing the strength of dipolar interactions (Soares et al., 2014). Sorption of citrate to ferrihydrite was not a concern due to the deprotonation of carboxyl groups (found in citric acid) to carboxylate groups, additionally sorption of citrate has been shown to make an insignificant contribution to C retention, see pg 68 for further information. Bicarbonate buffers the extraction solution at a circumneutral pH to prevent hydrolysis and re-adsorption of protonated OC in the co-precipitate (Mehra, 1958; Poulton and Canfield, 2005; Lalonde et al., 2012). The use of a circumneutral (7)

pH sets the OC-Fe extraction apart from alternative methods that would be typically used for easily reducible Fe_R phases (pH 4.8).

All dithionite-based extractions of Fe_R phases, including ferrihydrite, are performed on the principles of operational definition, whereby pools of Fe are separated by their ability to be reduced by methods of increasing "strength". This presumes that the ability of a phase to be reduced is consistent across that phase, i.e. that any two ferrihydrites regardless of formation conditions or coprecipitates will be equally (and fully) reduced by the same dithionite treatment. OM is known to interfere with ferrihydrite reactivity due to having both an increasing and decreasing effect on crystallinity of ferrihydrite dependent on whether precipitation occurs under oxic or anoxic conditions (Henneberry et al., 2012 and references within).

It has further been suggested that the surface reactivity of ferrihydrite can be affected by the adsorption of organic anions during precipitation (Fuller et al., 1993), which may have a subsequent effect on the reactivity of ferrihydrite towards reduction by dithionite. Structural disorder has also been identified as heightened in coprecipitated Fe phases compared to synthetic or OC free ferrihydrite (Eusterhues et al., 2008; Cismasu et al., 2011; Mikutta et al., 2008; Mikutta, 2011). Differences in structure, surface reactivity and crystallinity are all likely to affect the ability of dithionite to reduce Fe_R phases, currently presumed to exist in the same operationally defined 'pool' of Fe.

This inherent variability in mineral stability suggests a heterogenous set of mineral phases exist in soil and sediment samples, while chemical extractions can by their nature only discriminate by reactivity to a certain treatment. Therefore, there has been much caution placed on deriving mineral identity from chemical leachate, particularly as chemical extractions are often not additionally characterised for specific mineral identity (e.g. by XRD or TEM), largely due to purity constraints (Hepburn

et al., 2020 and references therein). This suggested caution in presuming the identity of mineral groupings has been recently validated empirically. In their study, Mössbauer spectroscopy is applied to determine the identity of synthetic Fe minerals extracted sequentially following Poulton and Canfield (2005). Thus study concludes that both incomplete and premature dissolution of the target phases can occur in different extraction steps (Hepburn et al., 2020). While Fe associated with organic compounds was not investigated, the incomplete and premature extraction of Fe phases could have a significant impact on our understanding of the abundance of OC-Fe. For example, does the CDB reduction extract less stable versions of phases which are unreactive for OC, thereby overestimating the OC-Fe pool (Barber et al., 2017), or may OC-Fe binding confer a stability preventing its full reduction? It should also be highlighted that the outcome of the chemical extraction depends on a variety of practical parameters, including sample grain sizes, sample storage, extraction temperature, even the freshness of chemical reagents, and utmost care must be taken to produce comparable and reproducible results.

The cross validation approach employed by Hepburn et al. (2020) highlights a lack of understanding regarding what sequential extractions do and do not extract. Further thought needs to be given to how environmental factors affecting deposition and sequestration may also shift Fe mineral phases from their intended chemical extraction pool. Understanding the molecular role OC plays in mineral stability will be key to this and may subsequently allow for the development of either a more specific method or at least a better understanding of the limitations of the current CDB method.

1.5 Degradation of organic carbon

OM preserved below the seafloor will eventually be liberated through microbial degradative processes, resulting in transformation to IC. Compared to terrestrial OC turnover (decadal) (Field et al., 1998), marine

OC turnover in the water column is very quick with phytoplankton turning over in one week (Middelburg, 2019b) and marine macrophytes in one year (Smith, 1981). Benthic communities are involved in the processing of sediment OC in several different ways. The physical interaction of macrobenthos (>0.5mm) with OM in the sediment results in mixing, or bioturbation, of particles. This movement is the main mode for transport of reactive compounds in sediment and affects the distribution of both OC and reactive metal oxides (Meysman et al., 2010; Aller, R.C. and Aller, J.Y., 1998; Berg et al., 2001), potentially across electron acceptor transition zones *(Figure 1.7)*.

Redox conditions of the ocean play an important role in determining OC fate, as can be seen in the palaeo record via enhanced OC preservation in black shales deposited during Oceanic Anoxic Events (OAEs) (Tessin et al., 2015; Kolonic et al., 2005). However, the direct influence of oxygen exposure on OC preservation is somewhat controversial; for example, Cowie, G. L. and Hedges, J. I. (1992) find indistinguishable undegraded OM fractions in OM-rich costal sediments deposited under anoxic and oxic conditions. It has instead been proposed that processes linked to oxygen limitation such as lack of bioturbation, reduced efficacy of O_2 dependent extracellular enzymes, and transformation of OM due to sulphurisation may limit the bioavailability of OM (Burdige, 2007; Raven et al., 2018 and references therein). In particular, abiotic reactions with sulphur can prevent OC reduction by removing functional groups required for enzyme binding in microbial degradation (Kohnen et al., 1990). Oxygen depletion results in sulphate reducing microbes producing reduced sulphur species (inc. hydrogen sulphide), enhancing sediment sulphur content and facilitating sulphurization (Raven et al., 2018). This coupling of sulphurization to anoxia may be an additional factor, beyond O_2 electron acceptor availability itself, explaining increased OM deposition in O_2 limited environments.

Microbial heterotrophs inhabiting sedimentary environments rely on OC consumption for growth and reproduction (Middelburg, 2019a) and are numerate in comparison to fauna (Snelgrove et al., 2018); as such they account for the majority of biological OC degradation in deep sediments. In oxic environments, oxygen serves as the main electron acceptor for OC metabolism, particularly for those sediments with low OC content (e.g. deep sea, low sedimentation rate) (Glud, 2008). Beyond the oxygen penetration depth, or for sediments with an anoxic bottom water interface, OC oxidation becomes dependent on a cascade of electron acceptors which have a decreasing energy yield *(Figure 1.7)*.

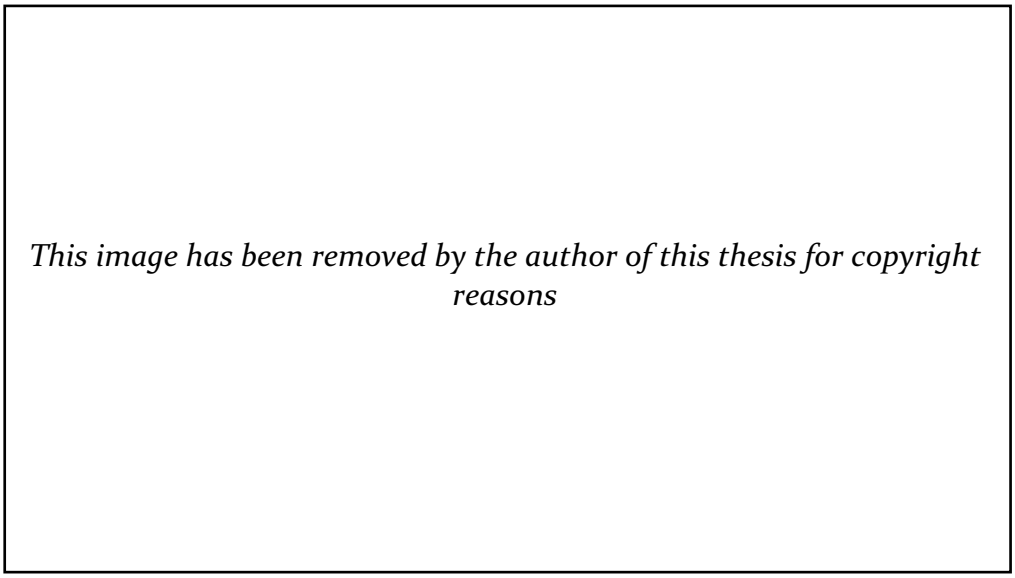

Figure 1.7 One dimensional profile of oxidants and their associated (an)oxic conditions (left). Relative concentration of electron acceptors involved in mineralisation of OM with depth (right). (Lindqvist, 2014)

OC oxidation by these species is determined by their concentration, which in turn is dependent on environmental factors and decreases with depth. Those electron acceptors higher in the cascade (NO_3^-, Mn^{4+}, Fe^{3+}) facilitate OC oxidation for environments where they exist at a high enough concentration or are rapidly recycled (Canfield et al., 1993; Sørensen and Jeørgensen, 1987). For example, the Ulleung Basin is characterised by high Mn and Fe oxide concentrations (> 200 μmol cm^{-3}, 100 μmol cm^{-3}) resulting in 45% total OC oxidation by Mn and 20% by Fe (Hyun et al., 2017). The contribution of OC oxidation by nitrate appears to be more

variable as its presence in marine sediments is influenced by proximity to riverine inputs and high OM input (Link et al., 2013 and references therein). Additionally, nitrate fluxes are highly coupled to oxygen, with oxidation by nitrate highest under oxygen limited conditions (Link et al., 2013 and references therein), as expected from the electron acceptor diagram.

Some of the most ubiquitous degradative processes rely on sulphate as electron acceptor or on OM fermentation to methane. These processes readily occur in marine sediments as their prevalence is less dependent on environmental inputs. OM degradation by sulphate reduction can account for 12-29% of global OC oxidation (Bowles et al., 2014), further enriched as high as 50% where the OC flux is high and there is sufficient sulphate available in pore waters (Hyun et al., 2017 and references therein). The final stage of anaerobic OC degradation produces methane by fermentation, which is typically a very inefficient processes with a low energy yield (Schlesinger and Bernhardt, 2013). Despite this, methanogenesis can be a dominant process in some anoxic ecosystems, such as wetlands and lakes, which are limited in other electron acceptors (Schlesinger and Bernhardt, 2013; Bastviken, 2009)

Evidence suggests that species dependent availability of electron acceptors influences the ability to degrade rDOC, particularly for oxygen which is thought to provide essential O_2 containing radicals interacting with specialised aerobic enzymes to facilitate the breakdown of complex OC molecules (Reimers et al., 2013 and references therein). As OC oxidation processes are facilitated by living microbes, there are additional physical controls on the enzyme implicated in degradative processes. For example, the rate of methanogenesis has been shown to double with a 10 ^{O}C increase in temperature (Segers, 1998). Additionally, the activity of more energy intense enzyme pathways required for the degradation of rDOC is expected to increase twice as fast as those enzymes degrading labile DOC under 2 ^{O}C warming (21% vs 10% increase) which has the potential to act

as a positive feedback on temperature (Davidson and Janssens, 2006). For deep sediment or anoxic environments, it has also been shown that subsequent electron acceptors (Mn and Fe) are involved in catalysing geo-polymerisation processes which have an inverse effect on OC degradation by increasing OC preservation (Moore et al., *in prep)*. Thus, we see a vast and complex set of abiotic and biotic parameters which determine the fate of buried OC, including the locality, depth and sedimentary chemistry surrounding buried OC. Understanding how these factors differentially affect and interact with OC moieties, particularly functional groups, will be crucial to uncovering the physiochemical mechanisms behind mineral based preservation of OC.

1.6 Iron phase mineralogy

Metals play a crucial role in the sedimentary cycling of OC, primarily through the use of metal ions as electron acceptors in OC oxidation. Iron is of particular importance for the additional role of Fe_R phases in physical OM preservation due to its higher sorption capacity compared to other minerals (Kaiser and Guggenberger, 2003). It is important to first recognise that the total Fe pool is comprised of differing phases, each of these phase 'pools' are differently reactive and are operationally defined by their chemical extractability, see Poulton and Canfield (2005). These are summarised below:

Table 1.1 Chemical treatments for the sequential extraction of Fe phases per Poulton & Canfield 2005.

Nomenclature	Phase(s)	Extraction method
$\mathbf{Fe_{carb}}$	Iron carbonates (siderite, ankerite)	Na Acetate, pH 4.5, 24 h
$\mathbf{Fe_{ox1}}$	Easily reducible oxides (ferrihydrite, lepidocrocite)	Hydroxylamine–HCl, 48 h
$\mathbf{Fe_{ox2}}$	Reducible oxides (goethite, hematitie, akagnéite)	Dithionite, 2 h
$\mathbf{Fe_{mag}}$	Magnetite	Oxalate, 6 h

$\mathbf{Fe_{PRS}}$	Poorly reactive sheet silicate	Boiling 12 N HCL
$\mathbf{Fe_{py}}$	Pyrite	Chromous chloride
$\mathbf{Fe_{U}}$	Unreactive silicate	Total Fe- above stages.

The multi-phase aspect of Fe minerals means only certain phases are of interest in terms of cycling with OC. Total Fe remains environmentally important, for example as a nutrient input for primary productivity; however, less reactive, more crystalline Fe phases cannot associate with or preserve OC. Of particular interest are the reactive Fe phases, defined as those which are reducible by dithionite (i.e. (oxyhyd)oxides); these phases are characterised by high surface area and correlate with increased OC concentrations (Keil and Mayer, 2014).

Fe_R phases are ubiquitous minerals across most environments, with a particular prevalence under oxic redox conditions where Fe readily precipitates (Gorski et al., 2016). Fe_R phases have been widely described in marine and freshwater sediments, soils, acid mine waste drains and springs (Postma, 1993; Sorensen, 1982; Lindsay and Schwab, 2008; Kim and Kim, 2003; Carlson and Schwertmann, 1981). The composition Fe_R phases is dependent upon both Fe speciation and the presence of environmental contaminants, such as metals, and OM (von der Heyden and Roychoudhury, 2015; Henneberry et al., 2012; Fuller et al., 1993).

Iron has been shown to protect OC in soils (Kaiser and Guggenberger, 2000; Mu et al., 2016) due to its high sorption capacity, as demonstrated by adsorption to humic substances (Tipping, 1981). Further, the presence of iron containing compounds can inhibit microbial degradation of organic compounds (Jones and Edwards, 1998), with the least soluble Fe_R phases (goethite, hematite) being the most resistant to microbial degradation (Bonneville et al., 2004).

Ferrihydrite is typically the youngest Fe_R phases, acting as a pre-cursor for subsequent Fe_R phases in soils and sediments, and decreases in concentration with sediment depth/age (Jiang et al., 2018; Konhauser et

al., 2017). It is also the phase most susceptible to microbial degradation, and therefore liberation of OC, due to its relatively high solubility compared to other Fe_R phases (Bonneville et al., 2004). In addition to the significant role of ferrihydrite in preserving OM, the ability to easily synthesise the mineral and coprecipitates (Schwertmann and Cornell, 2000) makes ferrihydrite a good subject for experimental investigation of OC-Fe interactions. X-ray absorption spectroscopy (XAS) has shown close similarity between natural sediments and synthetic coprecipitates at the alkene, carboxyl and alcohol peaks (Barber et al., 2017), demonstrating that synthetic coprecipitates suitably replicate the organochemistry of naturally occurring marine sediment coprecipitates.

1.6.1 Extraction of iron bound organic carbon

While various techniques have been applied to determine the amount of OC bound to Fe_R, a common wet chemical approach is the application of a chemical extraction technique known as citrate-dithionite-bicarbonate (CDB). The name is given from the reagents involved in the extraction: Dithionite for reductive dissolution of easily reducible Fe_R (see Poulton and Canfield, 2005).

All dithionite-based extractions of Fe_R phases, including ferrihydrite, are performed on the principles of operational definition, whereby pools of Fe are separated by their ability to be reduced by methods of increasing "strength". This presumes that the ability of a phase to be reduced is consistent across that phase, i.e. that any two ferrihydrites regardless of formation conditions or coprecipitates will be equally (and fully) reduced by the same dithionite treatment. OM is known to interfere with ferrihydrite reactivity due to having both an increasing and decreasing effect on crystallinity of ferrihydrite dependent on whether precipitation occurs under oxic or anoxic conditions (Henneberry et al., 2012 and references within).

It has further been suggested that the surface reactivity of ferrihydrite can be affected by the adsorption of organic anions during precipitation (Fuller et al., 1993), which may have a subsequent effect on the reactivity of ferrihydrite towards reduction by dithionite. Structural disorder has also been identified as heightened in coprecipitated Fe phases compared to synthetic or OC free ferrihydrite (Eusterhues et al., 2008; Cismasu et al., 2011; Mikutta et al., 2008; Mikutta, 2011). Differences in structure, surface reactivity and crystallinity are all likely to affect the ability of dithionite to reduce Fe_R phases, currently presumed to exist in the same operationally defined 'pool' of Fe.

This inherent variability in mineral stability suggests a heterogenous set of mineral phases exist in soil and sediment samples, while chemical extractions can by their nature only discriminate by reactivity to a certain treatment. Therefore, there has been much caution placed on deriving mineral identity from chemical leachate, particularly as chemical extractions are often not additionally characterised for specific mineral identity (e.g. by XRD or TEM), largely due to purity constraints (Hepburn et al., 2020 and references therein). This suggested caution in presuming the identity of mineral groupings has been recently validated empirically. In their study, Mössbauer spectroscopy is applied to determine the identity of synthetic Fe minerals extracted sequentially following Poulton and Canfield (2005). Thus study concludes that both incomplete and premature dissolution of the target phases can occur in different extraction steps (Hepburn et al., 2020). While Fe associated with organic compounds was not investigated, the incomplete and premature extraction of Fe phases could have a significant impact on our understanding of the abundance of OC-Fe. For example, does the CDB reduction extract less stable versions of phases which are unreactive for OC, thereby overestimating the OC-Fe pool (Barber et al., 2017), or may OC-Fe binding confer a stability preventing its full reduction? It should also be highlighted that the outcome of the chemical extraction depends

on a variety of practical parameters, including sample grain sizes, sample storage, extraction temperature, even the freshness of chemical reagents, and utmost care must be taken to produce comparable and reproducible results.

The cross validation approach employed by Hepburn et al. (2020) highlights a lack of understanding regarding what sequential extractions do and do not extract. Further thought needs to be given to how environmental factors affecting deposition and sequestration may also shift Fe mineral phases from their intended chemical extraction pool. Understanding the molecular role OC plays in mineral stability will be key to this and may subsequently allow for the development of either a more specific method or at least a better understanding of the limitations of the current CDB method.

1.7 Motivation and research context

From the literature we can see the importance of OC-Fe stabilisation for preservation of OC on geological timescales, and therefore for climate by acting as a 'rusty' carbon sink and hence a potential sink of the greenhouse gas CO2. Multiple mechanisms facilitating this interaction have been demonstrated either environmentally, through analysis of recovered sediment, or experimentally by coprecipitating OM with Fe_R phases. The physical protection of OC by Fe_R phases remains the most significant described mechanism for OC preservation.

While the carbon-iron hypothesis is well described, there is little insight into the behaviour and characteristics of the molecular level interaction. We know that OC-Fe binding is chemically facilitated by mineral hydroxyl and carbon carboxyl groups, however, the nature of this binding is unknown. For example, does the binding behave in an on/off fashion with two energy states, or does the chemical composition of OC affect the bond strength and therefore the preservative effect on OC?

Understanding this mechanism is important as any OC pool represents a vast heterogeneous pool of thousands of structurally differing organic compounds. The source of OC as well as the degradative processes which an individual compound has been exposed to will alter both its structure and subsequent reactivity (Middelburg, 1989). In addition, it is known that some OC is freshly photosynthesised at the sediment interface for shallow waters producing non degraded compounds (Middelburg, 2019a). It will be of particular importance to determine how the molecular structure of OC affects preservation for efforts to increase OC sequestration, e.g. blue carbon. For example, it may allow us to manipulate water column degradation processes to produce an end state OC structure which is more favourable to preservation. By investigating this interaction, we will also better understand the apparent barrier which prevents more than ~20-30% OC being preserved by Fe, an average value never exceeded by CDB extractions of OC-Fe in the literature. Ultimately, increasing the resolution at which we understand mechanistic interactions of OC will provide a new perspective on how OC is stored and how planetary homeostasis is maintained, with potential implications for our understanding of global biogeochemical cycles and the models which describe these.

1.8 Experimental aims

This study will begin by taking inspiration from the work of Eusterhues et al. (2014a), whereby OC-Fe compounds have been successfully synthesised. We will differ from this approach by controlling the composition of OC coprecipitated with ferrihydrite (Fe source), as opposed to using a heterogenous pool of OM, to better understand the molecular level controls of the OC-Fe interaction. In doing so we will focus on the carboxyl functional group, as most OM is carboxyl rich and the carboxyl group has been shown to facilitate OC-Fe binding. Hence, we aim to:

1) Determine the effect of carboxyl groups on the stability of Fe_R organominerals.

2) Examine any physical effects of carboxyl content on Fe_R minerals (e.g., size, crystallinity).

3) Examine the implications of carboxyl driven mineral binding mechanisms on the preservative strength of Fe for OC in marine sediments.

While these initial investigations are experimental it will be important to calibrate the behaviour of experimental coprecipitates against naturally sourced sediment to understand if results of laboratory-based experiments are translational to and have implications in an environmental context. This will also allow us to investigate the OC-Fe extraction method (CDB) used for sediment samples which has been poorly defined and suffers from misinterpretation. This will allow us to:

4) Understand how sample preparation techniques may affect the extractability of OC-Fe phases.
5) Quantify the efficiency of OC-Fe (CDB) extraction, allowing us to interpret whether current estimates of the global OC-Fe pool are accurate.

6) Test the experimental parameters of the CDB extraction to see if efficiency can be improved.

By achieving these later aims we will not only probe a potentially important molecular binding mechanism, but we will also provide the first critical assessment of an extraction technique which is routinely used to characterise OC-Fe in sediment cores. Improving this technique or producing an assessment of what the method does (and does not) achieve could provide a best approach which could both increase the quality of sediment extraction data and also crucially will allow the results of a common method to be comparable. At the moment, different investigators are known to apply the CDB method in different ways which makes it difficult to accurately compare sediment samples extracted from different sites. Providing a 'best method' to the sediment community could allow future sediment analyses to be much more comparative, which would be of great use in global process modelling and for refining approximations of the global sediment OC-Fe pool.

Chapter 2- Methodology

2.1 Ferrihydrite coprecipitate synthesis

Following a modified method of Schwertmann and Cornell (2000), 2-line ferrihydrite was precipitated in the presence of either i) pentanoic acid; ii) hexanedioic acid or iii) 1,2,4-butanetricarboxylic acid, which increase in their number of carboxyl groups from 1 to 3 respectively. The increase in the number of C molecules also assists in building a range close to the wt% C content of environmental sediments. A pure ferrihydrite sample containing no carbon was also precipitated, as a control.

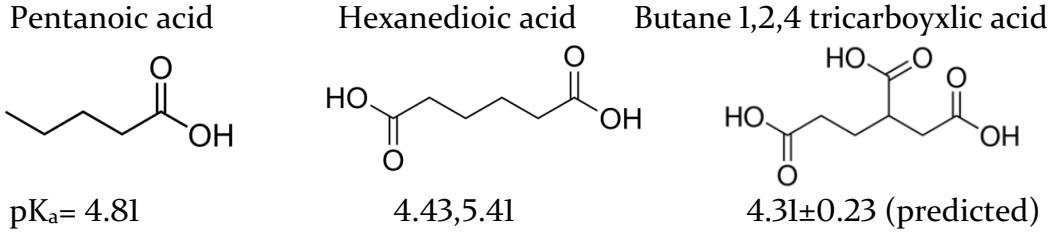

Figure 2.1 Chemical structure and pK_a values for selected organic acids.

Saturation concentrations for the three organic acids was determined by increasing organic acid concentration in the mineral coprecipitation stage and measuring end state wt% C (see *Table 2.1*). Saturation concentration refers to the point at which further increases in organic acid addition does not result in a further wt% C increase in the resultant mineral coprecipitate. Coprecipitation of ferrihydrite with the named organic acids was performed by dissolving organic acids in deionised water (DI) with Iron (Fe) (III) nitrate nonahydrate [$Fe(NO_3)_3.9H_2O$]. 1 M potassium hydroxide (KOH) was then added by titration to achieve a pH of 7.0 ± 0.3.

Following coprecipitation, the organomineral composites were rinsed in 5L of DI water and left to gravitationally settle out. This rinse step was repeated 5 times. The pentanoic acid (1 COOH) coprecipitate was only rinsed three times due to decreased settling and therefore a lower yield associated with the smaller 1 COOH particles. The resultant slurry was raised to pH 7 through dropwise addition of 0.1 M NaOH then centrifuged (2750 RCF, 20 minutes) with the precipitate being retained and the supernatant discarded.

Following this, half of the precipitate was frozen and subsequently freeze dried; whilst the other half was stored at 4°C. X-ray diffraction (XRD) was used to confirm the Fe mineralogy of the co-precipitate was 2-line ferrihydrite (Fig 1.6).

Table 2.1. Summary of organic acids used to form ferrihydrite co-precipitates.

IUPAC Name	COOH Groups	Stoichiometry	Organic Added[a]
Pentanoic acid	1	$C_5H_{10}O_2$	5 ml
Hexanedioic acid	2	$C_6H_{10}O_4$	3 g
1,2,4-Butanetricarboxylic acid	3	$C_7H_{10}O_6$	3 g

[a] values of organic acid addition at their saturation concentration are relative to 20 g of $Fe(NO_3)_3.9H_2O$, as per Schwertmann and Cornell (2000)

2.2 Field Site

Marine sediment was retrieved from the Barents Sea using a multicore sampler (Location Lat.: 75° 11.012 N, Long.: 17° 32.204 E; Water Depth 141 m; sediment core depth, 33.5 cm; station B6, E40; Cruise JR16006).

2.3 Sediment Spiking

To replicate OC-Fe conditions of natural sediments and create a concentration gradient for OC-Fe content relative to the total sediment weight, ferrihydrite composites were spiked into Arctic marine sediment. The sediment had been previously freeze-dried and was prepared by grinding to a powder using a pestle and mortar, followed by ashing (650°C, 12 hours) to oxidatively remove all OC. IC was later removed by fumigation with HCL vapour to form an inert, carbon free sediment sample. Spiked samples were prepared by agitation of carbon free sediment with ferrihydrite coprecipitates across a concentration gradient *(Table 2)*.

Table 2.2- Concentration matrix for spiked sediments.

%Fh-OC: Sediment	0	10	20	30	40	50	60	80	100
Fh-OC (mg)	0	25	50	75	100	125	150	200	250
Sediment (mg)	250	225	50	150	150	125	100	50	0

Values shown are contextualised for a total experimental sample mass of 250 mg, as per Lalonde et al. (2012).

2.4 Standard OC-Fe extraction approach.

Extraction of dithionite reducible Fe and associated OC was conducted according to the method by Lalonde et al. (2012). Briefly, 0.25 g of bulk spiked aliquots were weighed into centrifuge tubes with both total sediment and centrifuge tube mass recorded. 13 ml of 0.11 M sodium bicarbonate ($NaHCO_3$) and 0.27 M trisodium citrate ($Na_3C_6H_5O_7$) was added and heated to 80°C in a water bath. Sodium dithionite (0.25 g) was then dissolved in 2 ml of 0.11 M $NaHCO_3$ and 0.27 M $Na_3C_6H_5O_7$ and added, the mixture was vortexed and then heated again (80 °C, 15 minutes).

In parallel, a control extraction was conducted replacing sodium dithionite with sodium chloride at an equivalent ionic strength; 13 ml of 1.6 M NaCl and 0.11 M $NaHCO_3$, followed by 0.22 g NaCl dissolved in 2 ml of the NaCl and $NaHCO_3$ solution. All samples were then centrifuged (3000 g, 10 minutes) and the supernatant retained. This was followed by three rinses of the precipitate in artificial seawater (3000 g, 10 minutes) with 15 ml of each of these three supernatants retained and combined with one another. To prevent precipitation of the Fe all supernatants were acidified to pH <2 with 12N HCL. Precipitates were oven dried (60°C, 12 hours) and then decarbonated with HCL in vapour phase to avoid potential bicarbonate contamination. The final sample mass was recorded prior to elemental analysis to correct for any mass lost in the extraction procedure.

Coprecipitates extracted for OC-Fe to investigate the effect of carboxyl content (i.e those results presented in *Chapter 3*) were conducted singularly owing to mass limitations of coprecipitate synthesis. However, repeats were conducted by proxy through the inclusion of a concentration gradient *(Table 2.2)* which facilitated the identification of any outliers against trends in extraction values across the included concentrations.

2.5 Elemental Analysis- Iron

Fe concentrations were determined by atomic absorption spectroscopy (Thermo Fisher iCE3300 AAS), calibrated using specific standards (0-10 ppm) with the background matrix optimised to the extraction/control

reagents and organic acid in the co-precipitate. Each sample was auto-analysed 3 times with the mean value recorded, a calibration QC against a 0 ppm and 5 ppm standard was run following every 10 samples with a full recalibration if the drift was excessive (>2% error). Concentration determined using the iCE SOLAAR software package (Thermo).

Total Fe content of the spiked sediments was determined by digesting ~2 mg of the spiked sediment mixes in 1 ml concentrated HCL (37%) followed by a 1 in 10 dilution with 1% HCL. These were then further diluted in Milli-Q (MQ) water as necessary to reach the correct concentration window (0-10 ppm) for analysis. Control supernatants were diluted 20-fold to prevent salt blockages and washed supernatants were undiluted except for where the Fe concentration was >10 ppm, whereby these were diluted by 10-fold.

2.6 Elemental analysis – Carbon

Initial carbon content of synthetic samples was measured using a LECO-SC144DR C&S analyser. It was calibrated using manufacturer's standards (0.924%C and 10.80%C soil) for a detection window of 0-10 wt% C at a mass of 0.25 g. Post extraction carbon was determined by LECO analysis for the majority of samples (concentrations ≤ 50%) or by a Vario PYRO cube (Elementar Analysis) where post extraction sample mass was limiting and below the limits required for LECO analysis. The Vario PYRO cube was calibrated using a sulphanilamide ($C_6H_8N_2O_2S$) standard, both instruments were corrected for drift by running a standard after every 10-15 samples. All carbon samples were analysed in a dried (oven or freeze dried) state following the removal of IC as described above.

2.7 Mass balance calculation

To account for the loss of mass once Fe and associated OC has been reduced in the extraction, the mass balance calculation from Salvadó et al. (2015) (Equation S1) was adapted. Here we calculate %OC loss by applying bulk %C to the pre extraction mass and post extraction %C to the final mass. This approach was similarly applied by Peter and Sobek (2018) where Fe loss in their samples resulted in >20% mass loss, therefore

requiring a mass balance correction. Comparison by change in raw %C is likely to overestimate the final %C if start and end carbon concentrations are calibrated to the initial mass, as when %C reduces so does the sample mass. The below calculation was devised to determine %OC-Fe loss.

Equation 1

$$\Delta C(\%)=\frac{\left(M^{PreI} x\ \%C^{Bulk}\right)-\left(M^{PI(R)} x\ \%I\right)}{M^{Pre\ (R)} x\ \%C^{Bulk}}-\frac{\left(M^{Pre(C)} x\ \%C^{Bulk}\right)-\left(M^{Post(C)} x\ \%C^{Post(C)}\right)}{M^{Pre\ (C)} x\ \%C^{Bulk}} \times 100$$

$M^{Pre/Post(R/C)}$ = Mass I/post (R) Iuction / (C) control.

$\%C^{Post(R/C)}$ = %C Post reduction/control experiment.

$\%C^{Bulk}$ = %C in the sediment pre extraction (same for control and reduction).

2.8 Particle sizing

Nanotracking analysis

Sizing of the coprecipitate particle– between 0.01 - 1 μm was attempted using a Malvern NanoSight NS300. Wet ferrihydrite was diluted until particle separation was sufficient for visualisation (25-fold) and the system was flushed with MQ water between samples. Sizing was determined using the Nanotracking analysis (NTA) software (Malvern).

Optical sizing

In supplement to NTA, sizing of particles within the range of 0.1-10000 μm was conducted using a Malvern Mastersizer 2000. Wet ferrihydrite coprecipitates were added dropwise to water in the suspension mixer until within the detection limit of the machine, as determined by the Malvern software. Detection of the particle scattering pattern was conducted in triplicate by the detector array in the optical bench and interpreted for output by the Malvern software.

2.9 Sample preparation methods

To investigate the effect of drying on Fe extractability some ferrihydrite coprecipitates were retained in a 'wet' (i.e. not dried) form. Samples were

retained in a diluted slurry and stored short term at 4°C to inhibit transformation to a more stable mineral phase. For spiking of the wet sediments, coprecipitate concentration (mg/ml) was determined by oven drying 10x1 ml aliquots at 60 °C until the liquid phase was fully removed. Initial and final mass of the weighing boats was measured to determine the mass of the dried solid, and a mean of the 10 values taken. This allowed to calculate the volume of ferrihydrite coprecipitate (ml) needed to achieve the mass according to the matrix in *Table 2.2***.** Following spiking, the sediment and wet ferrihydrite were spun together and then centrifuged (3000 RCF, 20 mins) to remove residual water, leaving a slurry. After Fe extraction the slurry was dried and analysed in the same way as dried samples.

2.10 Optimising the CDB method

For the majority of conditions, sodium dithionite was added to the extraction in aqueous form, 0.25 g dissolved in 2 ml of 0.11 M $NaHCO_3$ and 0.27 M $Na_3C_6H_5O_7$. In addition, samples in the investigation of solid vs aqueous dithionite addition received sodium dithionite as an individual 0.25 g solid per sample. For these samples, their pair control also received the 0.22 g NaCl addition as a solid to maintain comparability.

The amount of sodium dithionite added was adjusted to determine its saturation point for Fe extraction. In these cases, 0.25 g dithionite addition is replaced with 0.125 g, 0.250 g, 0.375 g, 0.500 g or 0.625 g dissolved in 2 ml/sample of 0.11 M $NaHCO_3$ and 0.27 M $Na_3C_6H_5O_7$.

One experiment considers how the length of the extraction may change Fe extractability. Samples were retained in the water bath for either 15, 30, 45 or 60 minutes. All experiments conducted in this section and reported in *Chapter 4* were conducted in duplicate.

2.11 Preparation of natural samples

To understand the implications of experiments conducted on synthetic ferrihydrite to the environment, extractions for Fe-OC phases were conducted on environmental samples in triplicate. Sediment was sourced from the Barents Sea, *(see 2.2)*. This sediment was treated by freeze drying as described for synthetic samples. In addition, a portion of the environmental sediment was retained as 'wet', here the sediment slurry was first diluted in MilliQ water to a consistency suitable for pipetting before concentration determination and extraction as in *2.4*.

2.12 X-ray diffraction analysis

Ferrihdyrite-organic composites were structurally characterised for crystallinity by powder x-ray diffraction (XRD). The pattern was collected over a 2-90° 2θ range in 0.01969° intervals with a steptime of 930 ms using a Bruker D8 diffractometer with Cu-Kα radiation (λ ≈ 0.154 nm).

Chapter 3- Experimental evaluation of the extractability of Fe-bound organic carbon as a function of carboxyl content

3.1 Introduction

Organic carbon (OC) is preserved in soils and marine sediments through occlusion within, or sorption to reactive iron (Fe) phases (Kaiser and Guggenberger, 2000; Wagai and Mayer, 2007; Lalonde et al., 2012; Mu et al., 2016) . The interaction between OC and Fe (OC-Fe) physically protects OC from microbial degradation (Jones and Edwards, 1998), allowing OC to be 'locked away' on geological timescales, representing a large carbon sink (Lalonde et al., 2012).

Bonding between OC and Fe has been shown to be facilitated by carboxyl and hydroxyl groups within the OC structure (Karlsson and Persson, 2010, 2012; Mikutta, 2011). Additionally, carboxyl group banding (1,400 cm^{-1}) is prevalent in the FTIR spectra of ferrihydrite (Fh) precipitated with DOM (Yang et al., 2012).Carboxyl groups (COOH) are readily available in dissolved organic matter (DOM) due to degradation (hydrolysis) and conjugation of carboxyl containing amino acids to form carboxyl rich alicyclic molecules (CRAM) (Hertkorn et al., 2006). Subsequently, DOM may either coprecipitate within or adsorb to an iron mineral surface by ligand exchange (Fuller et al., 1993; Gu et al., 1994; Henneberry et al., 2012; Eusterhues et al., 2014a).

Fe_R coprecipitates have been previously synthesised, however the DOM source is typically natural in origin e.g. forest floor extract (Eusterhues et al., 2011; Eusterhues et al., 2014a; Eusterhues et al., 2014b; Chen et al., 2014). Use of natural OM in synthetic coprecipitates aims to replicate OC-Fe complexes precipitated under environmental conditions, but in order to do so uses organic matter for which the structural carbon content is inherently hetereogenous. Whilst using naturally sourced OC more closely replicates environmental settings, its speciation and structure are largely unknown and therefore the fundamental mechanisms controlling OC-Fe interactions are difficult to elucidate. Here, we aimed to control the OC coprecipitated for its

structural content by precipitating ferrihydrite with similar organic acids differing only in carboxyl group richness.

We propose that structural variability in OC, particularly the bonding carboxyl groups, would have an effect on the OC-Fe complex stability, and therefore on the preservative effect of Fe for OC on geological timescales. This chapter aims to 1) quantify the OC-Fe pool for synthetic marine sediments which differ in carboxyl richness 2) determine if the stability of iron oxide organominerals to reductive dissolution is affected by carboxyl richness 3) examine any physical effects of carboxyl content on iron oxide minerals (size, crystallinity).

3.2 Results

3.2.1 OC content calibration of spiked sediments

Following spiking labile sediment with ferrihydrite-organic coprecipitates at known concentrations, elemental analysis for C was conducted for the resultant composite sediments. This was done to ensure synthetic sediments contained the expected concentration of OC-Fe and to facilitate like for like sediment elemental analysis following OC-Fe extraction. The C content is a key variable in the extractions we conduct, varying with both C source and the concentration of organic coprecipitate spiked into sediment. Reference to wt% C in subsequent figures is made in terms of wt% Fh-OC in sediment, i.e., the dilution of coprecipitate relative to labile sediment. This term has been calibrated with true wt% C to describe the sediment composition used in subsequent experiments *(Figure 3.1).* As the number of carboxyl groups included in the organic acids was increased from 1 to 3 the wt% of C incorporated during the experiment similarly increased. Maximal wt% C (50% Fh-OC) for the 1-COOH precipitate was 1.36 % increasing to 3.64% (2-COOH) by a factor of 2.68x, then to 6.94% (3-COOH) by a factor of 1.90x. The 15 unique sample compositions represent a range of C concentrations from 0.33% (10%, 1-COOH) to 6.94% (50%, 3-COOH).

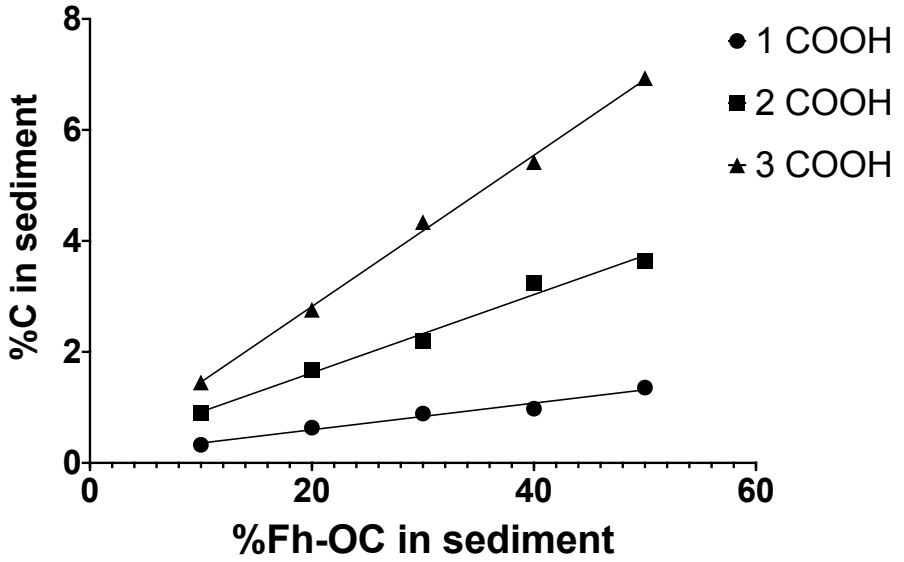

Figure 3.1 Calibration of sediment coprecipitate content and sediment wt% C. Coprecipitates show a tight linear regression trend across the series with R-squared values of: 1 COOH = 0.97; 2 COOH = 0.98; 3 COOH = 0.99. %Fh-OC refers to the content of ferrihydrite-organic coprecipitate in the sediment composite.1/2/3 COOH refers to the number of carboxyl groups per molecule in the three different organic acids coprecipitated with ferrihydrite. %C refers to the concentration of carbon in the overall sediment composite by wt%. Instrument error is too small (≤1% RSD) to be visualised.

3.2.2 Organic Carbon extraction

The Fe bound OC fraction (%OC-Fe) lost from the composite material during the extraction was determined for each of the carboxyl coprecipitate containing samples at concentrations of 20-50% Fh-OC, since C loss for coprecipitates at 10% Fh-OC was too small to be accurately determined *(Figure 3.2).* The 3-COOH sample was extractable for ~46% of OC, while 2-COOH and 1-COOH samples show 'negative' extractability of ~ -6% and ~ -90%, respectively. Negative values are labelled as "NaCl extractable" *(Figure 3.2)* and refer to sediment composites where treatment of the sample with sodium chloride liberated a greater amount of OC than treatment with dithionite. Precise values for all extractions including duplicate errors are detailed in *Table 3.1.*

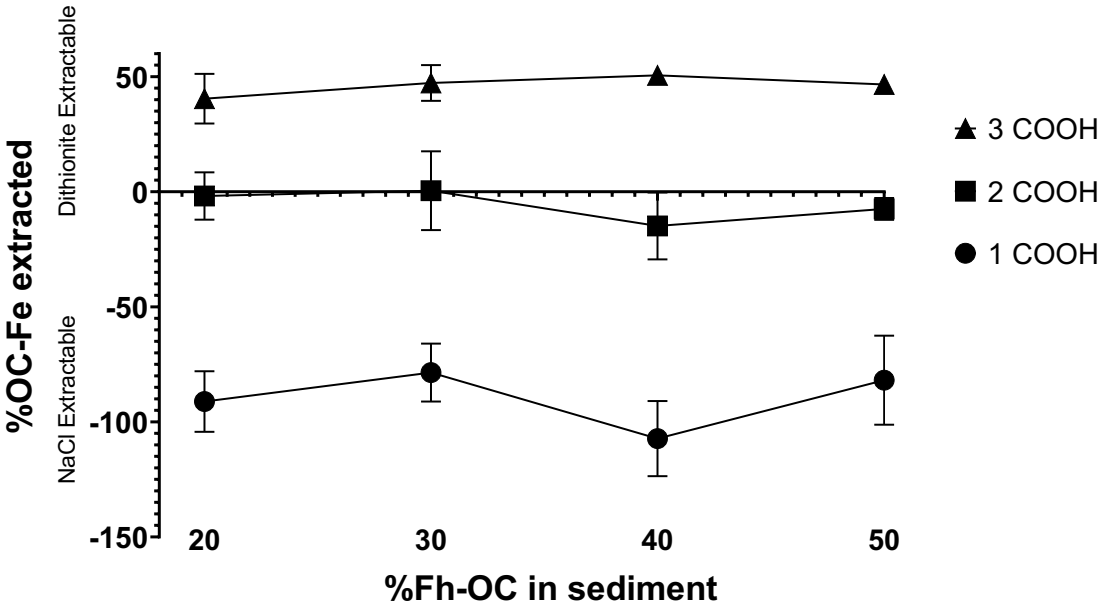

Figure 3.2- Dithionite extractable fraction of OC from carboxyl coprecipitate spiked sediments. %OC-Fe extracted from artificial sediments spiked with 1,2 or 3 carboxyl organic acids. Error bars show SEM of duplicate values, error for 40% and 50% Fh-OC, 3 COOH and 50%, 2 COOH are too small to be visualised on this scale. %OC-Fe refers to wt%C removed by reductive dissolution of the reactive iron phase for iron bound carbon. %Fh-OC describes the contribution of iron bound carbon to the initial sediment composite before extraction. Key descriptors, 1-3 COOH, represent the 3 different organic acids coprecipitated with ferrihydrite.

A breakdown of how these negative extraction values arise has been included for each carboxyl containing sediment at the 30% Fh-OC concentration *(Figure 3.3)*. The 1-COOH sediment composite shows negative %OC-Fe extraction, this is a function of greater %C loss in the NaCl control than with sodium dithionite reduction. The 2-COOH shows a similar loss of carbon in both the control and reduction stages, resulting in an apparent ~0 %OC-Fe content. The 3 COOH spiked sediment is favourable to the reductive stage, with a greater %C loss here than in the NaCl control. These trends were observed across the concentration series *(Figure 3.2)*. The mean difference between all three carboxyl coprecipitates was found to be significantly different for all pairwise combinations via a one-way ANOVA and Tukey's test post hoc (99% significance) *(Table 3.2)*.

Table 3.1 Raw carbon data for determining %OC-Fe.

%Fh-OC	Bulk %OC*	Reduction (Δ %OC)	Control (Δ %OC)	%OC-Fe
		1 COOH		
20	0.636	-12.527 (± 21.056)	78.606 (±11.716)	-91.132 (± 9.340)
30	0.968	17.398 (± 7.741)	95.968 (± 1.162)	-78.570 (± 8.903)
40	0.978	-19.607 (± 2.243)	87.622 (± 9.317)	-107.229 (± 11.560)
50	1.357	10.854 (± 9.315)	92.742 (± 4.386)	-81.888 (± 13.702)
		2 COOH		
20	1.681	74.066 (± 5.818)	75.944 (± 1.457)	-1.879 (± 7.275)
30	2.192	71.080 (± 2.150)	70.613 (± 9.976)	0.467 (± 12.126)
40	3.237	63.203 (± 8.030)	78.079 (± 2.245)	-14.876 (± 10.275)
50	3.639	70.423 (± 1.234)	77.892 (± 2.123)	-7.468 (± 3.357)
		3 COOH		
20	2.761	87.043 (± 3.224)	46.620 (± 4.390)	40.423 (± 7.615)
30	4.339	91.764 (± 1.881)	44.503 (± 3.625)	47.260 (± 5.506)
40	5.420	91.628 (± 0.686)	41.114 (± 0.629)	50.514 (± 1.315)
50	6.935	89.602 (± 0.487)	43.036 (± 0.485)	46.566 (± 0.973)

*Bulk %OC refers to the OC content prior to any treatment. Values shown are a mean of duplicates, ± indicates the standard error of the mean (SEM).

Table 3.2 Tukey's multiple comparisons test of extracted OC-Fe for carboxyl coprecipitates.

Comparison	Adjusted P Value	Significant?*
1 COOH vs 2 COOH	<0.0001	Yes
1 COOH vs 3 COOH	<0.0001	Yes
2 COOH vs 3 COOH	0.0001	Yes

*Significance was determined at the 99% significance level.

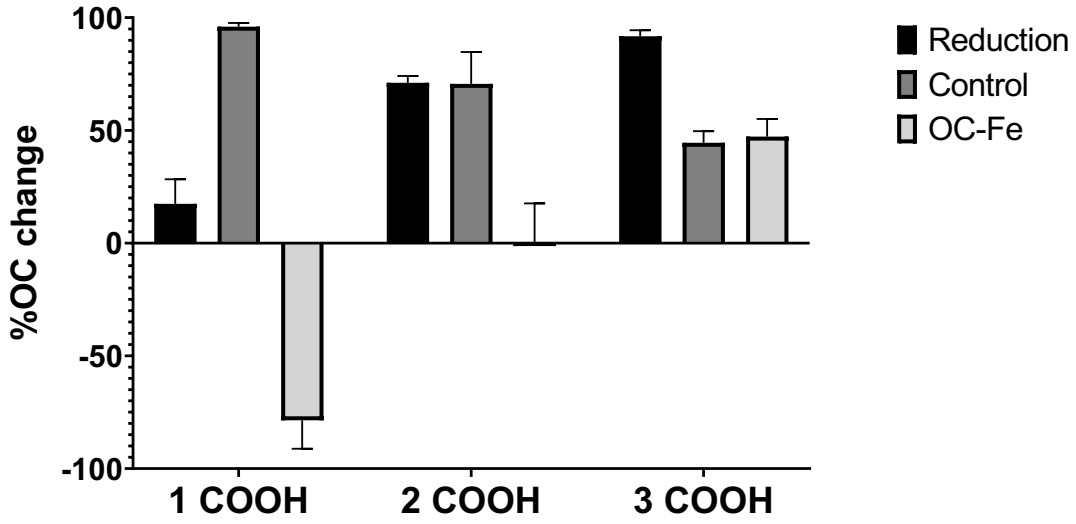

Figure 3.3- %OC change of spiked sediments in control and reduction conditions. An expanded dataset from *Figure 2*, showing the breakdown and calculation of %OC-Fe at 30% Fh-OC content for the three carboxyl coprecipitates (1-3 COOH). %OC change was determined from subtracting final %C from bulk %C and corrected for mass loss. Error bars show SEM of duplicate values. Reduction refers to treatment with CDB, control is treatment with NaCl and OC-Fe is a subtraction of the control value from the reduction.

3.2.3 Iron extraction

Extractable Fe shows an increasing stepwise trend with carboxyl richness for all concentrations of %Fh-OC *(Figure 3.4)*. All extractions for easily reducible Fe were incomplete (< 100% of added Fe) with a maximum yield of 61.6% achieved for the 3 COOH coprecipitate at 50% Fh-OC, and with a mean range of 50.5-61.6% across all concentrations. In decreasing order, the 2-COOH sediment was extractable for 40.0-45.7% and 1-COOH for 17.9-29.9%. The OC free (0-COOH) sediment composite achieved the lowest rate of Fe recoverability, between 6 and 14%. %Fe extracted was calculated from subtraction of Fe_{CDB} and Fe_{NaCL} from $Fe_{Total.}$ The contribution of Fe_{NaCl} was minimal (≤ 0.3%) and made no difference to the overall trend. Iron liberated in wash stages for both CDB and NaCl treatment are included in the overall %Fe extracted values. Relative to Fe liberated from the initial chemical treatment, the wash removed a further

6.7-34.0% Fe for CDB and 0.4 to 27.8% for NaCl. All sample means were calculated from the average of independent duplicates. A significant difference was found between the means of all coprecipitate pairwise combinations (>99% significance) by one-way ANOVA analysis and Tukey's test post hoc. A statistical summary is included in *Table 3.3*.

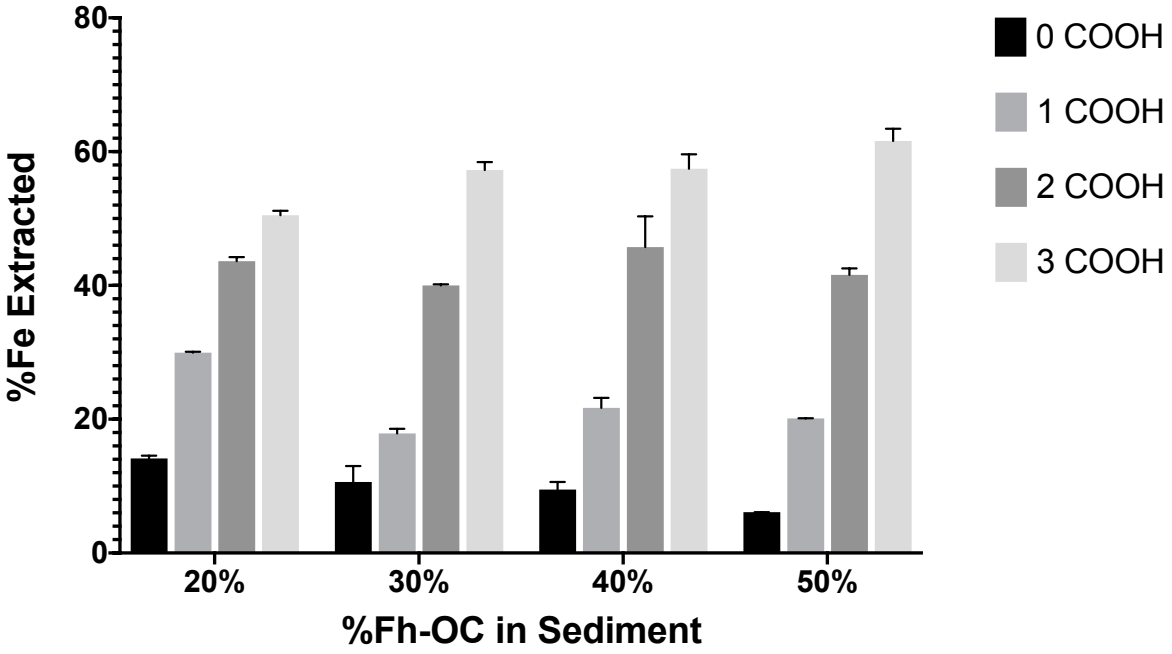

Figure 3.4 Dithionite extraction efficiency for reactive Fe phases in sediment samples differing in carboxyl richness**.** %Fe extracted from each carboxyl spiked sediment (0-3 COOH) is shown, values are control corrected. Error bars represent SEM of duplicate values.

Table 3.3 Tukey's multiple comparisons test of extracted %Fe for carboxyl coprecipitates.

Comparison	Adjusted P Value	Significant?*
0 COOH vs 1 COOH	0.0050	Yes
0 COOH vs 2 COOH	<0.0001	Yes
0 COOH vs 3 COOH	<0.0001	Yes
1 COOH vs 2 COOH	<0.0001	Yes
1 COOH vs 3 COOH	<0.0001	Yes
2 COOH vs 3 COOH	0.0019	Yes

*Significance was determined at the 99% significance level.

3.2.4 Coprecipitate grain size

Grain size of ferrihydrite composites was measured by optical analysis in the 0.01 to 10000 µm range. The 3-COOH coprecipitate showed a slight peak shift from 12.04 to 28.66 µm compared to the carboxyl free, pure ferrihydrite phase (0 COOH) *(Figure 3.5)*. One and two COOH coprecipitates showed no determinable difference in grain size distribution and sat between the 0 and 3 COOH sediments. The 0 and 3 COOH precipitates also had marginally taller, slimmer distributions indicating a narrower range of grain sizes and a greater proportion of the class existed at the mid-point compared to 1 and 2 COOH. These two samples have almost identical normal distribution curves and show no determinable difference in grain size or distribution. Due to the overlapping of all distributions, there cannot be any meaningful difference in the grain size of coprecipitates.

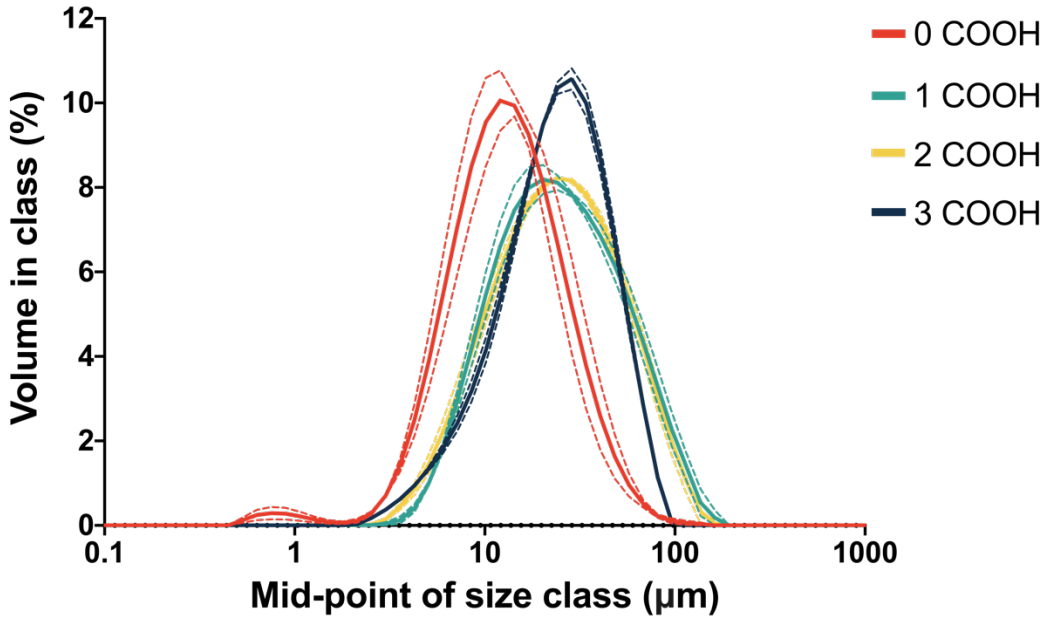

Figure 3.5 Grain size distribution of carboxyl coprecipitates**.** Grain size distribution is shown as percent in class, values are the mean of triplicate measurements.

3.2.5 X-ray diffraction analysis (XRD)

XRD was performed to determine the effect of carboxyl content on overall Fe mineral crystallinity *(Figure 3.6)*. All samples show a characteristic two peak signature, indicating successful synthesis, carboxyl free ferrihydrite resembles a characteristic two-line sample. As carboxyl richness increases, a decrease in relative intensity and softening of the two ferrihydrite characteristic peaks can be seen by a reduction in amplitude.

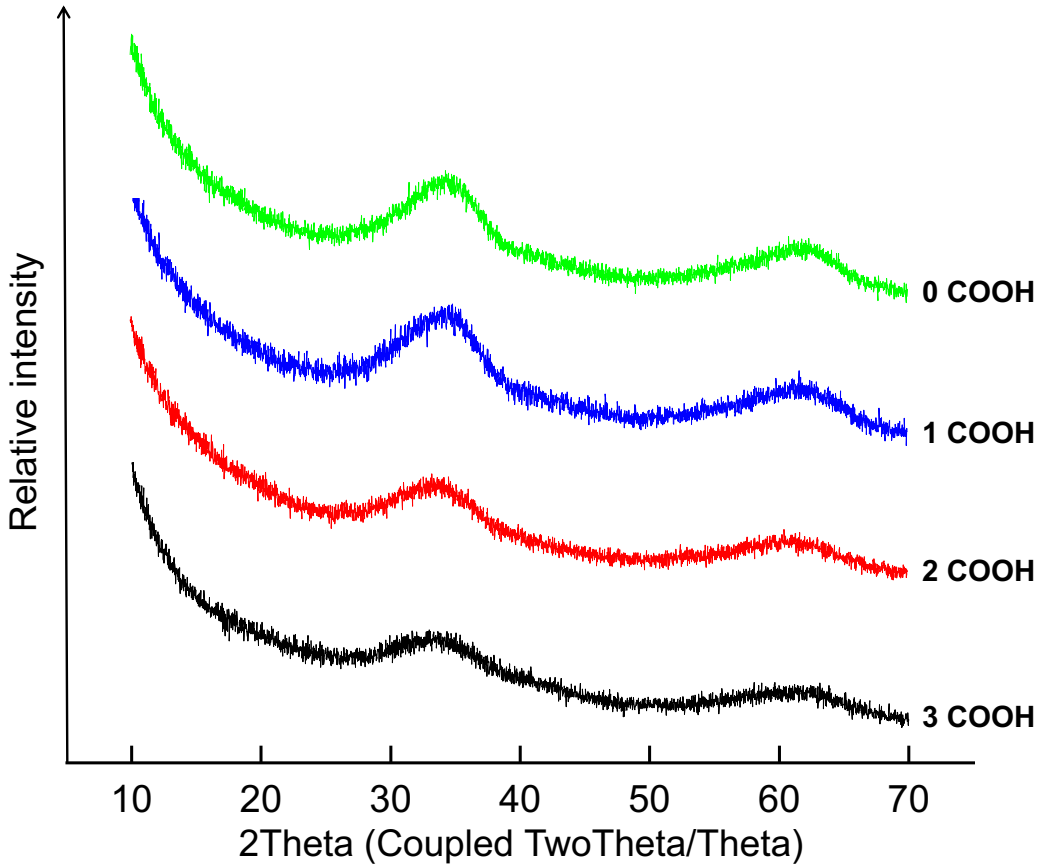

Figure 3.6 Stacked XRD of coprecipitates with increasing carboxyl rich organic content.

3.3 Discussion

Organic carbon bound to reactive Fe phases represents the largest described mechanism by which OC is preserved within soils and marine sediments, maintaining planetary homeostasis and having a potentially mitigating affect towards rising atmospheric CO_2. The CDB method, previously used to quantity OC-Fe in terrestrial environments, has been applied to marine sediments providing the first quantification of preserved sedimentary carbon on a global scale (Lalonde et al., 2012). Here we applied the same CDB method to synthetic samples, in an experimental investigation of OC-Fe, to uncover the influence of the molecular characteristics of OC in determining its ability to be preserved by Fe. By extracting OC-Fe from ferrihdyrite preciptated with short chain organic molecules, differing only in carboxyl content, we explore a regulatory mechanism, mediated by carboxyl groups, which we show to have a significant influence on OC preservation *(3.3.1)***.** Subsequently we demonstrate inefficiencies in the CDB method through calibration against synthetic standards which has the potential to transform our interpretation of CDB extractions performed on natural sediments and thus our understanding of marine sediment carbon preservation of a global scale *(3.3.2)*.

3.3.1 Current methods may underestimate the extent of OC-Fe interactions.

Preservation of OC by Fe is resultant from the physical protection conferred on OC by Fe and results from chemical bonding. OC-Fe interactions rely on high energy bonding between the two to maintain a preservative effect (Middelburg, 2019a); weaker interactions (e.g. Van der Waals) may exist but are not of sufficient strength to facilitate OC preservation (Burdige, 2007). Here, we assessed the extent to which OC composition varies the strength of this preservative OC-Fe interaction by subjecting different OC-Fe compounds to reduction by CDB *(Figure 3.2)*. Treatment with CDB has been described to dissolve “all solid reactive iron

phases and the organic carbon associated with these phases" (Lalonde et al., 2012). Therefore, in our samples we would expect full liberation of Fe_{Total} and C_{Total} given that for our synthetic coprecipitates spiked in carbon-free sediment C_{Total} was equal to the amount of C associated with ferrihydrite. Any shift from a balance of $C_{CDB} = C_{Total}$, as a result of altering the OC structure (carboxyl richness), would imply a change in the strength of chemical bonding from what would otherwise have been expected. This effect could therefore contribute to an overall bond strength diversification for OC-Fe in organic compounds comprised of variable carboxyl content, a diversified bond strength pool has been previously observed as a feature in the long term persistence of mineral bound OC (Hemingway et al., 2019). Across all concentrations and C structures we observed incomplete recovery of Fe, not exceeding 50.514 % of the added Fe content (± 1.315) (3-COOH, 40%) *(Figure 3.2)*. As OC-Fe (C_{CDB}) is less than C_{Total} this indicates either the chemical treatment or interpretation of the result contain a significant error. However, the OC-Fe values obtained, in particular for the 3 COOH containing sediment, are comparable to observations from some environmental samples.

Where CDB has been applied to marine sediments the %OC-Fe (= fraction of total OC bound to reactive Fe) ranges between 0-42% on continental shelves (Ma et al., 2018; Salvadó et al., 2015; Lalonde et al., 2012) with typical averages for sediments under oxic bottom waters of 21.7 ± 7.8% (Lalonde et al., 2012). While the calculation for our 3-COOH coprecipitate exceeds these ranges for %OC-Fe in marine sediments, it is agreeable with terrestrial environments, demonstrating that the values obtained for our extractions are in the same order of magnitude as those conducted on environmental samples. For example, Zhao et al. (2016) determined an OC-Fe pool of 37.8 ± 20% for forest soils, however it remains unknown as to why OC-Fe values for natural samples rarely exceed this range. The appearance of a less than complete OC extraction can be explained by the large loss of OC-Fe from NaCl treatment, designed to remove OC not

bound to Fe. Lalonde et al. (2012) note 7.2 ± 5.4% of OC is released from treatment of natural sediments with NaCl, while we recorded 43.81 ± 3.06% for synthetic coprecipitates, suggesting a large proportion of OC is weakly bound to Fe in our experiments. This ultimately reduces the %OC-Fe from an initial value of OC_{CDB} 90.00 ± 2.50 % to 46.19 ± 7.57 % (*Figure 3.3),* despite the initial OC_{CDB} being much closer to the true value of 100%. This demonstrates that this method of calculating the OC-Fe pool is misleading as it gives the impression that the pool is much smaller than in actuality due to subtraction of the control experiment, which contains Fe bound OC.

The effect of NaCl removal of OC is amplified by the inclusion of less structurally complex 1- and 2-COOH sediment composites. Here, the substantial extraction of OC by NaCl results in final %OC-Fe calculations of ~-90% and ~-6% respectively *(Figure 3.2),* which is physically implausible. This demonstrates that the NaCl control treatment is capable of removing less complex and comparatively weakly bound OC (e.g. 1 COOH, *Table 3.1)* from a reactive Fe mineral interface. By synthesising precipitates we have ensured that all OC in the sample is associated with Fe: i) ferrihydrite is the only reactive interface OC is exposed to; ii) residual OC not associated with ferrihydrite is already removed by multiple rinses following precipitation, at which point C/Fe ratio determination is recommended (Eusterhues et al., 2011; Han et al., 2019). This would not be the case if it was plausible that non-Fe associated OC remained in solution.

In addition to a high OC loss in the control, we may also be observing an artificially low OC loss in the CDB treatment stage. This may explain negative mean values for C% loss of -12.527 and -19.607 following CDB extraction at 20 and 40% (1-COOH), respectively. When dissolved with sodium dithionite, the reactive Fe phase breaks down, as observed by Fe loss *(Figure 3.4).* However, this Fe loss is incomplete and much of the phase (~77%) remains within the sediment. Liberation of OC from the

surface of ferrihydrite during reductive dissolution will increase the number of available surface binding sites and therefore could allow for either re-adsorption of liberated OC or sorption of organic reagents involved in the reduction stage (sodium bicarbonate, trisodium citrate). It has been shown that sorption of bicarbonate (HCO_3^-) to Fe_R phases at neutral pH is a thermodynamically favourable process via monodentate inner-sphere complexation (Acelas et al., 2017), a mechanism similar to that suggested by (Barber et al., 2017) for OC association with Fe. Sorption of OC or HCO_3^- on to dithionite reduced Fe phases could elevate sediment carbon concentration post extraction and therefore appear to artificially decrease %C loss in the reduction stage below what is observed in the non-dissolved control.

The CDB method as applied by (Lalonde et al., 2012) states that treatment of sediment with NaCl removes OC not associated with Fe. However, our results suggest that this NaCl-leached pool of OC is in fact bound to reactive Fe phases but less strongly than the CDB extractable pool. Whether this comparatively weakly bound interaction offers physical protection is unknown, however, a large co-localisation of OC with mineral phases (including Fe) has been observed via scanning transmission x-ray microscopy (STXM) at depths far beyond current quantification of OC-Fe (23.9 metres below seafloor) (Estes et al., 2019). While the direct binding of OC to Fe was not measured in this study, it suggests that the extent of OC association with Fe is larger than has been determined by CDB extraction to date. We suggest that the OC_{NaCl} pool is of importance when calculating the overall OC-Fe budget. While this step has been implemented to avoid overestimation of %OC-Fe, it has become apparent that NaCl has a capacity to liberate OC weakly bound to Fe from the sediment matrix beyond what would be reasonably expected to be removed in the ocean. This is demonstrated by the additional 7.2 ±, 5.4% OC removed with NaCl in treatment of surface marine sediment, previously exposed to seawater, by (Lalonde et al., 2012). Therefore, the

subtraction of OC_{NaCl} from the overall OC-Fe pool has the potential to underestimate the global OC-Fe budget. We suggest that to avoid excess extraction of non-Fe bound OC, a multiple (5x) wash stage in DI water could be implemented (as in the Fh synthesis method) as a suitable replacement of NaCl.

A recalculation on the presumption that all OC_{NaCl} extracted by Lalonde et al. (2012) in fact represents weakly bound OC-Fe suggests that Fe promoted preservation could be underestimated by ~33% relative to the estimates by Lalonde et al. (2012). However, while in a synthetic experiment it appears that NaCl removable OC is bound to reactive Fe phases, this may not be fully translational to environmental sediments due to the loss of OC from other sources, such as those bound to manganese oxides (Tipping and Heaton, 1983; Bernard, 1997; Allard et al., 2017) or DOC dissolved in the pore waters (Fox et al., 2018; Rossel et al., 2016). A change in the extent to which OC-Fe contributes to OC preservation has ramifications for both the global OC-Fe budget and for biogeochemical models aiming to include OC preservation mechanisms. The bias towards high removal of organic compounds of low structural complexity, as seen with the easy loss of 1 COOH organics from the coprecipitates, also suggests these may be being discarded from CDB extraction of natural sediment, however, the underlying mechanisms controlling the strength of OC-Fe bonds requires further investigation and appreciation for the molecular level characteristics of OC.

3.3.2 Carboxyl content of Fe bound OC determines the strength of preservation.

We observe that a greater proportion of CDB reducible Fe (i.e., OC-Fe) is extracted when carboxyl content of the organic matter is high *(Figure 3.2).* This relationship suggests a greater proportion of OC is preserved for carboxyl rich OC compared to that which is carboxyl poor. As increasingly carboxyl rich organic acids become introduced in to the coprecipitation reaction, the number of carboxyl groups available for

ferrihydrite bonding increases from 1 to 3. A greater overall number of OC-Fe bonds in carboxyl rich coprecipitates would explain the increase in the proportion of OC stabilised by Fh. As a result of increasing the number of COOH groups per molecule, the total organic carbon (TOC) also increases whereby the C/Fe molar ratio of the extracted coprecipitates roughly doubles (1 COOH = 0.2, 2 COOH = 0.5, 3 COOH = 1). It has been suggested that C/Fe ratios can be interpreted for mineral binding mechanism with values ~1 indicating surface mono-layer sorption (Barber et al., 2017) with higher values indicating coprecipitation of OC within the mineral matrix, allowing for greater overall C content (Chen et al., 2014). However, Barber et al. (2017) suggest that dithionite extraction of all reactive Fe, regardless of whether it is bound to OC or not, introduces negative bias in to the C:Fe calculation, producing much lower ratios than actually occur. The persistence of larger C/Fe ratios (up to 30) as recalculated by Barber et al. (2017) are suggested to indicate that large organic biomolecules may only associate with Fe_R phases through "one or a few" functional groups. If it were the case that large molecules bind reactive Fe through a minimal number of functional groups then we would not expect OC increasing in carboxyl richness to have a differing preservative strength when associated with Fe, as no additional OC-Fe bonds would form; however we do observe stronger OC-Fe preservation for carboxyl rich OC structures *(Figure 3.2).* This indicates that functional group (here, carboxyl) binding to Fe_R phases is a cumulative effect, limited by carboxyl content and not a simple "on/off" mechanism which reduces the surface area of a binding interaction.

Chen et al. (2014) analysed forest floor DOM extracts coprecipitated with synthetic Fh at varying C:Fe ratios (0.3-25) and proposed that higher C/Fe ratios may result from fewer carboxyl groups per molecule involved in binding interactions. This is suggested to be in part due to a decrease in available binding sites on the mineral surface when large amounts of natural organic matter become associated. As our C/Fe ratios are

determined by carboxyl group content, due to low variability in carbon chain length of the coprecipitated organic acids *(Figure 3.1),* we instead see that higher C/Fe ratios suggest more carboxyl groups are involved in OC-Fe binding. The increasing gradient between the 1-3 COOH precipitates shown in *Figure 3.1* supports this as for each increase in %Fh-OC concentration a greater number of C molecules are being included (due to a progressively larger number of carboxyl groups on each acid). The pattern of C/Fe ratios reflecting the number of carboxyl groups highlights a difference between the organic acids used in our precipitation and marine DOC, as the small carboxylic acids used here are less likely to block mineral surface sites compared to larger DOC structures. Indeed, according to the characterisation of CRAM, the carboxyl rich moiety representing the dominant molecular DOC structure, by Hertkorn et al. (2006), our largest organic (1,2,4-butanetricarboxylic acid) is approximately half the weight (190.15 Da) of the smallest CRAM (400-700 Da). As such it is important to note that short chain organics are used here to uncover a mechanistic trend in carboxyl binding, not to directly replicate physical and structural characteristics of natural DOC.

Here we suggest that OC-Fe preservation is influenced by carboxyl group richness. Thus, the translation of this finding into an environmental context requires an understanding of the moieties present in marine DOC. Much of the work aimed at probing the OC-Fe interaction has involved coprecipitations of Fh with DOM, containing OC (e.g., Eusterhues et al., 2011; Eusterhues et al., 2014a; Eusterhues et al., 2014b). Typical coprecipitation experiments for Fe bound OC use DOM from forest floor extracts or purchased standards (e.g., Swanee River). Chen et al. (2014) showed some appreciation for the importance of OM carboxyl content by using forest floor extract enriched for carboxyl content in their study. Coprecipitation with terrestrial organic matter is unlikely to be representative of marine DOM as the OC within DOM has been shown to

be enriched in carboxyl content, due to the refractory nature of CRAM (Hertkorn et al., 2006).

Additionally, marine (algae) OM further differs from terrestrial sources by exhibiting a lower C/N ratio (4-10) than terrestrial OM (>20) (Meyers, 1994). Higher plants, the largest contributor to terrestrial OM, contain less than 20% protein, hence have lower nitrogen contents and higher C/N ratios than protein rich (~80%) marine bacteria and benthic animals (Müller, 1977). OM preserved in ancient sediments (since 11.6 Ma) shows increased C/N ratios (>10) relative to marine surface (algal) OM (Twichell et al., 2002).This change is attributed to partial OM degradation during sinking and potentially post deposition. Verardo and McIntyre (1994), however, suggest that alteration of C/N ratios from shallow to deep burial in sediments occurs due to favourable decomposition of N-rich (C/N low) OM by microbial communities. This would imply that N-rich (C//N low) marine OM undergoes more extensive structural alteration during decomposition than C/N high terrestrial OM, reinforcing why coprecipitation of terrestrial OM cannot be considered to be comparative to the OC moieties within marine OM arriving at the seafloor.

For our coprecipitation experiments, the OC source was isolated to carboxyl groups as far as possible, with unavoidable inclusion of one additional short chain C molecules in the 1 and 2 COOH acid (4 non-COOH C's) compared to the 3 COOH molecule (3 non-COOH C's). It was neither expected nor observed that the inclusion of these additional C chain molecules had any significant effect on OC binding to Fe. In addition the coprecipitates were normalised to wt% C in *Figure 3.1* and showed the expected pattern whereby coprecipitates increase in wt% C content with an increase in the number of COOH groups, demonstrating COOH groups remain the primary control on sediment C content. As COOH and OH groups are thought to be crucial for OC-Fe binding (Karlsson and Persson, 2012, 2010; Mikutta, 2011; Yang et al., 2012) individual moieties of carboxylic acid were used to elucidate the precise

mechanisms of binding, as opposed to using a homogenous NOM source of unknown COOH and OH content. The occurrence of anion exchange bonding between the mineral surface and the COOH groups of OC (Kaiser and Guggenberger, 2003), coupled with the significant difference in OC preservation with carboxyl richness *(Table 3.1),* highlights the importance of accurately replicating COOH content in experimental coprecipitations. This demonstrates that carboxyl content of OM is crucial in determining the extent to which the OC pool will be preserved through mineral protection. Environmental conditions favouring high concentrations of Fe, such as close to continental margins and hydrothermal vents (Tagliabue et al., 2017), and carboxyl rich OC inputs, e.g. regions of high primary productivity and shallow waters, are likely to be more efficient at preserving OC through increased bonding to reactive Fe phases.

3.3.3 Ferrihydrite is incompletely extracted by Na dithionite.

Quantifying the efficiency of Fe phase extraction techniques has largely been neglected within the literature due to the nature of chemical methods being operationally defined, making it difficult to calibrate these against alternative methods of measuring Fe phases such as Mössbauer spectroscopy (Hepburn et al., 2020). In marine sediments, total Fe is comprised of phases of differing stability, requiring extraction techniques of increasing strength to remove them (Poulton and Canfield, 2005). Here, we isolated one phase (ferrihydrite) which is considered easily reducible by sodium dithionite and should be correspondingly removable for all reactive Fe phases (Lalonde et al., 2012). However, our measure of Fe extractability only shows a maximum extraction of ~60 wt% Fe when coprecipitated with a 3 COOH acid, comparable with the incomplete ($\leqslant$ 50%) sodium dithionite reduction of hematite-humic acid complexes by Adhikari and Yang (2015). Moreover, Fe extractability appears to be a function of carboxyl richness, with a stepwise trend observed across the carboxyl gradient *(Figure 3.4).*

The trend between carboxyl content of the coprecipitate and Fe extracted is concurrent with the theory of structural disorder (Mikutta, 2011; Mikutta et al., 2008; Cismasu et al., 2011). As OC of increasing carboxyl content sorbs to Fh, those phases become more amorphous, decreasing the crystallinity of the ferrihydrite and reducing the chemical stability of the mineral compared to OC free Fh. Our XRD analysis supports this theory as a weakening of peaks identifying 2-line ferrihydrite is observed when carboxyl content in the coprecipitates is increased *(Figure 3.6).* This demonstrates that an increase in carboxyl richness results in a decrease in ferrihydrite crystallinity. Decreasing crystallinity was similarly observed for samples where total OC (polygalacturonic acid) content was increased (C/Fe 0-2.5) which inhibits transformation of ferrihydrite to more stable phases (ThomasArrigo et al., 2018). The precipitation of a more amorphous organomineral with increasing carboxyl richness is consistent with the observed increasing trend in Fe extraction *(Figure 3.2)* as amorphous mineral phases would be less stable and, therefore, more susceptible to reduction by Na dithionite than crystalline phases. The presence of organic matter has previously been attributed to the reductive release of Fe through electron shuttling effects, due to the ability of organic compounds to act as electron carriers between redox reactions (Adhikari and Yang, 2015). Additionally, we see no difference in physical parameters of the coprecipitates, e.g., grain size *(Figure 3.5),* reinforcing our suggestion that internal mineral structure is responsible for differences in reactivity.

The CDB treatment employed was seen to be unsuccessful at fully liberating the added Fe from the artificial sediment mix. While reduction by Na dithionite is a well-established method, the adoption of CDB treatment at circumneutral pH, to avoid hydrolysis of OC, remains unique to the OC extraction application. Thompson et al. (2019) found that a CDB extraction at pH 7.6 fails to extract a large proportion of crystalline Fe_R phases in both modern and ancient sedimentary rocks. We make a similar

observation for OC free ferrihydrite phases, where only 9.91 ± 0.95 % Fe is recovered post extraction. While it is apparent that CDB treatment cannot fully extract easily reducible Fe_R phases, and therefore the entire associated OC pool, there is no obvious improvement that can be made to the current protocol due to the constraints of maintaining a neutral pH.

3.4 Conclusion

Carbon cycle feedbacks remain largely unconstrained on a molecular and mechanistic level, the lack of definition in processes controlling C sequestration and preservation represent a limiting factor in steps towards integrating biogeochemical processes in climate models. We aimed to understand how the specific bonding interactions which occur between OC and Fe may influence OC preservation by reactive Fe phases through artificially altering the functional group content of OC in coprecipitation with Fe_R phases and subjecting these compounds to a reductive dissolution treatment. We have shown that carboxyl richness of OC involved in sorption to reactive Fe phases exerts a primary control on mineral crystallinity and stability, and therefore the chemical extractability of the Fe. We found that the increased preservation of carboxyl rich OC is associated with an increased number of carboxyl mediated OC-Fe bonds requiring reductive dissolution to liberate the OC-Fe pool. Weaker bound organics are readily removed from the mineral phase by NaCl solution. The most carboxyl rich coprecipitate (3 COOH) showed a comparable OC-Fe pool to observations of natural marine sediments (30.07 ± 4.3 vs 21.5 ± 8.6) (Lalonde et al., 2012). And therefore, agreeing with Hertkorn et al. (2006), that preserved marine OC is rich in carboxyl content.

The %OC-Fe ≤ 0 pools shown for 1 and 2 COOH coprecipitates indicate a difference in behaviour between adsorbed high molecular weight organic matter saturating surface sites in ferrihydrite precipitated under environmental conditions, compared to largely 'naked' synthetic phases precipitated in the presence of low molecular weight compounds.

Subsequently, this could allow for re-adsorption of released OC or sorption of the organic reagents used in reduction on to synthetic phases. The sorption of OC on to residual Fe indicates that chemically resistant Fe remains after reduction, i.e., that release of Fe from sediment spiked with organically complexed ferrihydrite by Na dithionite extraction is incomplete (total yield ~60%). Further, Fe loss appears to be a function of carboxyl richness with those phases enriched in carboxyl groups releasing a greater amount of OC, concurrent with observed decreases in crystallinity and increased structural disorder (Mikutta et al., 2008; Mikutta, 2011; Cismasu et al., 2011). Whilst we have shown the current extraction protocol is of low efficiency for OC-Fe, at least for synthetic coprecipitates, other studies have typically counteracted this through use of a lower pH (Thompson et al., 2019). This cannot be readily translated to an OC-Fe determination application due to the hydrolysis of OC at low pH, decoupling it from the Fe phase. Our current work probes alternate ways of maximising Fe extraction by changing physical parameters within the current reagent framework. Crucially, it should be taken in to account that extractions of OC-Fe phases by the CDB method are likely incomplete and therefore provide an underestimation of the amount of OC preserved through mineral based protection in marine sediments.

Chapter 4- A review of the citrate-dithionite-bicarbonate (CDB) method for quantification of the iron bound carbon pool.

4.0 Preface

In *Chapter 3* we conclude that the incomplete extraction of reactive Fe phases by CDB treatment may facilitate (re)adsorption of organic reagents or previously liberated OC, leading to errors in the calculation of OC loss. The incomplete extraction of Fe, while documented, is not well understood for its implications on organic carbon and at odds with widely applied methods claiming that such a treatment will reduce all reactive iron phases. It is difficult to propose any chemical changes due to the requirement of buffering the reaction at circumneutral pH to which there are no alternatives, from either the pH or organic buffer (sodium bicarbonate). In this chapter we review and reassess the CDB method, by probing physical parameters of the method in an attempt to increase its extractability for reactive iron while maintaining the necessary chemical conditions.

4.1 Introduction

The extent to which OC preservation is influenced by association with reactive Fe minerals can be quantified using the CDB method of Lalonde et al. (2012), as applied in *Chapter 3***.** Obtaining accurate quantifications of OC-Fe interactions in marine sediments under different environmental conditions is essential for uncovering the factors which influence OC preservation, e.g. redox conditions, OC source, and Fe availability. Further, a better understanding of the conditions associated with high (> 25%) OC-Fe may aid efforts to increase sequestration and storage of OC in sediments and soils, mitigating against rising atmospheric CO_2.

Extraction of preserved OC has been conducted by proxy through reductive dissolution of the associated reactive Fe phase with sodium dithionite, thus liberating Fe bound OC from the sediment matrix. The dissolution is conducted at circumneutral pH buffered with sodium bicarbonate and trisodium citrate to prevent hydrolysis of OC (Mehra, 1958; Lalonde et al., 2012). Preventing hydrolysis of OC is an important precaution to avoid leaching of OC which is bound to interfaces in the sediment matrix other than Fe_R (e.g. silica minerals) Use of dithionite for reduction of reactive Fe phases is a long established method beyond the extraction of mineral protected OC and a similar method (citrate-dithionite-acetic acid (CDA)), buffered with acetic acid to pH 4.8, is widely applied in the sequential extraction of reducible Fe_R phases (Poulton and Canfield, 2005) *(Table 1.1).* It has been shown that compared to a CDA extraction, treatment with CDB at pH 7 results in incomplete extraction of reactive iron phases (Thompson et al., 2019) and thus is incomplete for OC-Fe also *(3.4.3).* Incomplete extraction of OC associated with reactive Fe was also observed by (Adhikari and Yang, 2015) with 5-44% of carbon released from hematite-humic acid complexes upon Fe dissolution. A trend additionally recorded by Gorbunov et al. (1961) in respect of the earlier (Mehra, 1958) method, noting that Fe_R phases were incompletely dissolved. This series of observations appears in contrast with current

interpretations of the CDB method which state that CDB extraction will "fully reduce all solid reactive iron phases and associated organic carbon" (Lalonde et al., 2012).

Improvements or alterations to the CDB method have largely been left untouched due to the constraints associated with trying to extract both OC and Fe. pH cannot be lowered due to the hydrolysis of OC even though lower pH approaches are shown to be more efficient at extracting the targeted Fe phases (Thompson et al., 2019). It is also preferable to avoid using organic reagents (e.g. sodium ascorbate) as these can contaminate the extracted OC pool (Ferdelman, 1988), however, the use of dithionite is unavoidable and retention of sodium citrate in the OC pool is minimal (< 0.08% of sediment dry weight) (Lalonde et al., 2012). Since the chemical "recipe" of the reductive dissolution method cannot easily be changed, our approach is targeted towards testing variations in the physical parameters of the CDB method.

Stages of the CDB method were individually tested for different extraction times, reagent concentrations and sample preparation methods. Subsequently, we aimed to establish whether there was one clear set of optimum conditions for all CDB extractions or whether this should be dynamic, i.e. differing dependent upon sediment Fe content, which was achieved through experimentally determining the saturation capacity of sodium dithionite. In doing so, we were able to quantify the saturation capacity of sodium dithionite, which has not been previously reported. Developing an understanding of the phases extracted by the CDB method as well as optimising the parameters for maximal extractability within the chemical constraints will provide both a more accurate and a more reproducible method for extracting OC-Fe. Establishing a standardised approach will allow future environmental OC-Fe datasets to be more comparable, increasing their usefulness for understanding the role of OC-Fe in global biogeochemical cycles.

4.2 Results

4.2.1 Effect of sample preparation on Fe extractability

Two forms of each carboxyl coprecipitate were prepared, one freeze dried according to the standard method, to prevent subsequent transformation, and one left as a slurry (referred to as 'wet'). Total Fe content of samples was determined for dried samples. As wet and dry samples came from the same batch of co-precipitate, the initial Fe content in the slurry was assumed to be the same as initial Fe content for dried samples. % Recovery of Fe following CDB extraction is shown in *Figure 4.1*. A greater proportion of Fe is extracted from the slurry than from freeze-dried samples for all coprecipitates at all concentrations. Dry samples achieve a maximum Fe extractability of 71% (3 COOH, 60%), while in slurries up to 87% is recovered (3 COOH, 100%). No samples recovered 100% of added Fe. Sample preparation method was the overriding determinant for %Fe extractability and was more important than the number of carboxyl groups in this context.

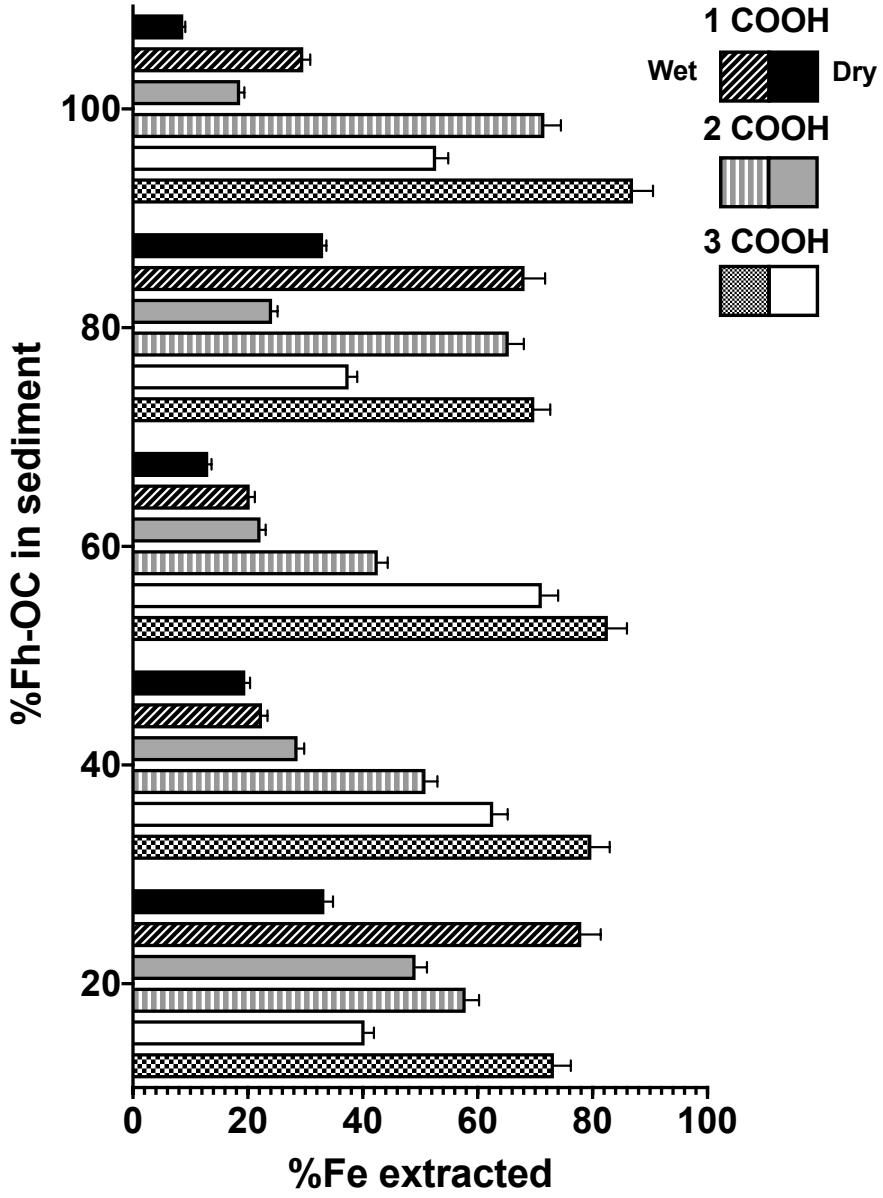

Figure 4.1- Fe recovery from freeze-dried vs slurry coprecipitates. Solid bars show dried samples while patterns show the wet (slurry) samples. Each bar shows maximum compound error.

4.2.2 Fe extractability from natural sediment samples

Following on from *4.2.1*, the effect of variable sample preparation of natural Arctic marine sediment was investigated. Triplicate samples were prepared of dried and freeze-thawed sediment samples which were treated with the CDB extraction. No significant difference was found between %Fe extracted for dried or freeze-thawed samples *(Figure 4.2)*.

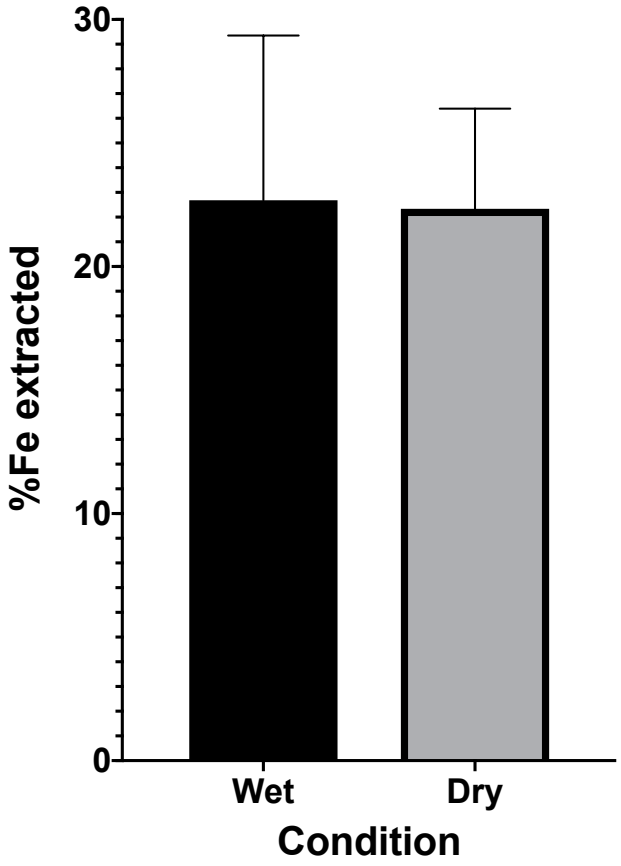

Figure 4.2 %Fe extracted from freeze-thawed (wet) natural sediment compared to freeze-dried sediment. Error bars show SEM of triplicate values (n=3).

4.2.3 Extraction time

Following the method of Lalonde et al. (2012) the CDB extraction is performed over a period of 15 minutes. Here we examined whether extending this time period would increase the amount of Fe extracted. All other parameters of the extraction remained the same, a 2 COOH coprecipitate at a 60% concentration relative to labile sediment was used in freeze-dried and wet forms. Times were advanced in 15-minute stages from 15 minutes to 60 minutes, and results from the subsequent extractions are shown in *Figure 4.3*. %Fe extracted remains consistent across the time series for both wet and dried samples, there is no evidence that increasing the extraction duration increases Fe liberation.

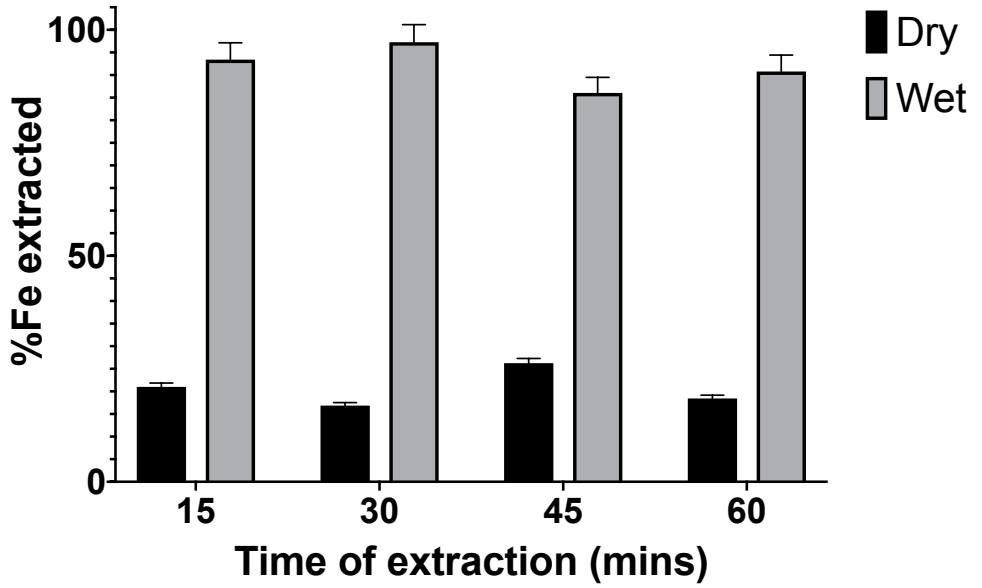

Figure 4.3 %Fe extracted across a time series for CDB extraction. Error bars show compound maximal instrument error. The sample used in this experiment was a synthetic sediment spiked with 2 COOH coprecipitate at 60% Fh-OC.

4.2.4 Na dithionite concentration

The standard addition of Na dithionite in the CDB method is 0.25g per 0.25g dried sediment. In our test, the mass of dithionite added was increased (0.25g, 0.35g, 0.50g, 0.75g, 1.00g) while the sediment mass remained at 0.25g or dry mass equivalent for slurry samples. Dithionite mass was increased to determine if increased dithionite addition would result in an increase in %Fe extracted. An initial decrease from the baseline addition (0.25 g, 21% dry, 93% wet) was measured at 0.35 g (7% dry, 82% wet) *(Figure 4.4)*. Subsequent measurements (0.5 g-1 g) showed an increase from the baseline for dried samples, approximately doubling the %Fe extracted (40-45%). Wet samples remained consistent within error (± 4%) of the baseline (93-101%).

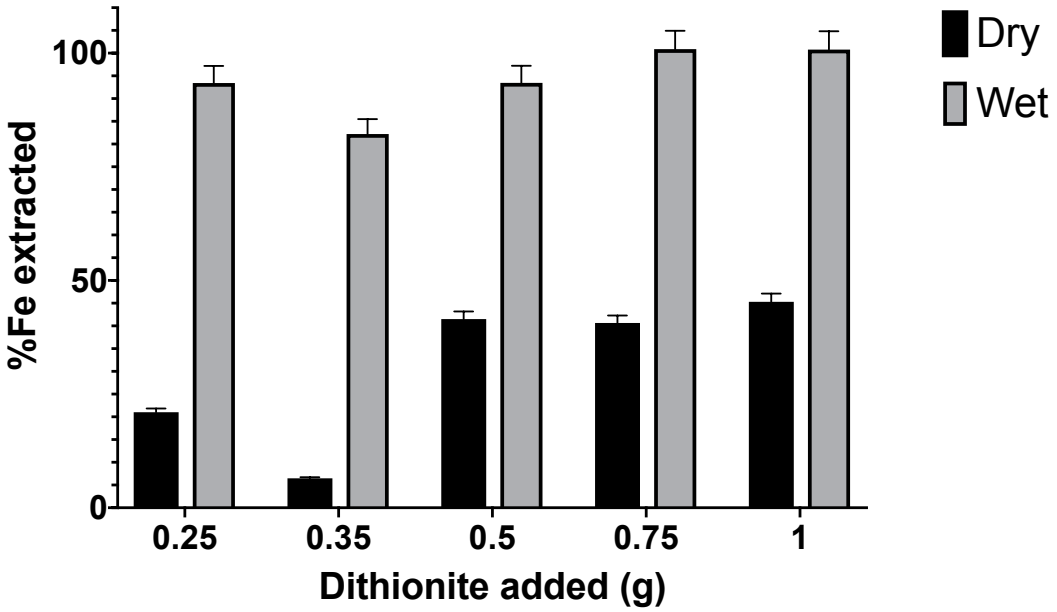

Figure 4.4 %Fe extracted across an addition gradient of Na dithionite addition in the CDB extraction**.** Error bars show compound maximal instrument error. The sample used in this experiment was a synthetic sediment spiked with 2 COOH coprecipitate at 60% Fh-OC.

To further investigate this discrepancy for dried samples (%Fe extracted decreased then further increased), an additional investigation at a higher resolution was conducted. Here, the concentration of Fh-OC (% mix relative to sediment) was re-established as a parameter (as seen in *Chapter 3,* here 20-50%), and duplicates of each Na dithionite addition mass were included in order to rule out outliers. An additional lower Na dithionite mass was included, so the full range of added Na dithionite masses were 0.125 g, 0.250 g, 0.375 g 0.500 g and 0.625 g. The %Fe extracted from these CDB extractions is shown in *Figure 4.5*, and this figure visualises the maximum Fe extractable as a function of the amount of Na dithionite added. For the 20% Fh-OC sediment mix, maximal Fe extraction occurs at the baseline 0.25 g addition. For sediments with a greater initial %Fh-OC (and therefore Fe) content, mean maximal Fe extraction occurs past the baseline. For the 30% and 40% Fh-OC mix, this is at 0.500 g Na dithionite addition where 88% of Fe is extracted. At 50% Fh-OC, 60% of total Fe is extracted at both 0.500 g and 0.625 g Na dithionite additions. From this,

we can deduce the maximal %Fe in sediment extractable by 0.25 g Na dithionite (0.1 M) lies between a 20 and 30% Fh-OC mix, equivalent to 7-10 wt% Fe in the sediment. The 30 and 40% Fh-OC mixes tracked almost identical paths for their extractable %Fe, while 20% Fh-OC is more readily extracted and 50% is less extractable.

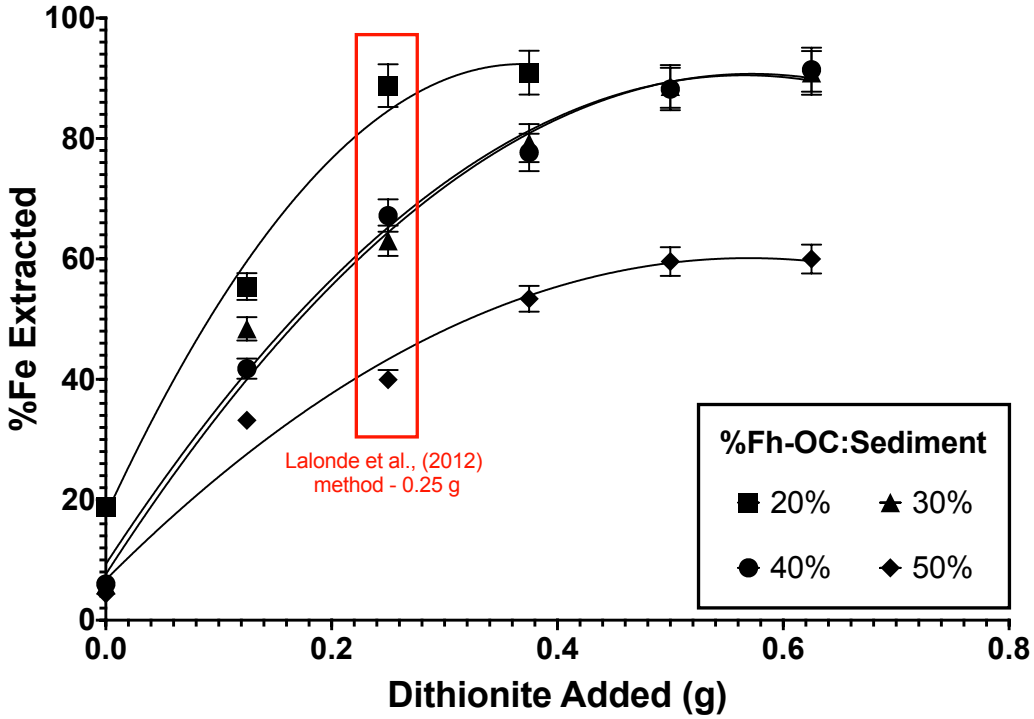

Figure 4.5- Extended analysis of %Fe extracted with varying Na dithionite addition across a %Fh-OC gradient**.** Error bars show SEM of duplicate value.

4.2.5 State of dithionite addition

Initially, Na dithionite was added in solid form to each extraction sample as per Lalonde et al. (2012). As this is labour-intensive, an alternative method was established whereby Na dithionite was added in solution (see *Methods 2.4*). *Figure 4.6* shows %Fe extracted following CDB extraction conducted under the two addition methods. This particular experiment was conducted with a one-way hypothesis, seeking to identify if addition in solution was significantly detrimental to Fe extractability. Four concentrations were tested, 40-100% Fh-OC to sediment mixes, and

all Fh-OC components were in a dry state. There was no significant difference between addition of Na dithionite as a solid or in solution at any of the tested concentrations with values for both methods reproducing similar values of Fe extractability.

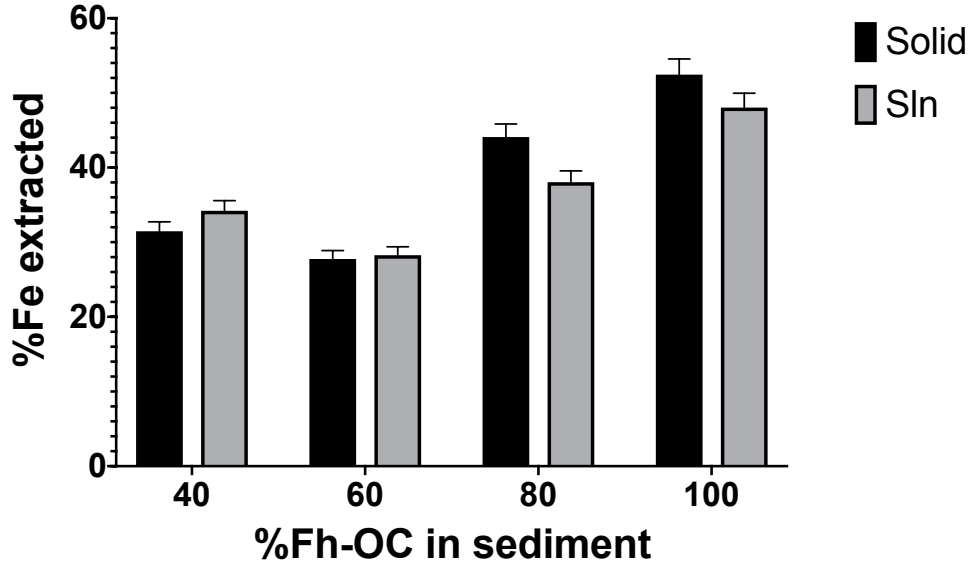

Figure 4.6- %Fe extractability across a Fh-OC gradient with Na dithionite addition in solid or solution (Sln) form**.** Error bars show maximum compound instrument error, n=1 sample measured in triplicate. The sample used in this experiment was a synthetic sediment spiked with 2 COOH coprecipitate at 60% Fh-OC.

4.3 Discussion

In order to improve the extraction efficiency of CDB treatment for reactive Fe, which has been shown to be incomplete, physical parameters of the extraction method were adjusted and applied to synthetic sediments with known Fe concentration, and %Fe extracted was measured. The process of sample preparation was found to be potentially important for chemical extraction through particle aggregation of synthetic sediments, but less important for natural samples *(4.3.1, 4.3.2).* Out of the varied experimental parameters, concentration of Na dithionite *(4.3.3)* was most successful in increasing %Fe liberated, particularly for sediments with a high Fe content, allowing for determination of the reduction capacity of Na

dithionite. Reaction time was found to have no effect on increasing Fe extractability *(4.3.4)*. In conclusion, it is shown that Fe extractability can be reasonably increased for sediments with high Fe and OC-Fe contents, and we suggest an overall extraction approach, from both the results described in this chapter and recent methods described in the literature, to achieve this higher efficiency CDB extraction.

4.3.1 Preparation of samples for CDB extraction.

The extraction efficiency of Fe from freeze-dried sediment samples was less than that measured for chemically identical samples retained in slurry form (i.e. not freeze-dried) *(Figure 4.1)*. The scope of CDB extractions has expanded over time and this wet-chemical treatment is now performed on a diverse range of solid phases, including soils (e.g. Deb, 1950; Mackenzie, 1954; Zhao et al., 2016; Wagai and Mayer, 2007; Schulten and Leinweber, 1995), clays (Aguilera and Jackson, 1953; Deb, 1950; Mehra, 1958; Mitchell and Mackenzie, 1954), plant roots (Taylor and Crowder, 1983), cryoconite accumulated on glaciers (Cong et al., 2018), estuarine sediments (e.g. Jokinen et al., 2020; Zhao et al., 2018) and marine sediments (e.g. Barber et al., 2017; Lalonde et al., 2012; Salvado et al., 2015), with each material possessing unique physical and chemical characteristics. To aid the retrieval of samples from often remote locations, freeze-drying has become established as an almost universal storage and preparation method for solid samples. Removal of the aqueous phase decreases sample mass and prevents the need for cold storage. Freeze-drying inhibits processes of microbial degradation from occurring in the sediment sample, preserving the biochemical profile. Alternative treatment such as air drying are considered to be more aggressive as they can alter the chemical composition of samples and may inflict significant changes on sediment chemistry, including losses of biomarkers (McClymont et al., 2007).

It can be reasonably assumed that drying-induced aggregation of sediment particles is responsible for limiting the extractability of Fe *(Figure 4.1),*

with grain size being a key factor in limiting determination of bioavailable Fe (Raiswell et al., 1994). Aggregation could reduce surface contact with dithionite, preventing reduction of 'shielded' sediment particles, while this could be overcome (e.g. by crushing), this in itself would introduce further variability in grain size (Raiswell et al., 1994).The influence of freeze-drying on grain particle size has been previously noted, particularly for sediment with a high clay content (>39%) (Keiser et al., 2014). McKeague and Day (1966) similarly report that finer grinding of sediment resulted in an increased extraction of Fe. These findings indicate that particle size is a critical parameter in determining the amount of Fe extracted, however, all methods fail to define what is meant by "finely ground". This lack of definition introduces an error of reproducibility as particle size is certain to vary with different sample preparation methods and therefore two identical chemical treatments may vary in strength because of physical differences in the sediment sample.

The alternate tested method of using wet samples has largely been avoided, with only van Bodegom et al. (2003) reporting use of a wet slurry sample. This method also carries error as it is much more difficult to determine the accurate dry weight of sediment in a slurry form due to the heterogeneity of samples and the fact that wet samples contain grains of variable sizes also. Density tests for the tested synthetic samples indicated this contributes up to ±5% error which, while significant, is less than the difference seen between Fe extraction from slurries compared to dried samples (up to 53%, 2 COOH, 100% Fh-OC, *Figure 4.1*). The use of fresh 'wet' samples, differing from the freeze thawed natural sediment we extracted from *(Figure 4.2)* in never having been frozen, appears to be the only method by which aggregation can be avoided as drying, freezing and thawing are all known to produce aggregates (IAEA, 2003).

The use of wet sediments may not be appropriate for all analyses. Fresh sediments retain their microbiological components which can result in biological degradation of pollutants, release of ammonia and chemical

degradation via hydrolysis and oxidation (Schwab, 1980). However, it has also been show that freeze-drying can result in elevation of DOC in sediment (Geffard et al., 2004), and Barbanti and Bothner (1993) also report an increased amount of OC (20-44 % greater) and some metals (Zn, Cu) in the coarse fraction of freeze-dried sediment compared to slurry samples, suggesting freeze-drying can similarly alter sediment chemistry. Therefore, it should be acknowledged that any storage method is likely to cause a variable level of chemical change.

Although extraction efficiency of Fe from ferrihydrite is improved through the use of wet samples, this only achieves a maximal extraction efficiency of 87% (3 COOH, 100% Fh-OC) (*Figure 4.1).* For Fe_R phases associated with less complex OC, the extraction efficiency is even lower, e.g. for the 1 COOH sample at the same concentration (100% Fh-OC) only 30% of Fe is liberated. Trends between Fe liberation and carboxyl content have been discussed in *3.4.2* and are mirrored here in *Figure 4.1*, besides an inflation in 1 and 2 COOH values at the 20% concentration, likely due to errors in small numbers as a result of the dilution. The 1 COOH complex at 80% Fh-OC also appears inflated with no obvious explanation, and extraction on this synthetic sediment would ideally have been repeated. The inability to fully extract Fe even when sediments are in a slurry form indicates that other limiting factors persist which prevent complete extraction of Fe_R phases by the CDB method.

4.3.2 Behaviour of natural sediment

While in synthetic samples we have established that sample preparation method can limit Fe extractability *(4.3.1),* it remained unclear whether this effect was translational to natural sediments due to the difference in chemical and physical complexity compared to our synthetic coprecipitates. Cismasu et al. (2011) note that ferrihydrite precipitated in environmental conditions shows a decrease in particle size and increase in structural disorder with increasing Al, Si and OM content. The presence of these impurities is predicted to have a significant effect on ferrihydrite

surface reactivity (Cismasu et al., 2011). Given the differences in particle size, crystallinity and reactivity for natural ferrihydrite it cannot be presumed that the sample preparation effects observed for synthetic ferrihydrites would apply to natural sediments.

Triplicate analysis of Arctic marine sediment was conducted, with sediment extracted for easily reducible Fe following the CDB procedure for both freeze-dried and non-freeze-dried samples from the same sediment sample. This showed no significant difference *(Figure 4.2)* in %Fe extraction for the two sample preparation methods. Here, the dried sediment was extractable for 22 ± 4 % while slurry "wet" samples were extractable for 23 ± 7 %. This lack of difference creates an important distinction between the behaviour of synthetic coprecipitates and natural marine sediment under the CDB procedure.

Subtle differences between the treatments applied to natural sediments compared to synthetic samples may play a larger role in the lack of difference in extractable Fe observed for natural samples. The slurry (wet) marine sediments differed from synthetic slurry samples in that they had been previously frozen, so represent a freeze-thawed sample as opposed to an untreated fresh slurry. According to the International Atomic Energy Agency (IAEA, 2003), "drying, freezing and thawing of thawing of the sediment can cause aggregation of particles and should be avoided". Similarly, Hofmann et al. (2004) observe that freezing and thawing of hydrous ferric oxides leads to formation of dense aggregates. Since similar aggregation processes occur in the freeze-drying process (Barbanti and Bothner, 1993), as discussed in *4.3.1,* then aggregation to the same extent under both preparation methods would explain the similarity in %Fe extraction for natural samples.

Hepburn et al. (2020) state that "grain size greatly affects the precision of individual extraction stages between natural and synthetic forms of the same mineral, […] and even between identical samples." And that the susceptibility of Fe minerals to chemical extractions is determined

primarily by the physical characteristics of a sample, with mineral identity being only a secondary factor. This indicates that grain size, and thus sample preparation method, is likely to be a significant factor in determining the extent to which chemical treatments can fully extract their targeted Fe phases. To fully understand the importance of this effect it would be necessary to perform extraction on pristine, unfrozen marine sediment, however, this is operationally challenging given the difficulties in performing extractions at sea or the biological degradation occurring within the sediment sample if it were to be stored unfrozen. Therefore, even if it was shown that extracting from fresh sediment improved the accuracy of CDB reduction, it is unlikely to be practically implementable as a general method recommendation.

4.3.3 Dithionite addition

Sodium dithionite as a reducing agent, buffered by bicarbonate and citrate, has been used to extract reactive Fe phases from a range of media. One of the most important variables across these methods is the ratio of Na dithionite relative to the sample size and its Fe_2O_3 (iron oxide) content. We altered the method of Lalonde et al. (2012) by changing the mass of Na dithionite added to the CDB extraction for four synthetic sediments, each differing in Fe wt%, to determine whether an increased concentration of Na dithionite would liberate more Fe than the standard method.

Early methods (e.g. Aguilera and Jackson, 1953; Mehra, 1958) use 1 g of dithionite per sample, suggested sample sizes are to not exceed 4 g for soils or 1 g for clays. Generally, 1 g of dithionite is considered to only be effective for Fe_2O_3 contents < 0.5g (i.e. a dithionite to extractable Fe ratio of 2:1); where sample composition exceeds 5% Fe_2O_3, the treatment should be repeated two or three times to ensure complete extraction. Wagai and Mayer (2007) similarly employ a triple treatment method and report almost identical Fe liberation in the first and second treatment of two Oxisol samples with ~50% of this value additionally removed upon the third treatment, indicating that on initial treatment, Na dithionite at this

concentration does not have the necessary capacity to fully reduce all extractable Fe. However, note that Wagai and Mayer (2007) employed a lower concentration of dithionite (0.049 M) than (Aguilera and Jackson, 1953; Mehra, 1958) (0.128 M). Accordingly, the sample mass is also lower than applied in earlier methods, with Wagai and Mayer (2007) introducing a solid to solution ratio of 4.3 mg mL^{-1} for Fe-rich soils and 7.1 for Fe-poor soils. This results in an effective treatment at least twice as strong as that previously used, see *Table 4.1* for comparative treatment strengths.

Table 4.1 Comparison of CDB treatments which differ by Na dithionite strength.

Reference*	**Dithionite concentration**	**Sample mass**	**Dithionite: Total Solid**
Aguilera and Jackson (1953)	0.128 M	Soils:88.89 mg ml^{-1} Clays:22.22 mg ml^{-1}	1:4
Mehra (1958)	0.128 M	If sample exceeds 5% Fe_2O_3 repeat 2-3 times.	1:1
Wagai and Mayer (2007)	0.049 M	Fe rich: 4.3 mg ml^{-1} Fe poor: 7.1 mg ml^{-1}	1:0.5 1:1.2
Lalonde et al. (2012) Zhao et al. (2016)	0.1 M	Sediments and Soils: 16.67 mg ml^{-1}	1:1

*Only the first paper which implemented a new concentration of Na dithionite is listed. Multiple references for the same method are included where a subsequent method built on a previous concentration or applied this to a new media type.

To increase the strength of a chemical treatment, either the sample size must be reduced or the reagent concentration must be increased. Wagai and Mayer (2007) reduced sample size, and this is effective as dithionite is known to interfere in quantification of Fe by AAS with potential errors of up to 100% (Taylor and Crowder, 1983). Dilution or substitution of dithionite with sodium sulphite have been shown to decrease the interference. Note however that we did not experience any interference of

dithionite with AAS quantification, possibly owing to the low concentrations of dithionite employed following sample dilution or improvements in AAS technology over the last 40 years. The method we follow (Lalonde et al., 2012), applied for marine sediments, uses a 0.1 M dithionite strength per 0.25 g of sediment added, and this does not vary for Fe content as in the soils method of Wagai and Mayer (2007). However, quantification of OC-Fe in sediments indicates that %OC-Fe is typically lower and less variable in marine sediments than in soils, making classification by Fe content less necessary (Lalonde et al., 2012; Zhao et al., 2016). We only deviate from the Lalonde et al. (2012) by addition of Na dithionite to the sample, citrate, bicarbonate (CB) solution in aqueous form (dissolved in a subsample of the CB solution). Despite some warnings against this approach due to rapid decomposition of Na dithionite (Varadachari et al., 2006), we noticed no significant difference in %Fe liberated *(Figure 4.6),* which allowed for addition by pipette from a master mix as oppose to individually weighed out dithionite aliquots for each sample, saving a large amount of time.

For the four synthetic samples we subjected to dithionite reduction, these differed in composition (7-24 wt% Fe, 20-50% OC-Fe). The concentration of Fe in these samples results in an effective dithionite to Fe reduction reaction ratio of 1:0.07-0.24, based on mass. This is multiple times stronger than the concentration of dithionite previously used in incomplete Fe extractions, e.g. <50 wt% Fe extracted with a dithionite to Fe ratio of 1:0.8 for a humic-hematite complex (Adhikari and Yang, 2015). While %Fe in natural sediments rarely exceeds 10 wt% Fe, inherent heterogeneity and clustering of Fe can be seen in the Iron L_3 edge XAS spectra of sediments (Barber et al., 2017) which has the potential to drive wt% Fe higher in small samples of sediment. Additionally, %Fe-OC has been observed at concentrations exceeding 40% in terrestrial environments (Zhao et al., 2016; Patzner et al., 2020) and 50% in sandy beach sediments of subterranean estuaries (e.g. 56.31% ± 5.56 Martinique

Beach, Canada (Sirois et al., 2018)), explaining the choice to include high %OC-Fe compositions in the matrix. We find that the sample containing 20% Fh-OC (~7 wt% Fe) is maximally extracted for its reactive Fe component under the 0.25 g (0.1 M) treatment as described by Lalonde et al. (2012) *(Figure 4.5).* Maximal extraction here is defined as the point at which further addition of Na dithionite does not further increase the extraction of Fe beyond the amount of Fe extracted under the previous dithionite addition mass. For 20% Fh-OC, 0.25 g treatment removes 88.79% ± 3.55 of Fe_{Total} while 0.375 g addition extracts 90.94% ± 3.64; as these values are within error, our method presents suitable extraction capacity for sediments containing 20% OC-Fe, conditions similar to those reported in natural marine sediments (Lalonde et al., 2012).

At increased concentrations of Fe-bound OC, this trend falls away. 30 and 40% Fh-OC follow almost identical trajectories and are not maximally extracted at 0.25 g/0.1 M Na dithionite addition; instead they reach maximal extraction at 0.5 g/0.2 M with 88.65% ± 3.54 and 88.22% ± 3.53 of Fe_{Total} recovered, respectively. These values are within the error of maximal extraction for 20% Fh-OC and significantly higher than the %Fe liberated under the standard 0.1 M extraction (63.03% ± 2.52 and 67.21% ±2.69, respectively). This finding demonstrates that the OC-Fe composition would not be correctly determined following the method of Lalonde et al. (2012) for these Fe-OC-rich sediments, and the overall extent of OC-Fe in the marine sediment pool would be underestimated. While 30-40% Fh-OC are above average for marine sediment OC-Fe composition, many samples exist in the 20-30% range. Indeed, the average value for marine sediment OC-Fe composition given by Lalonde et al. (2012) is greater than 20% with individual marine sediments recorded as exceeding 30% OC-Fe (e.g. Equatorial Pacific 0°N, 34.79% (Barber et al., 2017)).

The conclusion that Na dithionite is not present in a high enough concentration , and thus inefficient, for OC-Fe rich sediments is

confounded at the 50% Fh-OC composition. Here, %Fe extracted is increased from 39.96% ± 1.60 with 0.1 M (0.25g) Na dithionite to 59.58% ± 2.38 at double strength (0.2 M). Note, however, that this differs from the previous compositions in reaching a maximum at ~60% Fe, as opposed to the ~90% achieved for 20-40% Fh-OC. Given that %Fe removed does not increase with further addition of Na dithionite (0.625 g), that the amount of Na dithionite is no longer the limiting factor in extracting Fe from Fh-OC rich samples. It is likely that another reagent, potentially trisodium citrate, may become limiting. In the extraction reaction, citrate acts as a complexing agent to keep Fe dissolved in solution (Lalonde et al., 2012; Sirois et al., 2018). If the increased strength dithionite treatment increases dissolved Fe beyond the complexing capacity of citrate, then excess Fe likely precipitates out of solution before measurement.

It is apparent that Na dithionite concentration can limit the extractability of reducible Fe and associated OC in Fe-OC rich sediments, and that the generally applied method could benefit from using increased strength Na dithionite compared to the 0.1 M treatment currently used. Based on the set of experiments we conducted, an increase to 0.2 M would be sufficient. However, if increasing the amount of Na dithionite beyond its current level, other considerations need to be made, such as the decomposition of Na dithionite in AAS standards which may skew quantifications and a reassessment of the concentration of the other reagents, sodium bicarbonate and trisodium citrate, to maintain the buffering and complexation capacity of the extraction. While we observed no shift from pH 7.0 (±0.3) throughout the extraction at greater dithionite concentrations, there was some evidence that the citrate content dropped below the amount required to fully complex all dissolved Fe as described above. It is also important to note that by increasing the concentration of these organic reagents, the background DOC of the experiment will also increase, which has the potential to interfere in OC-Fe quantification. It would be useful to include background DOC detection for samples (as per

Patzner et al. (2020)) to avoid the accidental inclusion of organic reagents in OC-Fe determination. In this example, the input of C containing compounds into the sample in the extraction procedure (citrate and bicarbonate) is mitigated against by directly measuring the C content of the reaction matrix in aqueous phase by HPLC.

4.3.4 Length of extraction

One parameter of the extraction method which has remained largely consistent across all iterations of circumneutral pH CDB treatment is an extraction length of 15 minutes (Mehra, 1958; Wagai and Mayer, 2007; Lalonde et al., 2012). Compared to other Fe phase extractions, e.g. (Poulton and Canfield, 2005), 15 minutes can be considered a short extraction, and many other chemical treatments include dithionite extraction at pH 4.8 for several hours. However, the CDB method used by us is performed at 80 ^{0}C which provides a large amount of energy to the reaction and compensates for the short reaction time. As we observed incomplete Fe extraction *(Figure 4.1)* for all our samples, a range of CDB extraction times were trialled to understand whether increasing the length of a reaction would increase Fe liberated, as seen for other chemical Fe extractions; oxalate, for example, is known to continue to extract Fe beyond 1 hour (McKeague and Day, 1966). Additionally, as previously mentioned, some iterations of the CDB method have been repeated multiple times in succession to extract the full Fe_{CDB} pool, but it is unclear whether time or reagent concentration limit full extraction of this pool on the first treatment.

Exposure time of wet and dried synthetic samples (2-COOH, 60%) to CDB was increased from the standard 15-minute treatment in 15-minute intervals to 60 minutes *(Figure 4.6).* No difference was observed for the amount of extractable Fe across the time series, concluding that an increase in chemical exposure time has no difference on Fe extractability. This shows that time is not a limiting factor in the CDB extraction, and that reductive dissolution of the susceptible Fe phases occurs rapidly. We

would perhaps not expect any benefit from increasing the length of CDB treatment as dithionite, the reductive component, is known to undergo degradation to form sodium thiosulfate and bisulfite in aqueous solutions with a rapid second order rate constant (K_2) of 3.0 (g-molecule/L)$^{-1}$ min^{-1} at 79.4 °C, indicating reducing conditions are unlikely to be sustained for long (Lister and Garvie, 1959).

While increasing extraction time has no benefit for extracting Fe with the purpose of determining the OC-Fe pool, a recent adaptation of the CDB method has extended the time of the extraction in order to compensate for a reduction in the temperature of the reaction. Patzner et al. (2020) perform a 16-hour CDB extraction at room temperature on permafrost samples to, in the first instance, determine %OC-Fe, then subsequently apply scanning electron microscopy (SEM) and nanoscale secondary ion mass spectrometry (nanoSIMS) to analyse the extracted organominerals. Here the authors had to alter the CDB method as they were concerned that exposure of organic compounds to high temperature may alter OC structure and fate, which they wished to analyse. This raises an interesting question as to whether temperature and length of the extraction can compensate for each other to achieve the overall same %Fe extraction.

In our series of experiments, temperature was not altered as we saw no benefit to decreasing temperature, and therefore energy, of the reaction as we were focused on maximising %Fe extraction. While we saw no benefit from increasing extraction time, likely due to rapid decomposition of Na dithionite, the decomposition process may occur much slower at room temperature due to the decreased reaction energy. The authors of this pre-print (Patzner et al., 2020) have yet to calibrate their method against the standard 80 °C treatment, however, the values they obtain for %OC-Fe in permafrost soils appear agreeable, if not a little higher than much of the literature for terrestrial samples (e.g. Zhao et al., 2016). This could potentially be a benefit to the CDB method in preserving the structural component of OC, which would subsequently allow for much wider

analysis on the extracted OC, such as biomarkers, which has previously been limited by both transformation of C in extraction and by sample size. This may allow us to better understand the origins and molecular makeup of OC involved in mineral preservation processes and offers promising scope for future experimentation with the CDB method.

4.4 Conclusion

Reductive dissolution of solid reactive Fe phases by CDB treatment has been presumed to fully reduce these phases and all associated OC. We have shown that a significant amount of Fe is not reduced for ferrihydrite coprecipitated with organic acids under the conditions of (Lalonde et al., 2012), agreeing with similar earlier analyses (e.g. Adhikari and Yang, 2015). In this chapter, we have attempted to increase the proportion of the extractable Fe pool removed by CDB treatment in order to ensure estimations of the iron-bound organic carbon (OC-Fe) pool are accurate and not superficial underestimates due to inefficiencies in the method. Modifications to the method are limited by chemical constraints, due to the requirement to maintain circumneutral pH in order to prevent hydrolysis of OC. We therefore altered physical parameters (time of extraction, mass of dithionite added) and sample preparation methods (freeze drying vs slurry) and attempt to cross calibrate these between synthetic samples, as in *Chapter 3*, and natural marine sediments to account for any difference in behaviour.

We see that mass of dithionite added appears to be limiting in extracting the total easily reducible Fe pool for Fe-rich sediments (10-15 wt% Fe) and a doubling of Na dithionite addition for these sediments can increase Fe extracted from ~60% to ~90%, representing a much more complete removal of the OC-Fe pool. For extremely Fe-rich sediments, or small heterogeneous samples containing Fe clusters (>25 wt% Fe), increases in dithionite alone will not remove the full Fe pool and a parallel increase in addition of the complexing agent trisodium citrate could be useful here in order to prevent precipitation of the excess Fe. Freeze-drying induced

aggregation appears to have an effect on reducing Fe liberation relative to slurry samples for synthetic samples, however, we were unable to replicate this increased extraction for natural samples and obtaining accurate wt% of Fe is impossible for non-dried samples, so this appears unworkable as a mechanism for increasing Fe liberation.

Finally, increase of reaction time (up to 1 hr, 4x standard) showed no benefit for Fe extraction, however, a recent study has used time as a compensatory factor for reduction in temperature in order to maintain OC structure for post extraction C analysis (Patzner et al., 2020). The trade-off between time and temperature requires further investigation given the rapid degradation of Na dithionite in solution. We recommend the following changes to the CDB method:

- An increase in Na dithionite added to 0.5g in order to fully reduce as much of the OC-Fe pool as possible.
- This should be complemented by a parallel increase in the ionic strength of the NaCl control extraction.
- The background DOC exclusion step of Patzner et al. (2020) should be considered to remove interference of the increased strength organic reagents in calculation of OC-Fe.

By combining these methods, we expect the accuracy of the CDB method to be improved and from experimentation with synthetic samples we expect the Fe extracted for samples previously limited by the dithionite concentration to increase by up to 30%. Further investigation is required to understand how Fe not bound to OC responds to these adaptations as we have shown that “naked” Fe is much more resistant to CDB reduction, so may remain incompletely reduced even at a greater Na dithionite strength.

Chapter 5: Conclusions, implications of findings, and directions for future research.

5.1 Conclusions

In this thesis I set out to investigate the mechanistic basis of iron bound organic carbon interactions and its subsequent implications, both on an analytical level and how this may develop our understanding of carbon preservation and cycling on a global scale. In *Chapter 1*, the following research aims were set:

1) Determine the effect of carboxyl groups on the stability of Fe_R organominerals.

2) Examine any physical effects of carboxyl content on Fe_R phases (e.g., size, crystallinity).

3) Examine the implications of carboxyl driven mineral binding mechanisms on the preservative strength of Fe for OC in marine sediments.

4) Understand how sample preparation techniques may affect the extractability of OC-Fe phases.

5) Quantify the efficiency of OC-Fe (CDB) extraction, allowing us to interpret whether current estimates of the global OC-Fe pool are accurate.

6) Test the experimental parameters of the CDB extraction to see if efficiency can be improved.

Chapter 1.8

The first and third aim represent the bulk of work conducted and the most significant findings. In precipitating ferrihydrite with small organic compounds of differing carboxyl content, this was the first study of its type to form OC-Fe compounds in this mechanistic fashion, building on previous methodologies which utilise bulk OM samples. This allowed us to isolate the specific influence of binding carboxyl groups on the stability of OC bound Fe. Stability can be defined in different ways, here by the stability of preserved C and the structural stability of the resultant organomineral. We see that as the number of carboxyl groups is increased, stronger chemical treatment is

required to remove the carboxyl containing C from Fe minerals. While C appears more recalcitrant at higher carboxyl contents, the Fe phases which precipitated in the presence of this C source became increasingly amorphous and less structurally stable, releasing an increasing amount of Fe upon reductive dissolution due to the disorder introduced into the mineral structure by high affinity C.

In addressing the second aim, we were able to determine that the stability of Fe minerals was likely to be a function of crystallinity (as measured by XRD), due to the lack of difference in other physical parameters of the organic source on the resultant organomineral. In addition to crystallinity (an internal factor), coprecipitate size (an external factor) was measured but no significant difference was observed between the differing coprecipitates. To an extent the determination of ferrihydrite size was inhibited by technological limitations, particularly for NTA due to the refractory index of Fe when under laser light, potential solutions to this are discussed in *5.3*.

Through discovering the low levels of stability associated with carboxyl rich Fe organominerals, the high stability of those phases which were either carboxyl poor or C free became apparent. Upon reductive dissolution, pure ferrihydrite phases released approximately 20% of the expected Fe and reduction for all coprecipitates remained incomplete, regardless of the presence of carboxyl moieties. This demonstrated that one of the key assumptions in our methodological approach, the Lalonde et al. (2012) method, that treatment with dithionite would "fully reduce all solid reactive iron phases and associated organic carbon", was either untrue or at the least, open to interpretation beyond its factual basis. The fourth aim was explored through attempting to increase the extractability of Fe (and therefore OC) from OC-Fe complexes, initially by comparing Fe liberated when the extraction was performed on different sample types. There had been some suggestions in the literature that freeze-drying induced aggregation of sediment could reduce Fe extractability by limiting the surface area for the reductive dissolution reaction and therefore shield some Fe molecules,

leading to incomplete reduction. Our comparison with a sediment slurry showed a small advantage for not freeze drying the synthetic coprecipitates. However, when applied to natural marine sediment this trend was not replicated and sample preparation method appeared to have no effect on the amount of Fe extracted.

The final aim expanded on the theme of increasing Fe extractability through modifying non-chemical parameters of the CDB method. Length of extraction time, amount of dithionite added and addition of dithionite in solid or aqueous form were tested. While length of extraction and the state of addition showed no difference, addition of excess dithionite (0.2 M) did increase %Fe extracted from OC-Fe rich samples by ~30%, achieving a maximum of approximately 90%. By varying the amount of dithionite added against %Fe extracted we were able to determine the efficiency of CDB extraction, meeting the fifth aim and concluding that the current approach can underestimate OC-Fe in samples by up to 30%. However increasing extraction efficiency through increasing dithionite addition is highly variable and dependent on the concentration of OC-Fe and wt %Fe present in a sample with a skew towards those samples rich in OC-Fe (>20%).

In conclusion, this mechanistic and methodological study of iron bound carbon has uncovered the cumulative importance of carboxyl functional groups in the preservation of OC; demonstrating that an increasing number of carboxyl groups has an increasing effect on the strength of OC-Fe binding. By highlighting inefficiencies and misinterpretations of the CDB method for quantifying OC-Fe, we have shown that the extent of OC-Fe interactions in marine sediments could be underestimated by approximately a third. Finally, by combining the results from these experiments with the very latest literature we have suggested a series of changes which could improve the efficiency of the CDB method, providing a more accurate method by which OC-Fe can be analysed from marine and terrestrial samples.

5.2 Implications of findings

The motivation for this investigation was predominantly mechanistic and methodological, aiming to better understand the CDB extraction method and its limitations for quantification of Fe bound OC. However, by better defining and improving the efficiency of this method in the ways outlined, future integration of our findings by the wider community has a potential to further our understanding of the extent to which OC-Fe interactions persist under a range of environmental conditions.

A concern expressed at the start of this project was the way in which applications of CDB varied widely between different groups, in subtle but important ways. An example of this is the different concentrations of dithionite in different iterations of the method, which we saw exerted a significant control on the release of Fe, varying by up to 30%. These differences in method made it difficult to build any large-scale picture of the importance of OC-Fe as results from different methods which cannot be compared. In our suggestions (increased strength dithionite, measuring of background DOC), we provide a benchmark of the best method for extracting the most OC-Fe while being practicable, i.e. by not requiring the use of unfrozen sediment. However, it is important to note there are still some limitations in our approach and other important parameters such as grain size need to be better constrained in order to produce a fully translational method (*see 5.3*).

Conditional on adoption of a universal method, ultimately improving the accuracy of OC-Fe quantification and the size of the comparable data set available, this allows the much wider potential implications of this project to be realised. Constraining the processes of the global carbon cycle is one of the largest problems transecting all disciplines of geosciences. Writing recently in *carbonbrief.org*, Hausfather and Betts (2020) state that “Future warming scenarios developed by the climate modelling community [...] do not include any of the uncertainties in carbon-cycle feedbacks”. Instead, models often either leave out biogeochemical processes altogether or include

a ‘forcing’ scenario where one parameter is included in the model to account for carbon cycling and greenhouse gas releasing processes. With preservation of OC by reactive iron being the largest described mechanism through which OC is buried in marine sediments, and terrestrial environments, accurate estimations of the size of this preserved pool could be a crucial input in constraining the carbon cycle for earth system and climate models. It can be seen that the current uncertainty in biogeochemical cycles results in a vast range of model outputs for different climate models which increase with each Representative Concentration Pathway (RCP) prediction *(Figure 5.1)*. These resultant uncertainties of several degrees in future climate predictions ultimately weaken the ability of society to understand, respond and protect against a rapidly warming planet.

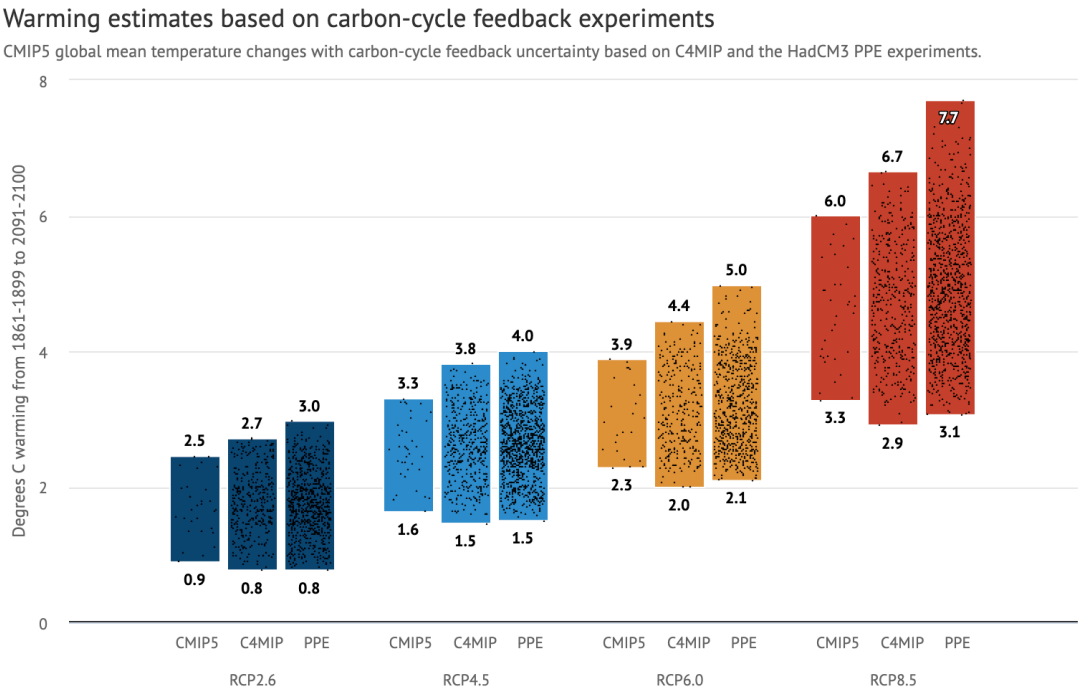

Figure 5.1 Warming estimates based on carbon cycle feedback experiments. CMIP5 global mean temperature changes with carbon cycle feedback uncertainty based on Coupled Climate Carbon Cycle Model Intercomparison Project (C4MIP) and the HadCM3 perturbed physics ensemble (PPE) experiments. Produced by Hausfather and Betts (2020), Source: https://www.carbonbrief.org/analysis-how-carbon-cycle-feedbacks-could-make-global-warming-worse (Accessed 24/05/2020)

In terms of other policy implications stemming from our findings, the physical instability due to the amorphous, gel like, nature of Fe organominerals highlights the importance of protecting marine sediments. Atwood et al. (2020) recently found that only ~2% of marine sediments are currently protected from physical disturbance and that "The lack of protection for marine C stocks makes them highly vulnerable to human disturbances that can lead to their remineralization to CO_2, further aggravating climate change impacts." In *Chapter 1* we discussed how little DOC actually becomes sequestered on meaningful timescales in the seafloor, our additional findings suggest that the chance of being preserved by reactive Fe minerals is increased when the OC structure is rich in carboxyl functional groups and therefore less degraded. It is therefore difficult to see any benefit to current geoengineering projects such as iron fertilisation, which aims to increase surface primary productivity and OC drawdown, but has no consideration for the fact very little of this OC will be sequestered due to limitations imposed by the structure of OC moieties. It would perhaps be a much better use of money and resources to build on the very little protection which currently exists for OC preserved in marine sediments, largely by reactive Fe.

5.3 Limitations and future work

As previously mentioned, one analysis that could not be completed was grain size determination using nano-tracking analysis (NTA). Initially this method was chosen for its ability to visualise as well as measure the size of different Fe organomineral grain sizes, giving an indication towards the composition of different sized fractions in the overall coprecipitate. This analysis works by shining a laser on to the coprecipitate containing solution to facilitate visualisation, however the high refractory index of Fe made this impossible to see due to light scattering and would have required use of a different filter to those available for use. In an attempt to overcome this, optical size analysis was used which similarly allows for size composition to be determined and this showed no difference in size amongst the various coprecipitates.

However, the two analyses work on different scales with NTA providing high resolution measurements at the 0.01-1 μm while optical analysis is at 0.1-10000 μm and the detected particles were at ~10 μm so may represent only one size fraction and not the complete composition.

Since particle size is postulated as one of the primary controls on Fe extractability (McKeague and Day, 1966), further work is needed in this area to understand both how particle size varies with organic content and sample preparation method. In our experiments a difference in Fe extractability of synthetic sediments was noted for those which were freeze dried vs slurried, thought to be due to particle aggregation, however no measurement of dried particle size was made. Microscopic techniques, particularly transmission electron microscopy (TEM) and scanning electron microscopy (SEM) are common tools used to measure the size of freeze dried particles and could be applied here (e.g. Greffié et al., 2001; Uramoto et al., 2014). Similarly, the lack of difference between freeze dried vs freeze thawed natural sediments was unexpected and would be better understood by applying the CDB method to non-freeze thawed sediments in order to make this comparable to the synthetic experiment. Particle sizing of the freeze thawed vs non freeze thawed sediment would further determine the impact of freeze thaw on particle aggregation and Fe extractability. Grain size of the sample remains the one important parameter of the CBD method which has yet to be constrained, this would be the final step in providing a universal approach towards OC-Fe quantification and should be considered as part of any further work in this area.

In determining OC-Fe, we noted that sometimes there was an apparent gain in %C for the control experiment which resulted in negative OC-Fe values, we hypothesised this may be due to retention of sodium bicarbonate in the mineral matrix. Treatment with concentrated hydrochloric acid significantly reduced but did not eliminate this interference. Additionally, we discussed the possibility of re-adsorption of previously liberated OC back on to the reactive Fe we know remains (due to incomplete reductive dissolution). An

experiment was planned using ^{13}C labelled sodium bicarbonate to determine whether the retained C is from the organic compound source, or added in the reaction. However, because of the relatively small addition of sodium bicarbonate relative to all other ^{12}C compounds (citrate, organic acids) a high amount of ^{13}C labelled bicarbonate would be needed to make a noticeable difference in the isotopic signature. This would have been both expensive, and it is also difficult to find a facility capable and willing to measure such highly enriched isotopic samples. Nevertheless, it would be interesting to understand the fate of organic reagents given their unusual involvement in this extraction of organic compounds.

Finally, there remains a range of other parameters and conditions that could be changed to further the scope of this study, for example:

- How does age of the sample affect OC-Fe extractability. Freshly synthesised sediments likely behave differently to those which have been in the seafloor for thousands of years. This may explain why we have such a high contribution of small, less structurally complex organics being removed in the control experiment of the CDB method. Perhaps these molecules are physically removed by diagenetic processes , ocean current circulation at the seafloor or bioturbation and we are not replicating that stage in laboratory experiments.
- How do different functional groups contribute to OC-Fe interactions? While it is known that carboxyl groups are the primary binding group for OC moieties to Fe the role of other groups, both in isolation and alongside carboxyl groups is unknown. Extraction of coprecipitates containing carboxyl + other functional groups could be compared to our carboxyl only samples to determine this effect.
- Similarly to the previous point, the extractability of large compounds, such as those produced by geopolymerisation is unknown. Determining whether these compounds are extracted by CDB is important to decipher whether preservation of OC through geopolymerisation has been included in the ~22% of OC estimated to

be preserved by reactive Fe or whether this is an individual process which should be considered separately in terms of extraction and quantification.

- Finally, further variation could be considered in terms of the mineral counterpart of the coprecipitate. The Fe phase could be changed from ferrihydrite to others in the same Fe_{OXI} extractability bracket (e.g. lepidocrocite) to determine if other Fe phases are involved in the preservation of OC. Similarly, it would be interesting to coprecipitate OC with other minerals such as manganese oxide (birnessite) to determine whether OC preserved by other reactive mineral interfaces (as established by Allard et al. (2017)) are extracted by the CDB method or not.

In summary, there remains a wide scope for further work to be conducted on the preservation of OC on reactive minerals interfaces. The proposed further work here largely aims to understand which processes are included in the CDB OC-Fe extracted pool and which processes are supplementary to this. As we know, while reactive Fe minerals explain the largest amount (21.5 % ± 8.6) of OC preservation, it does not explain it all. Consideration of these additional processes are aimed to improve the overall picture of how OC is preserved in marine sediments. The implications of which, as discussed, have widespread consequences for both the geosciences and biogeochemical communities and potentially our response as a society to future projections of a warming planet.

Appendix 1: Conference presentations

1.1 Quaternary Research Association Annual Discussion Meeting, 8-10th January 2020, Leeds, UK. Oral Presentation.

Implications of organic ligand dependent preservation of iron in the seafloor for marine carbon cycling.

Ben Fisher*, Christian März, Johan Faust, Oliver Moore, Caroline Peacock
*eebf@leeds.ac.uk
University of Leeds, Earth Surface Science Institute, School of Earth and Environment, United Kingdom of Great Britain and Northern Ireland

1.2 European Geosciences Union General Assembly, 4-8th May 2020, Vienna, Austria. Oral Presentation in Session BG4.1 "Biogeochemistry of costal seas and continental shelves".

What's af(Fe)cting OC-Fe interactions? An experimental approach to understanding iron bound organic carbon in sediments.

Ben Fisher*, Christian März, Johan Faust, Oliver Moore, and Caroline Peacock
University of Leeds, Earth Surface Science Institute, School of Earth and Environment, United Kingdom of Great Britain and Northern Ireland
*eebf@leeds.ac.uk
https://doi.org/10.5194/egusphere-egu2020-855

Note: Conference cancelled due to COVID-19, presentation was instead given online on 6th May as part of "shareEGU", a virtual alternative to the physical meeting.

Appendix 2: Determination of OC-Fe including non-presented data. *Shaded data indicates that which is presented.*

Repeat 1

Sample	%Fh-OC	Initial C (wt %)	Initial reduction mass (g)	Reduction C (wt %)	Reduction end mass (g)	Initial control mass (g)	Control C (wt %)	Control end mass (g)	% OC-Fe
0 COOH	0	0.032123	0.2537	0.16899	0.2928	0.2540	0.13956	0.3052	-85.12
0 COOH	10	0.01962	0.2462	0.26345	0.2928	0.2490	0.12335	0.3072	-821.27
0 COOH	20	0.098327	0.2493	0.25056	0.3118	0.2558	0.18034	0.3384	-76.08
0 COOH	30	0.13719	0.2454	0.10605	0.3234	0.253	0.10605	0.3503	5.16
0 COOH	40	0.16569	0.2536	0.42558	0.3456	0.2559	0.14074	0.3744	-225.76
0 COOH	50	0.16423	0.2554	0.29987	0.3871	0.2459	0.12772	0.3764	-157.71
1 COOH	0	0.032123	0.2565	0.25153	0.3038	0.2491	0.1902	0.3002	-213.85
1 COOH	10	0.32763	0.2457	0.30135	0.3133	0.2477	0.15287	0.3046	-59.91
1 COOH	20	0.63632	0.2476	0.70178	0.2999	0.2513	0.16054	0.3298	-100.47
1 COOH	30	0.891	0.2466	0.32749	0.3155	0.2568	0.13506	0.3619	-25.66
1 COOH	40	0.97759	0.2557	0.86772	0.3381	0.2566	0.14821	0.3672	-95.67
1 COOH	50	1.3567	0.2516	0.80076	0.3403	0.2456	0.1024	0.3789	-68.19
2 COOH	0	0.032123	0.2550	0.31155	0.2973	0.2520	0.21239	0.2848	-383.51
2 COOH	10	0.89403	0.2507	0.49677	0.1836	0.2550	0.29459	0.3134	-0.20
2 COOH	20	1.6811	0.2525	0.51541	0.2615	0.2497	0.30307	0.313	-9.15
2 COOH	30	2.1917	0.2499	0.6912	0.2462	0.2539	0.33205	0.3253	-11.66
2 COOH	40	3.2373	0.2472	0.89542	0.2571	0.243	0.55328	0.3436	-4.60
2 COOH	50	3.6391	0.2519	1.1352	0.2488	0.2445	0.48585	0.366	-10.83
3 COOH	0	0.032123	0.2444	0.2246	0.264	0.2434	0.28243	0.2756	240.27
3 COOH	10	1.4512	0.2514	0.28128	0.2561	0.2607	0.54913	0.3261	27.59
3 COOH	20	2.7608	0.2569	0.44328	0.2589	0.2428	1.0863	0.3023	32.81
3 COOH	30	4.3386	0.2498	0.43168	0.254	0.2527	1.7022	0.3341	41.75
3 COOH	40	5.4203	0.2467	0.63015	0.1922	0.254	2.3194	0.3458	49.20
3 COOH	50	6.9348	0.2558	0.93963	0.1871	0.2544	2.7639	0.3667	47.54

Sample	%Fh-OC	Initial C (wt %)	Initial reduction mass g)	Reduction C (wt %)	Reduction end mass (g)	Initial control mass (g)	Control C (wt %)	Control end mass (g)	OC-Fe
0 COOH	0	0.032123	0.2531	0.064796	0.3232	0.2497	0.04373	0.2925	-98.11
0 COOH	10	0.01962	0.2475	0.050552	0.3106	0.2483	0.036668	0.3254	-78.42
0 COOH	20	0.098327	0.2454	0.091367	0.3092	0.2500	0.055273	0.3107	-47.22
0 COOH	30	0.13719	0.2539	0.17859	0.3193	0.2494	0.016907	0.3858	-144.64
0 COOH	40	0.16569	0.2526	0.1795	0.2911	0.2547	0.034869	0.3232	-98.14
0 COOH	50	0.16423	0.2486	0.1969	0.3007	0.2565	0.0041936	0.3088	-141.95
1 COOH	0	0.032123	0.2580	0.03631	0.3280	0.2553	0.0064916	0.2991	-120.03
1 COOH	10	0.32763	0.2500	0.20277	0.3130	0.2552	0.20025	0.3302	1.60
1 COOH	20	0.63632	0.2478	0.4953	0.2912	0.2459	0.042731	0.3544	-81.79
1 COOH	30	0.891	0.2467	0.6158	0.3059	0.2461	0.86016	0.3724	60.38
1 COOH	40	0.97759	0.2499	1.0006	0.2975	0.2542	0.023506	0.3236	-118.79
1 COOH	50	1.3567	0.2549	1.0789	0.3156	0.2570	0.031297	0.3199	-95.59
2 COOH	0	0.032123	0.2561	0.14293	0.3223	0.2564	0.1237	0.3293	-65.39
2 COOH	10	0.89403	0.2504	0.14454	0.2882	0.2565	0.27596	0.3471	23.16
2 COOH	20	1.6811	0.2567	0.28679	0.3027	0.2574	0.31751	0.3477	5.40
2 COOH	30	2.1917	0.2555	0.51216	0.2927	0.2535	0.57417	0.3809	12.59
2 COOH	40	3.2373	0.2516	1.3453	0.2714	0.2502	0.46141	0.3454	-25.15
2 COOH	50	3.6391	0.2533	1.1213	0.233	0.2534	0.6886	0.3245	-4.11
3 COOH	0	0.032123	0.2469	0.18238	0.2998	0.2595	0.13633	0.3342	-142.83
3 COOH	10	1.4512	0.2422	0.17372	0.2629	0.2560	0.49993	0.3352	32.11
3 COOH	20	2.7608	0.2482	0.25118	0.2655	0.2428	1.1615	0.3334	48.04
3 COOH	30	4.3386	0.2579	0.30733	0.2314	0.2518	1.6655	0.3878	52.77
3 COOH	40	5.4203	0.2572	0.47018	0.2279	0.2556	2.5039	0.3293	51.83
3 COOH	50	6.9348	0.2553	0.90434	0.2131	0.2586	2.898	0.3495	45.59

Notes on additional data: The very low values of %C for <20% Fh-OC produce widely variable and mathematically impossible values (<0 or >100) for OC-Fe so are not included in the thesis analysis, it would be difficult to find an instrument with the necessary precision for these traces of C and the trends at higher concentrations provide enough information to come to valid conclusions. Similarly, 0 COOH is not shown as this contains no C, but proved to be useful as a control experiment to validate other results.

Collated References

Acelas, N.Y., Hadad, C., Restrepo, A., Ibarguen, C. and Florez, E. 2017. Adsorption of Nitrate and Bicarbonate on Fe-(Hydr)oxide. *Inorg Chem.* **56**(9), pp.5455-5464.

Adhikari, D. and Yang, Y. 2015. Selective stabilization of aliphatic organic carbon by iron oxide. *Sci Rep.* **5**(1), p11214.

Aguilera, N.H. and Jackson, M.L. 1953. Iron Oxide Removal from Soils and Clays. *Soil Science Society of America Journal.* **17**(4), pp.359-364.

Alexander, M. 1981. Biodegradation of chemicals of environmental concern. *Science.* **211**(4478), pp.132-138.

Allard, S., Gutierrez, L., Fontaine, C., Croue, J.P. and Gallard, H. 2017. Organic matter interactions with natural manganese oxide and synthetic birnessite. *Sci Total Environ.* **583**, pp.487-495.

Aller, R. and Aller, J. 1998. The effect of biogenic irrigation intensity and solute exchange on diagenetic reaction rates in marine sediments. *Journal of Marine Research.* **56**, pp.905-936.

Aller, R.C. and Aller, J.Y. 1998. The effect of biogenic irrigation intensity and solute exchange on diagenetic reaction rates in marine sediments. *Journal of Marine Research.* **56**(4), pp.905-936.

Anderson, L.G. and Macdonald, R.W. 2015. Observing the Arctic Ocean carbon cycle in a changing environment. *Polar Research.* **34**(1), p26891.

Arndt, S., Jørgensen, B.B., LaRowe, D.E., Middelburg, J.J., Pancost, R.D. and Regnier, P. 2013. Quantifying the degradation of organic matter in marine sediments: A review and synthesis. *Earth-Science Reviews.* **123**, pp.53-86.

Arrieta, J.M., Mayol, E., Hansman, R.L., Herndl, G.J., Dittmar, T. and Duarte, C.M. 2015. Ocean chemistry. Dilution limits dissolved organic carbon utilization in the deep ocean. *Science.* **348**(6232), pp.331-333.

Atwood, T.B., Witt, A., Mayorga, J., Hammill, E. and Sala, E. 2020. Global Patterns in Marine Sediment Carbon Stocks. *Frontiers in Marine Science.* **7**(165).

Baldock, J.A. and Skjemstad, J.O. 2000. Role of the soil matrix and minerals in protecting natural organic materials against biological attack. *Organic Geochemistry.* **31**(7-8), pp.697-710.

Barbanti, A. and Bothner, M.H. 1993. A procedure for partitioning bulk sediments into distinct grain-size fractions for geochemical analysis. *Environmental Geology.* **21**(1-2), pp.3-13.

Barber, A., Brandes, J., Leri, A., Lalonde, K., Balind, K., Wirick, S., Wang, J. and Gelinas, Y. 2017. Preservation of organic matter in marine sediments by inner-sphere interactions with reactive iron. *Sci Rep.* **7**(1), p366.

Barber, R.T. 1968. Dissolved organic carbon from deep waters resists microbial oxidation. *Nature.* **220**(5164), pp.274-275.

Bastviken, D. 2009. Methane. In: Likens, G.E. ed. *Encyclopedia of Inland Waters.* Oxford: Academic Press, pp.783-805.

Bender, M.L. and Heggie, D.T. 1984. Fate of organic carbon reaching the deep sea floor: a status report. *Geochimica et Cosmochimica Acta.* **48**(5), pp.977-986.

Berg, P., Rysgaard, S., Funch, P. and Sejr, M.K. 2001. Effects of bioturbation on solutes and solids in marine sediments. *Aquatic Microbial Ecology.* **26**, pp.81-94.

Bernard, S. 1997. Removal of organic compounds by adsorption on pyrolusite (β-MnO2). *Water Research.* **31**(5), pp.1216-1222.

Berner, R.A. 1987. Models for carbon and sulfur cycles and atmospheric oxygen; application to Paleozoic geologic history. *American Journal of Science.* **287**(3), pp.177-196.

Boetius, A., Albrecht, S., Bakker, K., Bienhold, C., Felden, J., Fernandez-Mendez, M., Hendricks, S., Katlein, C., Lalande, C., Krumpen, T., Nicolaus, M., Peeken, I., Rabe, B., Rogacheva, A., Rybakova, E., Somavilla, R., Wenzhofer, F. and Party, R.V.P.A.-.-S.S. 2013. Export of algal biomass from the melting Arctic sea ice. *Science.* **339**(6126), pp.1430-1432.

Bongiorno, G., Bünemann, E.K., Oguejiofor, C.U., Meier, J., Gort, G., Comans, R., Mäder, P., Brussaard, L. and de Goede, R. 2019. Sensitivity of labile carbon fractions to tillage and organic matter management and their potential as comprehensive soil quality indicators across pedoclimatic conditions in Europe. *Ecological Indicators.* **99**, pp.38-50.

Bonneville, S., Van Cappellen, P. and Behrends, T. 2004. Microbial reduction of iron(III) oxyhydroxides: effects of mineral solubility and availability. *Chemical Geology.* **212**(3-4), pp.255-268.

Bosatta, E. and Ågren, G.I. 1999. Soil organic matter quality interpreted thermodynamically. *Soil Biology and Biochemistry.* **31**(13), pp.1889-1891.

Bowles, M.W., Mogollon, J.M., Kasten, S., Zabel, M. and Hinrichs, K.U. 2014. Global rates of marine sulfate reduction and implications for sub-sea-floor metabolic activities. *Science.* **344**(6186), pp.889-891.

Burdige, D.J. 2007. Preservation of organic matter in marine sediments: controls, mechanisms, and an imbalance in sediment organic carbon budgets? *Chem Rev.* **107**(2), pp.467-485.

Canfield, D.E. 1993. Organic Matter Oxidation in Marine Sediments. *Interactions of C, N, P and S Biogeochemical Cycles and Global Change.* pp.333-363.

Canfield, D.E. 1994. Factors influencing organic carbon preservation in marine sediments. *Chem Geol.* **114**(3-4), pp.315-329.

Canfield, D.E., Thamdrup, B. and Hansen, J.W. 1993. The anaerobic degradation of organic matter in Danish coastal sediments: iron reduction, manganese reduction, and sulfate reduction. *Geochim Cosmochim Acta.* **57**(16), pp.3867-3883.

Carlson, L. and Schwertmann, U. 1981. Natural ferrihydrites in surface deposits from Finland and their association with silica. *Geochimica et Cosmochimica Acta.* **45**(3), pp.421-429.

Cartapanis, O., Bianchi, D., Jaccard, S.L. and Galbraith, E.D. 2016. Global pulses of organic carbon burial in deep-sea sediments during glacial maxima. *Nat Commun.* **7**(1), p10796.

Cavan, E.L., Trimmer, M., Shelley, F. and Sanders, R. 2017. Remineralization of particulate organic carbon in an ocean oxygen minimum zone. *Nat Commun.* **8**(1), p14847.

Chen, C., Dynes, J.J., Wang, J. and Sparks, D.L. 2014. Properties of Fe-organic matter associations via coprecipitation versus adsorption. *Environ Sci Technol.* **48**(23), pp.13751-13759.

Cismasu, A.C., Michel, F.M., Tcaciuc, A.P., Tyliszczak, T. and Brown, J.G.E. 2011. Composition and structural aspects of naturally occurring ferrihydrite. *Comptes Rendus Geoscience.* **343**(2-3), pp.210-218.

Clark, P.U., Dyke, A.S., Shakun, J.D., Carlson, A.E., Clark, J., Wohlfarth, B., Mitrovica, J.X., Hostetler, S.W. and McCabe, A.M. 2009. The Last Glacial Maximum. *Science.* **325**(5941), pp.710-714.

Cong, Z., Gao, S., Zhao, W., Wang, X., Wu, G., Zhang, Y., Kang, S., Liu, Y. and Ji, J. 2018. Iron oxides in the cryoconite of glaciers on the Tibetan Plateau: abundance, speciation and implications. *The Cryosphere.* **12**(10), pp.3177-3186.

Connolly, C.T., Cardenas, M.B., Burkart, G.A., Spencer, R.G.M. and McClelland, J.W. 2020. Groundwater as a major source of dissolved organic matter to Arctic coastal waters. *Nat Commun.* **11**(1), p1479.

Cooper, R.E., Eusterhues, K., Wegner, C.-E., Totsche, K.U. and Küsel, K. 2017. Ferrihydrite-associated organic matter (OM) stimulates reduction by Shewanella oneidensis MR-1 and a complex microbial consortia. *Biogeosciences.* **14**(22), pp.5171-5188.

Cowie, G.L. and Hedges, J.I. 1992. The role of anoxia in organic matter preservation in coastal sediments: relative stabilities of the major biochemicals under oxic and anoxic depositional conditions. *Organic Geochemistry.* **19**(1-3), pp.229-234.

Cowie, G.L. and Hedges, J.I. 1992. Sources and reactivities of amino acids in a coastal marine environment. *Limnology and Oceanography.* **37**(4), pp.703-724.

Cowie, G.L., Hedges, J.I. and Calvert, S.E. 1992. Sources and relative reactivities of amino acids, neutral sugars, and lignin in an intermittently anoxic marine environment. *Geochimica et Cosmochimica Acta.* **56**(5), pp.1963-1978.

Dasgupta, R. and Hirschmann, M.M. 2010. The deep carbon cycle and melting in Earth's interior. *Earth and Planetary Science Letters.* **298**(1), pp.1-13.

Davidson, E.A. and Janssens, I.A. 2006. Temperature sensitivity of soil carbon decomposition and feedbacks to climate change. *Nature.* **440**(7081), pp.165-173.

Deb, B.C. 1950. The Estimation of Free Iron Oxides in Soils and Clays and Their Removal. *Journal of Soil Science.* **1**(2), pp.212-220.

Dicen, G.P., Navarrete, I.A., Rallos, R.V., Salmo, S.G. and Garcia, M.C.A. 2018. The role of reactive iron in long-term carbon sequestration in mangrove sediments. *Journal of Soils and Sediments.* **19**(1), pp.501-510.

Ding, Q., Schweiger, A., L'Heureux, M., Battisti, David S., Po-Chedley, S., Johnson, Nathaniel C., Blanchard-Wrigglesworth, E., Harnos, K., Zhang, Q., Eastman, R. and Steig, Eric J. 2017. Influence of high-latitude atmospheric circulation changes on summertime Arctic sea ice. *Nature Climate Change.* **7**(4), pp.289-295.

Emerson, S. and Hedges, J.I. 1988. Processes controlling the organic carbon content of open ocean sediments. *Paleoceanography.* **3**(5), pp.621-634.

Estes, E.R., Pockalny, R., D'Hondt, S., Inagaki, F., Morono, Y., Murray, R.W., Nordlund, D., Spivack, A.J., Wankel, S.D., Xiao, N. and Hansel, C.M. 2019. Persistent organic matter in oxic subseafloor sediment. *Nature Geoscience.* **12**(2), pp.126-131.

Eusterhues, K., Hädrich, A., Neidhardt, J., Küsel, K., Keller, T.F., Jandt, K.D. and Totsche, K.U. 2014a. Reduction of ferrihydrite with adsorbed and

coprecipitated organic matter: microbial reduction by Geobacter bremensis vs. abiotic reduction by Na-dithionite. *Biogeosciences.* **11**(18), pp.4953-4966.

Eusterhues, K., Neidhardt, J., Hädrich, A., Küsel, K. and Totsche, K.U. 2014b. Biodegradation of ferrihydrite-associated organic matter. *Biogeochemistry.* **119**(1-3), pp.45-50.

Eusterhues, K., Rennert, T., Knicker, H., Kogel-Knabner, I., Totsche, K.U. and Schwertmann, U. 2011. Fractionation of organic matter due to reaction with ferrihydrite: coprecipitation versus adsorption. *Environ Sci Technol.* **45**(2), pp.527-533.

Eusterhues, K., Wagner, F.E., Hausler, W., Hanzlik, M., Knicker, H., Totsche, K.U., Kogel-Knabner, I. and Schwertmann, U. 2008. Characterization of ferrihydrite-soil organic matter coprecipitates by X-ray diffraction and Mossbauer spectroscopy. *Environ Sci Technol.* **42**(21), pp.7891-7897.

Feng, X., Simpson, A.J. and Simpson, M.J. 2005. Chemical and mineralogical controls on humic acid sorption to clay mineral surfaces. *Organic Geochemistry.* **36**(11), pp.1553-1566.

Ferdelman, T.G. 1988. *The distribution of sulfur, iron, manganese, copper, and uranium in a salt marsh sediment core as determined by a sequential extraction method*. Masters thesis, University of Delaware.

Field, C.B., Behrenfeld, M.J., Randerson, J.T. and Falkowski, P. 1998. Primary production of the biosphere: integrating terrestrial and oceanic components. *Science.* **281**(5374), pp.237-240.

Fox, C.A., Abdulla, H.A., Burdige, D.J., Lewicki, J.P. and Komada, T. 2018. Composition of Dissolved Organic Matter in Pore Waters of Anoxic Marine Sediments Analyzed by 1H Nuclear Magnetic Resonance Spectroscopy. *Frontiers in Marine Science.* **5**(172).

Fuller, C.C., Davis, J.A. and Waychunas, G.A. 1993. Surface chemistry of ferrihydrite: Part 2. Kinetics of arsenate adsorption and coprecipitation. *Geochimica et Cosmochimica Acta.* **57**(10), pp.2271-2282.

Gattuso, J.P., Gentili, B., Duarte, C.M., Kleypas, J.A., Middelburg, J.J. and Antoine, D. 2006. Light availability in the coastal ocean: impact on the distribution of benthic photosynthetic organisms and their contribution to primary production. *Biogeosciences.* **3**(4), pp.489-513.

Geffard, O., His, E., Budzinski, H., Chiffoleau, J.F., Coynel, A. and Etcheber, H. 2004. Effects of storage method and duration on the toxicity of marine sediments to embryos of Crassostrea gigas oysters. *Environ Pollut.* **129**(3), pp.457-465.

Glud, R.N. 2008. Oxygen dynamics of marine sediments. *Marine Biology Research.* **4**(4), pp.243-289.

Gorbunov, N., Dzyadevich, G. and Tunik, B. 1961. Methods of determining non-silicate amorphous and crystalline sesquioxides in soils and clays. *Soviet Soil Science.* **11**, pp.1252-1259.

Gorski, C.A., Edwards, R., Sander, M., Hofstetter, T.B. and Stewart, S.M. 2016. Thermodynamic Characterization of Iron Oxide-Aqueous Fe(2+) Redox Couples. *Environ Sci Technol.* **50**(16), pp.8538-8547.

Greffié, C., Amouric, M. and Parron, C. 2001. HRTEM study of freeze-dried and untreated synthetic ferrihydrites: consequences of sample processing. *Clay Minerals.* **36**(3), pp.381-387.

Gu, B., Schmitt, J., Chen, Z., Liang, L. and McCarthy, J.F. 1994. Adsorption and desorption of natural organic matter on iron oxide: mechanisms and models. *Environ Sci Technol.* **28**(1), pp.38-46.

Gu, B., Schmitt, J., Chen, Z., Liang, L. and McCarthy, J.F. 1995. Adsorption and desorption of different organic matter fractions on iron oxide. *Geochimica et Cosmochimica Acta.* **59**(2), pp.219-229.

Han, L., Sun, K., Keiluweit, M., Yang, Y., Yang, Y., Jin, J., Sun, H., Wu, F. and Xing, B. 2019. Mobilization of ferrihydrite-associated organic carbon during Fe reduction: Adsorption versus coprecipitation. *Chemical Geology.* **503**, pp.61-68.

Hansell, D., Carlson, C., Repeta, D. and Schlitzer, R. 2009. Dissolved Organic Matter in the Ocean: A Controversy Stimulates New Insights. *Oceanography.* **22**(4), pp.202-211.

Hansell, D.A. 2013. Recalcitrant dissolved organic carbon fractions. *Ann Rev Mar Sci.* **5**(1), pp.421-445.

Hansen, J., Johnson, D., Lacis, A., Lebedeff, S., Lee, P., Rind, D. and Russell, G. 1981. Climate impact of increasing atmospheric carbon dioxide. *Science.* **213**(4511), pp.957-966.

Hausfather, Z. and Betts, R. 2020. Analysis: How 'carbon-cycle feedbacks' could make global warming worse. *Carbonbrief.* [Online]. Available from: https://www.carbonbrief.org/analysis-how-carbon-cycle-feedbacks-could-make-global-warming-worse

Hayes, M.H.B. 2006. Solvent Systems for the Isolation of Organic Components from Soils. *Soil Science Society of America Journal.* **70**(3), pp.986-994.

He, W., Chen, M., Schlautman, M.A. and Hur, J. 2016. Dynamic exchanges between DOM and POM pools in coastal and inland aquatic ecosystems: A review. *Science of The Total Environment.* **551-552**, pp.415-428.

Hedges, J.I. 1992. Global biogeochemical cycles: progress and problems. *Marine Chemistry.* **39**(1-3), pp.67-93.

Hedges, J.I. 1999. Sedimentary organic matter preservation; a test for selective degradation under oxic conditions. *American Journal of Science.* **299**(7-9), pp.529-555.

Hedges, J.I. and Keil, R. 1995. Sedimentary organic matter preservation: an assessment and speculative synthesis. *Marine Chemistry.* **49**(2-3), pp.81-115.

Hedges, J.I. and Keil, R.G. 1995. Sedimentary organic matter preservation: an assessment and speculative synthesis. *Marine Chemistry.* **49**(2-3), pp.81-115.

Hedges, J.I. and Oades, J.M. 1997. Comparative organic geochemistries of soils and marine sediments. *Organic Geochemistry.* **27**(7-8), pp.319-361.

Hemingway, J.D., Rothman, D.H., Grant, K.E., Rosengard, S.Z., Eglinton, T.I., Derry, L.A. and Galy, V.V. 2019. Mineral protection regulates long-term global preservation of natural organic carbon. *Nature.* **570**(7760), pp.228-231.

Henneberry, Y.K., Kraus, T.E.C., Nico, P.S. and Horwath, W.R. 2012. Structural stability of coprecipitated natural organic matter and ferric iron under reducing conditions. *Organic Geochemistry.* **48**, pp.81-89.

Hepburn, L.E., Butler, I.B., Boyce, A. and Schröder, C. 2020. The use of operationally-defined sequential Fe extraction methods for mineralogical applications: A cautionary tale from Mössbauer spectroscopy. *Chemical Geology.* **543**.

Hertkorn, N., Benner, R., Frommberger, M., Schmitt-Kopplin, P., Witt, M., Kaiser, K., Kettrup, A. and Hedges, J.I. 2006. Characterization of a major refractory component of marine dissolved organic matter. *Geochimica et Cosmochimica Acta.* **70**(12), pp.2990-3010.

Hofmann, A., Pelletier, M., Michot, L., Stradner, A., Schurtenberger, P. and Kretzschmar, R. 2004. Characterization of the pores in hydrous ferric oxide aggregates formed by freezing and thawing. *J Colloid Interface Sci.* **271**(1), pp.163-173.

Holland, P.R., Bracegirdle, T.J., Dutrieux, P., Jenkins, A. and Steig, E.J. 2019. West Antarctic ice loss influenced by internal climate variability and anthropogenic forcing. *Nature Geoscience.* **12**(9), pp.718-724.

Hood, E., Battin, T.J., Fellman, J., O'Neel, S. and Spencer, R.G.M. 2015. Storage and release of organic carbon from glaciers and ice sheets. *Nature Geoscience.* **8**(2), pp.91-96.

Hoogakker, B.A.A., Elderfield, H., Schmiedl, G., McCave, I.N. and Rickaby, R.E.M. 2014. Glacial–interglacial changes in bottom-water oxygen content on the Portuguese margin. *Nature Geoscience.* **8**(1), pp.40-43.

Hyun, J.-H., Kim, S.-H., Mok, J.-S., Cho, H., Lee, T., Vandieken, V. and Thamdrup, B. 2017. Manganese and iron reduction dominate organic carbon oxidation in surface sediments of the deep Ulleung Basin, East Sea. *Biogeosciences.* **14**(4), pp.941-958.

IAEA. 2003. *Collection and preparation of bottom sediment samples for analysis of radionuclides and trace elements.* Vienna.

IPCC. 2013. *Climate Change 2013: The Physical Science Basis. Contribution of Working Group I to the Fifth Assessment Report of the Intergovernmental Panel on Climate Change.* Cambridge, United Kingdom and New York, NY, USA: Cambridge University Press.

Jannasch, H.W. 1994. The microbial turnover of carbon in the deep-sea environment. *Global and Planetary Change.* **9**(3-4), pp.289-295.

Jiang, Z., Liu, Q., Roberts, A.P., Barrón, V., Torrent, J. and Zhang, Q. 2018. A new model for transformation of ferrihydrite to hematite in soils and sediments. *Geology.*

Jiao, N., Herndl, G.J., Hansell, D.A., Benner, R., Kattner, G., Wilhelm, S.W., Kirchman, D.L., Weinbauer, M.G., Luo, T., Chen, F. and Azam, F. 2010. Microbial production of recalcitrant dissolved organic matter: long-term carbon storage in the global ocean. *Nat Rev Microbiol.* **8**(8), pp.593-599.

Jiao, N., Robinson, C., Azam, F., Thomas, H., Baltar, F., Dang, H., Hardman-Mountford, N.J., Johnson, M., Kirchman, D.L., Koch, B.P., Legendre, L., Li, C., Liu, J., Luo, T., Luo, Y.W., Mitra, A., Romanou, A., Tang, K., Wang, X., Zhang, C. and Zhang, R. 2014. Mechanisms of microbial carbon sequestration in the ocean – future research directions. *Biogeosciences.* **11**(19), pp.5285-5306.

Jokinen, S.A., Jilbert, T., Tiihonen-Filppula, R. and Koho, K. 2020. Terrestrial organic matter input drives sedimentary trace metal sequestration in a human-impacted boreal estuary. *Science of The Total Environment.* **717**, p137047.

Jones, D.L. and Edwards, A.C. 1998. Influence of sorption on the biological utilization of two simple carbon substrates. *Soil Biology and Biochemistry.* **30**(14), pp.1895-1902.

Kaiser, K. and Guggenberger, G. 2000. The role of DOM sorption to mineral surfaces in the preservation of organic matter in soils. *Organic Geochemistry.* **31**(7-8), pp.711-725.

Kaiser, K. and Guggenberger, G. 2003. Mineral surfaces and soil organic matter. *European Journal of Soil Science.* **54**(2), pp.219-236.

Karlsson, T. and Persson, P. 2010. Coordination chemistry and hydrolysis of Fe(III) in a peat humic acid studied by X-ray absorption spectroscopy. *Geochimica et Cosmochimica Acta.* **74**(1), pp.30-40.

Karlsson, T. and Persson, P. 2012. Complexes with aquatic organic matter suppress hydrolysis and precipitation of Fe(III). *Chemical Geology.* **322-323**, pp.19-27.

Kaushik, N.K. and Hynes, H.B.N. 1971. The fate of the dead leaves that fall into streams. *Arch. Hydrobiol.* **68**, pp.465-515.

Keil, R. and Mayer, L. 2014. Mineral matrices and organic matter.

Keil, R.G., Montluçon, D.B., Prahl, F.G. and Hedges, J.I. 1994. Sorptive preservation of labile organic matter in marine sediments. *Nature.* **370**(6490), pp.549-552.

Keiser, L., Soreghan, G.S. and Joo, Y.J. 2014. Effects Of Drying Techniques On Grain-Size Analyses of Fine-Grained Sediment. *Journal of Sedimentary Research.* **84**(10), pp.893-896.

Kim, J.T. and Kim, S.J. 2003. Environmental, mineralogical, and genetic characterization of ochreous and white precipitates from acid mine drainages in Taebaeg, Korea. *Environ Sci Technol.* **37**(10), pp.2120-2126.

Kleber, M. 2010. What is recalcitrant soil organic matter? *Environmental Chemistry.* **7**(4).

Kleber, M., Eusterhues, K., Keiluweit, M., Mikutta, C., Mikutta, R. and Nico, P.S. 2015. Mineral–Organic Associations: Formation, Properties, and Relevance in Soil Environments. *Advances in Agronomy.* **130**, pp.1-140.

Koç, N. and Jansen, E. 1994. Response of the high-latitude Northern Hemisphere to orbital climate forcing: Evidence from the Nordic Seas. *Geology.* **22**(6), pp.523-526.

Kohnen, M.E.L., Damsté, J.S.S., Kock-van Dalen, A.C., Haven, H.L.T., Rullkötter, J. and De Leeuw, J.W. 1990. Origin and diagenetic transformations of C25 and C30 highly branched isoprenoid sulphur compounds: Further evidence for the formation of organically bound sulphur during early diagenesis. *Geochimica et Cosmochimica Acta.* **54**(11), pp.3053-3063.

Kolonic, S., Wagner, T., Forster, A., Sinninghe Damsté, J.S., Walsworth-Bell, B., Erba, E., Turgeon, S., Brumsack, H.-J., Chellai, E.H., Tsikos, H., Kuhnt, W. and Kuypers, M.M.M. 2005. Black shale deposition on the northwest African Shelf during the Cenomanian/Turonian oceanic

anoxic event: Climate coupling and global organic carbon burial. *Paleoceanography.* **20**(1), pp.n/a-n/a.

Konhauser, K.O., Planavsky, N.J., Hardisty, D.S., Robbins, L.J., Warchola, T.J., Haugaard, R., Lalonde, S.V., Partin, C.A., Oonk, P.B.H., Tsikos, H., Lyons, T.W., Bekker, A. and Johnson, C.M. 2017. Iron formations: A global record of Neoarchaean to Palaeoproterozoic environmental history. *Earth-Science Reviews.* **172**, pp.140-177.

Kwon, E.Y., Primeau, F. and Sarmiento, J.L. 2009. The impact of remineralization depth on the air–sea carbon balance. *Nature Geoscience.* **2**(9), pp.630-635.

Lalonde, K., Mucci, A., Ouellet, A. and Gelinas, Y. 2012. Preservation of organic matter in sediments promoted by iron. *Nature.* **483**(7388), pp.198-200.

Lang, S.Q., Osburn, M.R. and Steen, A.D. 2019. Carbon in the Deep Biosphere: Forms, Fates, and Biogeochemical Cycling. In: Orcutt, B.N., et al. eds. *Deep Carbon: Past to Present.* Cambridge: Cambridge University Press, pp.480-523.

LaRowe, D.E., Arndt, S., Bradley, J.A., Estes, E.R., Hoarfrost, A., Lang, S.Q., Lloyd, K.G., Mahmoudi, N., Orsi, W.D., Shah Walter, S.R., Steen, A.D. and Zhao, R. 2020. The fate of organic carbon in marine sediments - New insights from recent data and analysis. *Earth-Science Reviews.* **204**, p103146.

Lawson, E.C., Wadham, J.L., Tranter, M., Stibal, M., Lis, G.P., Butler, C.E.H., Laybourn-Parry, J., Nienow, P., Chandler, D. and Dewsbury, P. 2014. Greenland Ice Sheet exports labile organic carbon to the Arctic oceans. *Biogeosciences.* **11**(14), pp.4015-4028.

le B. Williams, P.J. 1998. The balance of plankton respiration and photosynthesis in the open oceans. *Nature.* **394**(6688), pp.55-57.

Lehmann, J. and Kleber, M. 2015. The contentious nature of soil organic matter. *Nature.* **528**(7580), pp.60-68.

Li, X., Zhang, Z., Wade, T.L., Knap, A.H. and Zhang, C.L. 2017. Sources and compositional distribution of organic carbon in surface sediments from the lower Pearl River to the coastal South China Sea. *Journal of Geophysical Research: Biogeosciences.* **122**(8), pp.2104-2117.

Lindqvist, S. 2014. *Transport by Benthic Macrofauna: Functional Classification and Biogeochemical Response*. PhD thesis, University of Gothenburg.

Lindsay, W.L. and Schwab, A.P. 2008. The chemistry of iron in soils and its availability to plants. *Journal of Plant Nutrition.* **5**(4-7), pp.821-840.

Link, H., Chaillou, G., Forest, A., Piepenburg, D. and Archambault, P. 2013. Multivariate benthic ecosystem functioning in the Arctic – benthic fluxes explained by environmental parameters in the southeastern Beaufort Sea. *Biogeosciences.* **10**(9), pp.5911-5929.

Lister, M.W. and Garvie, R.C. 1959. Sodium Dithionite, Decomposition in Aqueous Solution and in the Solid State. *Canadian Journal of Chemistry.* **37**(9), pp.1567-1574.

Lopes, C., Kucera, M. and Mix, A.C. 2015. Climate change decouples oceanic primary and export productivity and organic carbon burial. *Proc Natl Acad Sci U S A.* **112**(2), pp.332-335.

Lush, D.L. and Hynes, H.B.N. 1973. The Formation of Particles in Freshwater Leachates of Dead Leaves1. *Limnology and Oceanography.* **18**(6), pp.968-977.

Lush, D.L. and Hynes, H.B.N. 1978. Particulate and dissolved organic matter in a small partly forested Ontario stream. *Hydrobiologia.* **60**(2), pp.177-185.

Ma, W.-W., Zhu, M.-X., Yang, G.-P. and Li, T. 2018. Iron geochemistry and organic carbon preservation by iron (oxyhydr)oxides in surface sediments of the East China Sea and the south Yellow Sea. *Journal of Marine Systems.* **178**, pp.62-74.

Mackenzie, R.C. 1954. Free Iron-Oxide Removal from Soils. *Journal of Soil Science.* **5**(1), pp.167-172.

Marschner, B., Brodowski, S., Dreves, A., Gleixner, G., Gude, A., Grootes, P.M., Hamer, U., Heim, A., Jandl, G., Ji, R., Kaiser, K., Kalbitz, K., Kramer, C., Leinweber, P., Rethemeyer, J., Schäffer, A., Schmidt, M.W.I., Schwark, L. and Wiesenberg, G.L.B. 2008. How relevant is recalcitrance for the stabilization of organic matter in soils? *Journal of Plant Nutrition and Soil Science.* **171**(1), pp.91-110.

Mayer, L.M. 1994. Relationships between mineral surfaces and organic carbon concentrations in soils and sediments. *Chemical Geology.* **114**(3-4), pp.347-363.

Mayer, L.M. 1995. Sedimentary organic matter preservation: an assessment and speculative synthesis—a comment. *Marine Chemistry.* **49**(2-3), pp.123-126.

McClymont, E.L., Martínez-Garcia, A. and Rosell-Melé, A. 2007. Benefits of freeze-drying sediments for the analysis of total chlorins and alkenone concentrations in marine sediments. *Organic Geochemistry.* **38**(6), pp.1002-1007.

McKeague, J.A. and Day, J.H. 1966. Dithionite and oxalate extractable Fe and Al as aids in differentiating various classes of soil. *Canadian Journal of Soil Science.* **46**(1), pp.13-22.

Mehra, O.P. 1958. Iron Oxide Removal from Soils and Clays by a Dithionite-Citrate System Buffered with Sodium Bicarbonate. *Clays and Clay Minerals.* **7**(1), pp.317-327.

Mentges, A., Feenders, C., Deutsch, C., Blasius, B. and Dittmar, T. 2019. Long-term stability of marine dissolved organic carbon emerges from a neutral network of compounds and microbes. *Sci Rep.* **9**(1), p17780.

Meybeck, M. 1982. Carbon, nitrogen, and phosphorus transport by world rivers. *American Journal of Science.* **282**(4), pp.401-450.

Meyers, P.A. 1994. Preservation of elemental and isotopic source identification of sedimentary organic matter. *Chemical Geology.* **114**(3-4), pp.289-302.

Meysman, F.J.R., Boudreau, B.P. and Middelburg, J.J. 2010. When and why does bioturbation lead to diffusive mixing? *Journal of Marine Research.* **68**(6), pp.881-920.

Middelburg, J.J. 1989. A simple rate model for organic matter decomposition in marine sediments. *Geochimica et Cosmochimica Acta.* **53**(7), pp.1577-1581.

Middelburg, J.J. 2019a. Carbon Processing at the Seafloor. In: Middelburg, J.J. ed. *Marine Carbon Biogeochemistry.* Cham: Springer International Publishing, pp.57-75.

Middelburg, J.J. 2019b. The Return from Organic to Inorganic Carbon. *Marine Carbon Biogeochemistry.* pp.37-56.

Mikutta, C. 2011. X-ray absorption spectroscopy study on the effect of hydroxybenzoic acids on the formation and structure of ferrihydrite. *Geochimica et Cosmochimica Acta.* **75**(18), pp.5122-5139.

Mikutta, C., Mikutta, R., Bonneville, S., Wagner, F., Voegelin, A., Christl, I. and Kretzschmar, R. 2008. Synthetic coprecipitates of exopolysaccharides and ferrihydrite. Part I: Characterization. *Geochimica et Cosmochimica Acta.* **72**(4), pp.1111-1127.

Mitchell, B.D. and Mackenzie, R.C. 1954. Removal of Free Iron Oxide from Clays. *Soil Science.* **77**(3), pp.173-184.

Moran, M.A., Kujawinski, E.B., Stubbins, A., Fatland, R., Aluwihare, L.I., Buchan, A., Crump, B.C., Dorrestein, P.C., Dyhrman, S.T., Hess, N.J., Howe, B., Longnecker, K., Medeiros, P.M., Niggemann, J., Obernosterer, I., Repeta, D.J. and Waldbauer, J.R. 2016. Deciphering ocean carbon in a changing world. *Proc Natl Acad Sci U S A.* **113**(12), pp.3143-3151.

Mu, C.C., Zhang, T.J., Zhao, Q., Guo, H., Zhong, W., Su, H. and Wu, Q.B. 2016. Soil organic carbon stabilization by iron in permafrost regions of

the Qinghai-Tibet Plateau. *Geophysical Research Letters.* **43**(19), pp.10,286-210,294.

Müller, P.J. 1977. CN ratios in Pacific deep-sea sediments: Effect of inorganic ammonium and organic nitrogen compounds sorbed by clays. *Geochimica Et Cosmochimica Acta.* **41**(6), pp.765-776.

Munroe, J. and Brencher, Q. 2019. Holocene Carbon Burial in Lakes of the Uinta Mountains, Utah, USA. *Quaternary.* **2**(1).

Mylotte, R., Sutrisno, A., Farooq, H., Masoom, H., Soong, R., Hayes, M.H.B. and Simpson, A.J. 2016. Insights into the composition of recalcitrant organic matter from estuarine sediments using NMR spectroscopy. *Organic Geochemistry.* **98**, pp.155-165.

Patzner, M.S., Mueller, C.W., Malusova, M., Baur, M., Nikeleit, V., Scholten, T., Hoeschen, C., Byrne, J., Borch, T., Kappler, A. and Bryce, C. 2020. Iron mineral dissolution during permafrost thaw releases associated organic carbon. *EarthArXiv (Pre-print).*

Peter, S. and Sobek, S. 2018. High variability in iron-bound organic carbon among five boreal lake sediments. *Biogeochemistry.* **139**(1), pp.19-29.

Poli, M.S., Meyers, P.A., Thunell, R.C. and Capodivacca, M. 2012. Glacial-interglacial variations in sediment organic carbon accumulation and benthic foraminiferal assemblages on the Bermuda Rise (ODP Site 1063) during MIS 13 to 10. *Paleoceanography.* **27**(3), pp.n/a-n/a.

Postma, D. 1993. The reactivity of iron oxides in sediments: A kinetic approach. *Geochimica et Cosmochimica Acta.* **57**(21-22), pp.5027-5034.

Poulton, S.W. and Canfield, D.E. 2005. Development of a sequential extraction procedure for iron: implications for iron partitioning in continentally derived particulates. *Chemical Geology.* **214**(3-4), pp.209-221.

Quigley, L.N.M., Edwards, A., Steen, A.D. and Buchan, A. 2019. Characterization of the Interactive Effects of Labile and Recalcitrant Organic Matter on Microbial Growth and Metabolism. *Front Microbiol.* **10**(493), p493.

Raiswell, R., Canfield, D.E. and Berner, R.A. 1994. A comparison of iron extraction methods for the determination of degree of pyritisation and the recognition of iron-limited pyrite formation. *Chem Geol.* **111**(1-4), pp.101-110.

Raven, M.R., Fike, D.A., Gomes, M.L., Webb, S.M., Bradley, A.S. and McClelland, H.O. 2018. Organic carbon burial during OAE2 driven by changes in the locus of organic matter sulfurization. *Nat Commun.* **9**(1), p3409.

Reimers, C.E., Alleau, Y., Bauer, J.E., Delaney, J., Girguis, P.R., Schrader, P.S. and Stecher, H.A. 2013. Redox effects on the microbial degradation of refractory organic matter in marine sediments. *Geochimica et Cosmochimica Acta.* **121**, pp.582-598.

Romero-Olivares, A.L., Allison, S.D. and Treseder, K.K. 2017. Decomposition of recalcitrant carbon under experimental warming in boreal forest. *PLoS One.* **12**(6), pe0179674.

Rossel, P.E., Bienhold, C., Boetius, A. and Dittmar, T. 2016. Dissolved organic matter in pore water of Arctic Ocean sediments: Environmental influence on molecular composition. *Organic Geochemistry.* **97**, pp.41-52.

Salvadó, J.A., Tesi, T., Andersson, A., Ingri, J., Dudarev, O.V., Semiletov, I.P. and Gustafsson, Ö. 2015. Organic carbon remobilized from thawing permafrost is resequestered by reactive iron on the Eurasian Arctic Shelf. *Geophysical Research Letters.* **42**(19), pp.8122-8130.

Schillawski, S. and Petsch, S. 2008. Release of biodegradable dissolved organic matter from ancient sedimentary rocks. *Global Biogeochemical Cycles.* **22**(3), pp.n/a-n/a.

Schlesinger, W.H. and Bernhardt, E.S. 2013. Wetland Ecosystems. *Biogeochemistry.* pp.233-274.

Schmidt, M.W., Torn, M.S., Abiven, S., Dittmar, T., Guggenberger, G., Janssens, I.A., Kleber, M., Kogel-Knabner, I., Lehmann, J., Manning, D.A., Nannipieri, P., Rasse, D.P., Weiner, S. and Trumbore, S.E. 2011. Persistence of soil organic matter as an ecosystem property. *Nature.* **478**(7367), pp.49-56.

Schulten, H.R. and Leinweber, P. 1995. Dithionite-Citrate-Bicarbonate-Extractable Organic Matter in Particle-Size Fractions of a Haplaquoll. *Soil Science Society of America Journal.* **59**(4), pp.1019-1027.

Schwab, K. 1980. *Effect-directed identification of bioavailable toxic organic compounds in contaminated sediments*. PhD thesis, Martin-Luther-universität halle-wittenberg.

Schwertmann, U. and Cornell, R.M. 2000. *Iron Oxides in the Laboratary.* Wiley.

Segers, R. 1998. Methane production and methane consumption: a review of processes underlying wetland methane fluxes. *Biogeochemistry.* **41**(1), pp.23-51.

Shaffer, G. and Lambert, F. 2018. In and out of glacial extremes by way of dust-climate feedbacks. *Proc Natl Acad Sci U S A.* **115**(9), pp.2026-2031.

Singh, M., Sarkar, B., Sarkar, S., Churchman, J., Bolan, N., Mandal, S., Menon, M., Purakayastha, T.J. and Beerling, D.J. 2018. Stabilization of Soil Organic Carbon as Influenced by Clay Mineralogy. In: Sparks, D.L. ed. *Advances in Agronomy.* Academic Press, pp.33-84.

Sirois, M., Couturier, M., Barber, A., Gélinas, Y. and Chaillou, G. 2018. Interactions between iron and organic carbon in a sandy beach subterranean estuary. *Marine Chemistry.* **202**, pp.86-96.

Smith, R.W., Bianchi, T.S., Allison, M., Savage, C. and Galy, V. 2015. High rates of organic carbon burial in fjord sediments globally. *Nature Geoscience.* **8**(6), pp.450-453.

Smith, S.V. 1981. Marine macrophytes as a global carbon sink. *Science.* **211**(4484), pp.838-840.

Snelgrove, P.V.R., Soetaert, K., Solan, M., Thrush, S., Wei, C.L., Danovaro, R., Fulweiler, R.W., Kitazato, H., Ingole, B., Norkko, A., Parkes, R.J. and Volkenborn, N. 2018. Global Carbon Cycling on a Heterogeneous Seafloor. *Trends Ecol Evol.* **33**(2), pp.96-105.

Soares, P.I., Alves, A.M., Pereira, L.C., Coutinho, J.T., Ferreira, I.M., Novo, C.M. and Borges, J.P. 2014. Effects of surfactants on the magnetic properties of iron oxide colloids. *J Colloid Interface Sci.* **419**, pp.46-51.

Sollins, P., Homann, P. and Caldwell, B.A. 1996. Stabilization and destabilization of soil organic matter: mechanisms and controls. *Geoderma.* **74**(1-2), pp.65-105.

Sorensen, J. 1982. Reduction of ferric iron in anaerobic, marine sediment and interaction with reduction of nitrate and sulfate. *Appl Environ Microbiol.* **43**(2), pp.319-324.

Sørensen, J. and Jeørgensen, B.B. 1987. Early diagenesis in sediments from Danish coastal waters: Microbial activity and Mn-Fe-S geochemistry. *Geochimica et Cosmochimica Acta.* **51**(6), pp.1583-1590.

Tagliabue, A., Bowie, A.R., Boyd, P.W., Buck, K.N., Johnson, K.S. and Saito, M.A. 2017. The integral role of iron in ocean biogeochemistry. *Nature.* **543**(7643), pp.51-59.

Taylor, G.J. and Crowder, A.A. 1983. Use of the Dcb Technique for Extraction of Hydrous Iron Oxides from Roots of Wetland Plants. *American Journal of Botany.* **70**(8), pp.1254-1257.

Tessin, A., Hendy, I., Sheldon, N. and Sageman, B. 2015. Redox-controlled preservation of organic matter during “OAE 3” within the Western Interior Seaway. *Paleoceanography.* **30**(6), pp.702-717.

ThomasArrigo, L.K., Byrne, J.M., Kappler, A. and Kretzschmar, R. 2018. Impact of Organic Matter on Iron(II)-Catalyzed Mineral

Transformations in Ferrihydrite-Organic Matter Coprecipitates. *Environ Sci Technol.* **52**(21), pp.12316-12326.

Thompson, J., Poulton, S.W., Guilbaud, R., Doyle, K.A., Reid, S. and Krom, M.D. 2019. Development of a modified SEDEX phosphorus speciation method for ancient rocks and modern iron-rich sediments. *Chemical Geology.* **524**, pp.383-393.

Tipping, E. 1981. The adsorption of aquatic humic substances by iron oxides. *Geochimica et Cosmochimica Acta.* **45**(2), pp.191-199.

Tipping, E. and Heaton, M.J. 1983. The adsorption of aquatic humic substances by two oxides of manganese. *Geochimica et Cosmochimica Acta.* **47**(8), pp.1393-1397.

Tissot, B.P. and Welte, D.H. 1984. *Petroleum Formation and Occurrence.* Springer.

Tombácz, E., Libor, Z., Illés, E., Majzik, A. and Klumpp, E. 2004. The role of reactive surface sites and complexation by humic acids in the interaction of clay mineral and iron oxide particles. *Organic Geochemistry.* **35**(3), pp.257-267.

Torn, M.S., Trumbore, S.E., Chadwick, O.A., Vitousek, P.M. and Hendricks, D.M. 1997. Mineral control of soil organic carbon storage and turnover. *Nature.* **389**(6647), pp.170-173.

Twichell, S.C., Meyers, P.A. and Diester-Haass, L. 2002. Significance of high C/N ratios in organic-carbon-rich Neogene sediments under the Benguela Current upwelling system. *Organic Geochemistry.* **33**(7), pp.715-722.

Uramoto, G.-I., Morono, Y., Uematsu, K. and Inagaki, F. 2014. An improved sample preparation method for imaging microstructures of fine-grained marine sediment using microfocus X-ray computed tomography and scanning electron microscopy. *Limnology and Oceanography: Methods.* **12**(7), pp.469-483.

van Bodegom, P.M., van Reeven, J. and Denier van der Gon, H.A.C. 2003. Prediction of reducible soil iron content from iron extraction data. *Biogeochemistry.* **64**(2), pp.231-245.

Varadachari, C., Goswami, G. and Ghosh, K. 2006. Dissolution of Iron Oxides. *Clay Research.* **25**.

Verardo, D.J. and McIntyre, A. 1994. Production and destruction: Control of biogenous sedimentation in the tropical Atlantic 0–300,000 years BP. *Paleoceanography.* **9**(1), pp.63-86.

Volkman, J.K. and Tanoue, E. 2002. Chemical and Biological Studies of Particulate Organic Matter in the Ocean. *Journal of Oceanography.* **58**(2), pp.265-279.

von der Heyden, B.P. and Roychoudhury, A.N. 2015. Application, Chemical Interaction and Fate of Iron Minerals in Polluted Sediment and Soils. *Current Pollution Reports.* **1**(4), pp.265-279.

Wagai, R. and Mayer, L.M. 2007. Sorptive stabilization of organic matter in soils by hydrous iron oxides. *Geochimica et Cosmochimica Acta.* **71**(1), pp.25-35.

Walker, M., Johnsen, S., Rasmussen, S.O., Popp, T., Steffensen, J.-P., Gibbard, P., Hoek, W., Lowe, J., Andrews, J., Björck, S., Cwynar, L.C., Hughen, K., Kershaw, P., Kromer, B., Litt, T., Lowe, D.J., Nakagawa, T., Newnham, R. and Schwander, J. 2009. Formal definition and dating of the GSSP (Global Stratotype Section and Point) for the base of the Holocene using the Greenland NGRIP ice core, and selected auxiliary records. *Journal of Quaternary Science.* **24**(1), pp.3-17.

Wang, D., Zhu, M.X., Yang, G.P. and Ma, W.W. 2019. Reactive Iron and Iron-Bound Organic Carbon in Surface Sediments of the River-Dominated Bohai Sea (China) Versus the Southern Yellow Sea. *Journal of Geophysical Research: Biogeosciences.* **124**(1), pp.79-98.

Wang, Y., Zhang, R., He, Z., Van Nostrand, J.D., Zheng, Q., Zhou, J. and Jiao, N. 2017. Functional Gene Diversity and Metabolic Potential of the Microbial Community in an Estuary-Shelf Environment. *Front Microbiol.* **8**, p1153.

Ward, B.B. 2008. Nitrification in Marine Systems. In: Capone, D.G., et al. eds. *Nitrogen in the Marine Environment.* San Diego: Academic Press, pp.199-261.

Wetzel, R.G. 2001. The Inorganic Carbon Complex. *Limnology.* pp.187-204.

Williams, P.M. and Druffel, E.R.M. 1987. Radiocarbon in dissolved organic matter in the central North Pacific Ocean. *Nature.* **330**(6145), pp.246-248.

Winton, M., Griffies, S.M., Samuels, B.L., Sarmiento, J.L. and Frölicher, T.L. 2013. Connecting Changing Ocean Circulation with Changing Climate. *Journal of Climate.* **26**(7), pp.2268-2278.

Wu, X., Fang, H., Zhao, Y., Smoak, J.M., Li, W., Shi, W., Sheng, Y., Zhao, L. and Ding, Y. 2017. A conceptual model of the controlling factors of soil organic carbon and nitrogen densities in a permafrost-affected region on the eastern Qinghai-Tibetan Plateau. *Journal of Geophysical Research: Biogeosciences.* **122**(7), pp.1705-1717.

Yang, Y., Lohwacharin, J. and Takizawa, S. 2017. Analysis of adsorption processes of dissolved organic matter (DOM) on ferrihydrite using surrogate organic compounds. *Environ Sci Pollut Res Int.* **24**(27), pp.21867-21876.

Yang, Y., Takizawa, S., Sakai, H., Murakami, M. and Watanabe, N. 2012. Removal of organic matter and phosphate using ferrihydrite for reduction of microbial regrowth potential. *Water Sci Technol.* **66**(6), pp.1348-1353.

Zhao, B., Yao, P., Bianchi, T.S., Shields, M.R., Cui, X.Q., Zhang, X.W., Huang, X.Y., Schröeder, C., Zhao, J. and Yu, Z.G. 2018. The Role of Reactive Iron in the Preservation of Terrestrial Organic Carbon in Estuarine Sediments. *Journal of Geophysical Research: Biogeosciences.* **123**(12), pp.3556-3569.

Zhao, Q., Poulson, S.R., Obrist, D., Sumaila, S., Dynes, J.J., McBeth, J.M. and Yang, Y. 2016. Iron-bound organic carbon in forest soils: quantification and characterization. *Biogeosciences.* **13**(16), pp.4777-4788.

In prep/review

Faust, J.C., Tessin, A., Fisher, B.J., Zindorf, M., Papdaki, S., Hendry, K., Doyle, K., März, C., *(submitted to Nature Geoscience)* Millennial scale persistence of organic carbon bound to iron in Arctic marine sediments.

Moore, O.W., Curti, L., Woulds, C., Bradley, J.A., Xiao, K., Babakhani, P., Bray, A.W., Fisher, B.J, Kazemian, M., Kaulich, B., Dale, A.W., Peacock, C.L. *(in prep)* Formation of geopolymerised organic carbon in marine sediments promoted by iron and manganese.